

A Mechanistic Approach towards the Reconstitution of Division in a Prospective Minimal Cell

Jard Mattens

To obtain the degree of Bachelor of Science in Nanobiology,
Delft University of Technology and the Erasmus Medical Center
Public defence on 27-03-2018

Supervisor: Elisa Godino, M.Sc.
Dr. Christophe Danelon
Delft University of Technology

March 2019



Abstract

Different approaches have been taken to reconstitute liposome deformation and division in an attempt to construct an artificial cell. Approaches adopted include thermal division, mechanical division, electrical division, osmotically stimulated division as well as protein based division. Here, we give an overview of the methods that have been used and their feasibility in the construction of a minimal cell. On top of that, we provide experimental evidence for the feasibility to use cholesterol to generate stably elongated liposomes as a first step towards division. We present a method to create stably elongated liposomes that are compatible with liposome-based gene-expression. Furthermore, we demonstrate initial compatibility of the method developed with two membrane-dependent proteins that form part of the *E. coli* bacterial division system.

Keywords: *Cell-free expression, In vitro transcription/translation, (Gene - Expressing) Liposomes (GUVs), Division, Membrane (Electro)Deformation, Cholesterol Membrane Partitioning, FtsZ, Min System, Minimal Cell.*

Contents

I	Building Synthetic Cells	6
0.1	Essential Criteria of Life	6
0.1.1	Compartmentalisation, Reproduction and Environmental Dependence	8
0.2	Bottom-up Cells	8
0.3	Top-down Cells	8
0.4	Artificial Cells	9
0.5	Protocells	9
0.6	Minimal Cells	10
0.6.1	The Christophe Danelon Lab Approach	10
0.7	Current Research Objective	13
II	Review: Division in a Minimal Cell	17
1	Introduction	18
2	Shaping Minimal Division	18
3	Morphology Associated Energy Considerations	20
3.1	Elongation as a Requirement for Intracellular-Content-Representative Division	20
3.2	Membrane Dynamics and Fission	21
3.3	Intermediate Membrane Structures in Content- Preserving Division	24
3.4	Multigenerational Division and Membrane Growth Limitation	28
3.5	Comparing Approaches towards Division	30
4	Thermal Division	31
5	Electrical Division	36
6	Mechanical Division	43
7	Osmolarity Induced Division	46
8	Lipid/Sterol Membrane Components and Division	49
8.1	Cholesterol	49
8.2	Sphingolipids	50
8.3	Excess Membrane Synthesis	50

9 Protein-based Fission	52
9.1 Reproduction in Mycoplasmas	52
9.2 <i>E. coli</i> division system	53
9.3 Archaeal Division	56
9.4 Virally Induced Fission	56
10 Conclusion	58
III Experimental Approach towards Division in Gene-Expressing Liposomes	77
11 Introduction	78
12 Material and Methods	80
12.1 Preparing GUVs	80
12.2 Preparing Lipid-Coated Silica Beads (\pm cholesterol)	80
12.3 Swelling and Freeze-Thaw cycles	81
12.4 Osmolarity assays	83
12.5 Kinetics	83
12.5.1 Surface functionalisation	84
12.6 Electrodeformation Approach	84
12.7 FtsZ bundle formation	85
12.8 Min System	85
12.9 Cholesterol titrations	86
12.10 Laser Scanning Confocal Microscopy Imaging	86
12.10.1 Image Analysis	87
12.11 Cleaning Chambers	88
12.12 Imaging Flow Cytometry	88
12.12.1 PBS addition during initiation of expression	89
12.12.2 Imaging Flow Cytometry Analysis	90
13 Results	91
13.1 Membrane cholesterol (30%) and increased external sucrose concentrations appear to independently elongate DO-liposomes, while showing compatible with YFP expression in the PURE system	91
13.1.1 The addition sucrose (200 mM) at transcription initiation shows uninhibited YFP expression, especially in cholesterol liposomes	94
13.2 Cholesterol (30%) liposomes may be stable for 5 hours in elongated shape	94
13.3 Imaging flow cytometry (IFC) studies corroborate that membrane cholesterol (30%) induces elongation and confirm cholesterol liposome stability over 24 hours	95

13.3.1	PBS induces liposome morphology changes similar to sucrose and is compatible with the PURE system and liposomal YFP-expression	97
13.4	Electrodeformation requires specialised high voltage equipment	97
13.5	30%-cholesterol in the liposome membrane does not appear to inhibit FtsA binding and FtsZ polymerisation	98
13.6	MinD is recruited to 30% cholesterol membranes, although no waves have been observed	100
13.7	Sucrose addition (100mM) facilitates Min waves in pronouncedly elongated liposomes	101
13.8	Direct cholesterol addition to the liposome environment destroys the liposomes	102
14	Discussion	104
14.1	Cholesterol elongation in context	104
14.2	Overall Project in Perspective	104
15	The future for division in gene-expression liposomes	107
16	Acknowledgements	112
17	Appendix A: Lipid/Sterol Nomenclature	113
18	Appendix B: Electrodeformation Chamber Construction	115
19	Appendix C: Additional Images and Data on the Morphology and Expression of Cholesterol Liposomes (30%) under the Addition of External Sucrose (0-200 mM)	116
20	Appendix D: Observed Events that resemble or suggest Fission	118
21	Appendix E: Fischer Linear Discriminant Analysis	119
22	Appendix F: Imaging Flow Cytometry Data Analysis	122

Part I

Building Synthetic Cells

Synthetic biologists use inspiration from nature to construct artificial life in order to acquire more understanding of living matter. Before understanding, and possibly recreating life however, one should have an idea on what life actually is. Should the living entity internally regulate all its life-essential processes, or may some essential internal processes depend on external cues? Does the being have to be build according to existing organisms, or can we create completely new living structures? Different branches of synthetic cell construction represent differing views on the methods and components used to reconstruct life. The branches range from artificial cells to protocells, and minimal cells with either a bottom-up, or top-down approach. Varying in their resemblance with the cells we are familiar with from nature, all approaches have in common the desire to build a system that fulfills the essential criteria of life.

0.1 Essential Criteria of Life

From Ancient Greek times, speculations have been issued on what life is. From these early times on, materialist perspectives went out to life being no more than a specially organised material. Life as an organised material could be seen as compatible with the current outlook of synthetic biologists. However, what is the meaning of organisation in this context?

In 1970 John Conway, a famous mathematician, published his Game of Life [Gardner, 1970]. The Game of Life comprises a two-dimensional raster of which each cell can take on two colours, representing life and death respectively, depending on the state of its neighbour (see figure 0.1.1). With a set of three simple rules quickly complex patterns emerge resulting from processes, or rules, resembling death and reproduction. The Game of Life is an example of a cellular automaton with two states: ‘alive’ and ‘death’. Even before the Game of Life, in 1966, John von Neumann developed a cellular automaton representing reproduction of a multicellular system [Von Neumann *et al.*, 1966]. The Von Neuman cellular automaton consists of finite state automata (FSA) that can each take on 29 states in a two-dimensional Cartesian space. Based on this cellular automaton environment, even before the discovery of DNA, Von Neuman designed a universal constructor, functioning similarly to the Central Dogma of Biology. In later years people elaborated on the Von Neumann’s cellular automata creating computer programs that improvingly mimick living cells. An example of these are the Langton loops and their successors [Langton, 1984; Byl, 1989; Sayama, 1999; Oros *et al.*, 2007].

Christopher Langton, after whom the first loops were named, designed a self-replicating entity containing hereditary information [Langton, 1984]. In 1999, Langton loops were improved to include a form of evolution [Sayama, 1999], and in 2007 the *Sexyloops* (see figure 0.1.1) were developed that could additionally

combine genetic information from several entities to form a new entity with different hereditary information [Oros *et al.*, 2007]. The computer programs that have been developed however, can constitute systems that self-organise, grow and adapt in response to external changes [Sayama, 1999; Oros *et al.*, 2007], many properties we recognise from living systems. However, we generally do not classify computer programs as living entities. Hence, one could pose the question: *What is life?*

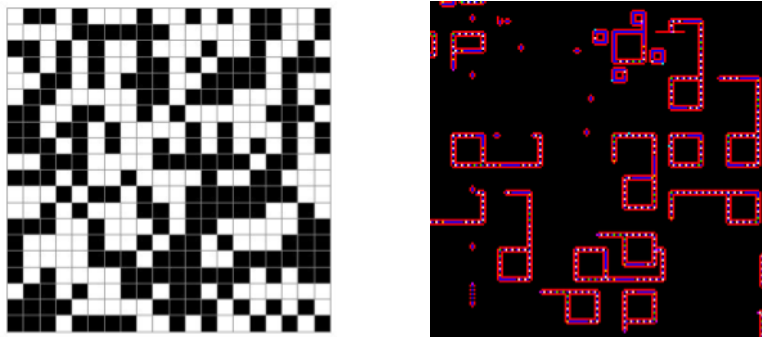


Figure 0.1.1. Cellular Automata. **Left:** Cellular Grid used in the Game of Life. [Kun *et al.*, 2011], **Right:** Sexyloops can evolve and transmit hereditary information to recombine in other entities. [Erkiaga, 2018].

In 1944 the famous physicist Erwin Schrödinger published his book called *What is Life? The Physical Aspect of the Living Cell*. In the book, Schrödinger described the storage form of hereditary information as an *aperiodic crystal* before the discovery of DNA. On top of that, in his book, Schrödinger also elicits living matter as matter that actively maintains a state of negative entropy [Schrödinger, 1944], as has been done more often in later times [Margulis *et al.*, 1995]. From a physical perspective, a living system could, more broadly, be described as an autopoietic self-organised thermodynamically open system that is able to grow, to maintain homeostasis and to sustain metabolism, whilst adapting to its environment and responding to stimuli [Schrödinger, 1944; Koshland *et al.*, 2002; McKay *et al.*, 2004; Trifonov *et al.*, 2012].

Apart from a direct description of the requirements of life in space time, life could on the contrary also be characterized by the ability to loose the functionalities described above to reach a state called death. Empirical evidence from everyday life suggests death to be inherent to any form of life on the short or long term. However, apart from death being inherent to any form of life we know, death might not necessarily be an essential criterion for life. Death might rather be the negation of life that is merely a consequence of how life as we know it is generally structured.

To maintain an autopoietic system functioning on negative entropy, as described to be essential for life, living entities need to be able to reliably store and copy information. In many living entities known to us, including ourselves, the

information is stored in compartments surrounded by lipid bilayers [Bretscher *et al.*, 1975; Zhang *et al.*, 2008]. For reproduction of such units of life enclosed by lipid bilayers, the lipid compartments need to be able to divide. Division in many organisms is a highly complex and extensively regulated task that may be dependent on environmental cues in addition to internal timing mechanisms. An example of environmental impact on division is the case of nutrient depletion. In times of starvation, an increase in guanosine pentaphosphate or tetraphosphate ((p)ppGpp) presence may be induced. As a result, the cell cycle is halted in G1-phase [Potrykus *et al.*, 2008; Jonas, 2014].

0.1.1 Compartmentalisation, Reproduction and Environmental Dependence

In order to maintain an open system with negative entropy and selective uptake of different molecular compounds, living systems generally make use of semipermeable membranes enclosing a lumen in which chemical reactions happen contributing to homeostasis and metabolism. The essential criteria for life in combination with an evolutionary perspective raise a compelling question: to what extent may a living system depend on cues from the environment to establish its essential functionality? Need all essential functions be under full internal control of the living entity? On these questions, synthetic biologists differ in opinion, giving rise to a plethora of reconstruction types that can be broadly categorised in *artificial cells*, *protocells*, and *minimal cells*. The approaches taken within the reconstruction type may then either rely on a *bottom-up*, or a *top-down approach*, each of which will first be shortly described in the following sections.

0.2 Bottom-up Cells

Bottom-up synthetic biology focuses on the construction of life from scratch. By constructing life in a bottom-up manner, individually added reactions can be evaluated for their functionality and metabolic interplay. Hereby, bottom-up synthetic biology may reveal a plethora of insights as regards physiological behaviour on all levels. Bottom-up studies are therein certainly not confined to the recreation of existing forms of life, but may rather focus on integrating components and/or metabolic pathways across species. Examples of bottom-up synthetic biology abound throughout the upcoming sections on artificial cells, protocells and minimal cells.

0.3 Top-down Cells

Top-down synthetic biology is the more conventional approach towards discovering components' functions. In contrast to the bottom-up approach, top-down synthetic biology starts from functional organisms such as *Mycoplasmas* [Glass *et al.*, 2006; Hutchison *et al.*, 2016], and further reduces their complexity in

order to find genes, and chemical and physical processes that provide essential contributions to the properties of life.

In the light of top-down synthetic biology, Craig Venter attracted significant attention with his work on the construction of a minimal genome [Glass *et al.*, 2006; Hutchison *et al.*, 2016]. Before focussing on a minimal genome, Venter and his team characterized the genome of *Mycoplasma genitalium*, that contains only 470 predicted coding regions and is therefore one of the organisms with the least genes known to us up until today [Fraser *et al.*, 1995].

Apart from the minimal genome studies by Craig Venter *et al.* [Glass *et al.*, 2006; Hutchison *et al.*, 2016], top-down synthetic biology can also focus on the minimisation of metabolic networks [Gabaldón *et al.*, 2007], or on the introduction of new components to an existing system to possibly optimise it. An example of the latter is the extension of the amino acid library, as contributed to by Summerer *et al.* (2006), which restructures the lines between bottom-up and top-down synthetic biology by introducing newly engineered components to existing organisms.

0.4 Artificial Cells

Artificial cells make up what could be seen as the broadest niche in synthetic biology. Artificial cells may consist of organic and inorganic components that are not standard in life as we know it. Artificial cells may make use of newly engineered components and mechanisms to obtain their organizational characteristics. Nevertheless, artificial cells may also be a product of a combination of components from different existing organisms. In respect of this organismal mixing, artificial cells encompass the protocells as well as the minimal cells that will be described below. An example of an artificial cell approach is an *E. coli* cell-free expression system, encapsulated in phospholipid GUVs, expressing eGFP, being facilitated therein through membrane-incorporated alpha-hemolysin pores from *Staphylococcus aureus* [Noireaux *et al.*, 2004]. The creation of artificial cells however, may reach further and include the reconstitution of example given cell communication. One way in which this can be achieved is through the combination of elements from different organisms, as achieved by Chen *et al.* (2005) in their integration of signalling elements from *Arabidopsis thaliana* in *Saccharomyces cerevisiae*. In contrast, new mechanisms may be invented to convey information in an artificial cell system. Booth *et al.* (2016) in this respect, created a 3D printed vesicle network in which alpha-hemolysin pores were synthesised controllably through a light-activated DNA-promoter, allowing electrical signals to travel through the tissue upon incorporation of the pores in the membranes [Booth *et al.*, 2016].

0.5 Protocells

In contrast to the relative freedom in the of artificial cells, the development of protocells adheres more strictly to the expected lines of evolution, oftentimes with ribozyme-based reaction catalysis and fatty acid membranes. Fatty acid

vesicles form a stable semipermeable enclosure that has been shown to allow for growth and reproducible division [Gebicki *et al.*, 1976; Hanczyc *et al.*, 2003, Chen *et al.*, 2004; Berclaz *et al.*, 2001; Blochliger *et al.*, 1998; Luisi *et al.*, 2004; Rasi *et al.*, 2003; Rasi *et al.*, 2004]. Upon the administration of fatty acid micelles, big multilamellar fatty acid vesicles have been shown to elongate and divide upon contact with shear forces without leakage of their content [Zhu *et al.*, 2009]. In combination with earlier evidence towards enhanced polymerization and encapsulation of RNA in such vesicles in the presence of certain naturally occurring clay species [Hanczyc *et al.*, 2003], this branch of bottom-up synthetic biology may give insights into the origins of life.

0.6 Minimal Cells

Research on minimal cells focuses more on reconstituting the essential parts of life through the combination of components and processes from different organisms in order to resemble a minimalistic system covering the essential properties of life [Schrödinger, 1944; Koshland *et al.*, 2002; McKay, 2004; Trifonov, 2012]. The goals encompass the identification of the processes and genes essential to life, along with the recognition of the dispensable ones, and any biochemical parameter that may affect the behavior of a living entity [Forster *et al.*, 2006]. In this study, there is no single envisioned minimal cell, rather a plethora. One interesting early example is the reconstitution of enzymatic RNA replication in self-reproducing vesicles as achieved by Oberholzer *et al.* (1995). In their research, Oberholzer *et al.* (1995) catalysed RNA replication through Q β replicase in oleate/oleic acid vesicles that they externally stimulated to divide through the addition of the vesicle-binding oleic anhydride. Upon adhering to the vesicles' bilayer, the oleic anhydride hydrolyses, forming carboxylate surfactant that triggers vesicle growth and division. In time, DNA encoded information in phospholipid bilayer vesicles may provide more stability however, leading to the question whether the same (i.e. replication and division) could be achieved for DNA-containing phospholipid vesicles. The final goal: to supplement the minimal set of properties described to give rise to a cell that resembles life better and better.

0.6.1 The Christophe Danelon Lab Approach

In the Christophe Danelon Lab at Delft University of Technology the focus is on the creation of a minimal DNA-based cell. In this process, phospholipid Giant Unilamellar Vesicles (GUVs) are used as a platform for gene-expression through the incorporation of the PURE system (protein synthesis using recombinant elements) [Shimizu *et al.*, 2001] that enables *in vitro* gene-expression and protein translation. *In vitro* expression and translation are essential in the construction of a minimal cell to allow for both self-sustainment as well as for prospective reproduction over multiple generations that is envisioned by the lab.

There is a plethora of mechanism with which GUVs can be formed. Examples include electroformation [Angelova *et al.*, 1986; Angelova *et al.*, 2007] and

microfluidic approaches [reviewed by Van Swaay *et al.*, 2013]. Drawbacks of these methods however are either a high dependence on lipid types and medium parameters such as osmolarity, temperature and ionic strength as observed in electroformation [Angelova *et al.*, 2007], or, as in double emulsion preparation, the necessity of a lipid-carrying organic solvent that renders the technique less compatible with protein systems that may be damaged by the hydrophobic interactions with organic solvents [Shum *et al.*, 2008].

In the Christophe Danelon lab, therefore the GUVs used for experimentation are created in a 3-step method containing an adapted process of natural swelling [Kumazawa *et al.*, 1996]. Natural swelling included higher volumes that are not compatible with the use of the relatively expensive buffer solutions. Therefore, the method was adapted by covering glass beads with lipids, thereby allowing the use of lower volumes. The natural swelling method is accompanied with sample heterogeneity. Nevertheless, this method is compatible with the formation of gene-expressing liposomes, containing components including DNA, ribosomes, initiation factors, ATP, GTP and possibly some proteins under study. In 2018, Van Nies *et al.* demonstrated linear DNA self-replication through encoded $\Phi 29$ virus proteins in GUVs in this lab. One of the present challenges is to instigate vesicle division that is compatible with gene-expression for replication and homeostasis.

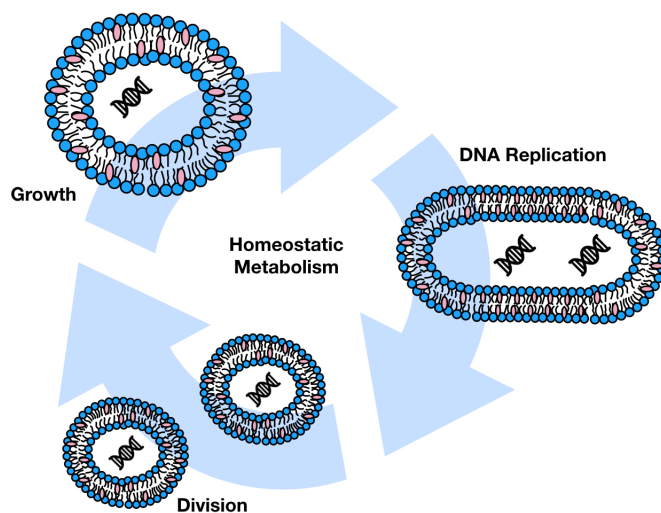


Figure 0.5.1 The creation of a minimal cell in GUVs involves DNA replication, compartment division, membrane growth, and transcription and translation for (multi-generational) homeostasis and metabolism, each of which is a topic of study in the Christophe Danelon lab.

Cell-Free Gene Expression In mimicking the essential characteristics of life with DNA-based systems, the Central Dogma of Biology has to be followed.

DNA in time stably stores hereditary information that may be controllably transcribed to mRNA and subsequently translated to essential proteins. Reconstruction in this system requires some essential components found in natural living systems such as ribosomes, ATP, and initiation factors. The cell free systems may therefore be based on crude cell extracts to obtain the necessary components. However, using crude cell extracts one cannot know or control the exact composition. Crude cell extracts often contain e.g. proteases and nucleases that may interfere with expression. On top of that, the approach is certainly not minimal. Therefore, a cell-free transcription and translation system may be used that consists of a controllable composition of purified components. An example of such a system is the PURE system [Shimizu *et al.*, 2001]. The components of the PURE system have been purified from *E. coli*, except for some factors including the RNA polymerase that stems from a T7-bacteriophage. Along with the DNA, the PURE system [Shimizu *et al.*, 2001] is essentially sufficient for protein synthesis as it contains all components necessary for aminoacylation, transcription, translation, and energy regeneration (see figure 0.5.2). Currently, different variants of the PURE system are under commercial production. PURE*flex*2.0 (Gene Frontier Corporation®) is at present the main system used in the Christophe Danelon Lab due to its relative predictability as a result of its confidentially disclosed composition. In the experimental section of this work, PURE*flex*2.0 has therefore been used for all experiments that required protein synthesis.

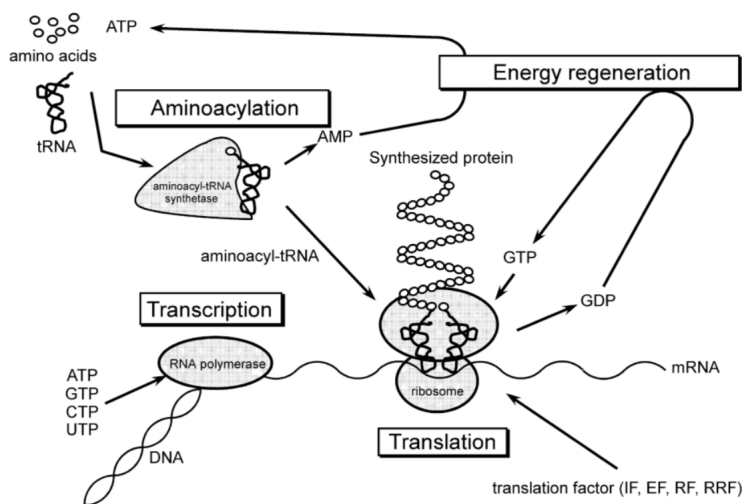


Figure 0.5.2 Overview of the four essential catalysing reactions in the PURE system. (*IF*=Initiation Factor, *EF*=Elongation Factor, *RF*=Releasing Factor, *RRF*= Ribosome Recycling Factor) [Figure adapted from Shimizu *et al.*, 2005].

0.7 Current Research Objective

As indicated above, one prominent current challenge in the context of minimal cells is to establish minimal, controllable, content-preserving division in vesicles that contain the necessary machinery to allow for cell-free gene expression, e.g. the PURE system. In the present work, a review is presented in which different methods used towards the establishment of division in liposomes are evaluated for their feasibility in the context of a minimal cell. Thereafter, an experimental section follows in which three promising division techniques are practically tested to assess their compatibility with gene-expression in PURE system-containing GUVs.

References

- [1] Berclaz, N.; Muller, M.; Walde, P.; Luisi, P. L. J. (2001). Matrix Effect in Oleate Micelles-Vesicles Transformation. *Phys. Chem. B*, 105, 1056–1064.
- [2] Blochliger, E.; Blocher, M.; Walde, P.; Luisi, P. L. J. (1998). Matrix Effect in the Size Distribution of Fatty Acid Vesicles. *Phys. Chem. B*, 102, 10383–10390.
- [3] Bretscher, M.S. *et al.* (1975). Mammalian plasma membranes. *Nature*, 258: 43–49.
- [4] Booth, M.J. (2016). Light-activated communication in synthetic tissues. *Science Advances*, 2(4), e1600056.
- [5] Byl, J. (1989). Self-Reproduction in small cellular automata. *Physica D*. 34: 295–299.
- [6] Chen, I. A.; Szostak (2004). Coupled Growth and Division of Model Procell Membranes. *J. W. Biophys. J.*, 87, 988–998.
- [7] Erkiaga, A. (2018). Own work, CC BY-SA 4.0, <https://commons.wikimedia.org/w/index.php?curid=54538407>
- [8] Forster, A.C. *et al.* (2006). Towards synthesis of a minimal cell. *Molecular Systems Biology*, 2 (1): 45. DOI 10.1038/msb4100090.
- [9] Fraser, C.M. *et al.* (1995). The Minimal Gene Complement of *Mycoplasma genitalium*. *Science*: 270 (5235): 397-404. DOI: 10.1126/science.270.5235.397.
- [10] Gabaldón, T. (2007) Structural analyses of a minimal metabolic network. *Philosophical Transactions of the Royal Society B*. DOI 10.1098/rstb.2007.2067.
- [11] Gardner, M. (1970). MATHEMATICAL GAMES The fantastic combinations of John Conway’s new solitaire game ”life”. *Scientific American* 223:120-123.
- [12] Glass, J.I. *et al.* (2006). Essential genes of a minimal bacterium. *PNAS* 103 (2) 425-430; <https://doi.org/10.1073/pnas.0510013103>.
- [13] Hanczyc, M.M. *et al.* (2003). Experimental Models of Primitive Cellular Compartments: Encapsulation, Growth, and Division. *Science*, 302(5645): 618-622.
- [14] Hutchison, C.A. *et al.* (2016). Design and synthesis of a minimal bacterial genome. *Science* 351 (6280), aad6253. DOI: 10.1126/science.aad6253.
- [15] Jonas, K. (2014). To divide or not to divide: control of the bacterial cell cycle by environmental cues. *Current Opinion in Microbiology* 18: 54-60. <https://doi.org/10.1016/j.mib.2014.02.006>.

- [16] Koshland, Jr., Daniel E. (22 March 2002). "The Seven Pillars of Life". *Science*. 295 (5563): 2215–16. doi:10.1126/science.1068489. PMID 11910092. Archived from the original on 28 February 2009. Retrieved 25 May 2009.
- [17] Kumazawa, N. *et al.* (1996). Novel method to form giant liposome entrapping DNA. *Macromol Symp*, 106: 219.
- [18] Kun, J. (2011). The Wild World of Cellular Automata. Retrieved on 23-01-2019 from: <https://jeremykun.com/2011/06/29/conways-game-of-life/>
- [19] Langton, C. G. (1984). Self-reproduction in cellular automata. *Physica D*. 10: 135–144.
- [20] Luisi, P. L.; Stano, P.; Rasi, S.; Mavelli, F. (2004). A Possible Route to Prebiotic Vesicle Reproduction. *Artificial Life*, 10 (3), 297-308.
- [21] Margulis, Lynn; Sagan, Dorion (1995). *What is Life?*. University of California Press. ISBN 978-0-520-22021-8.
- [22] McKay, Chris P. (14 September 2004). "What Is Life—and How Do We Search for It in Other Worlds?". *PLoS Biology*. 2 (2(9)): 302. doi:10.1371/journal.pbio.0020302. PMC 516796. PMID 15367939.
- [23] Von Neumann, J. and A. W. Burks (1966). *Theory of self-reproducing automata*. Urbana, University of Illinois Press.
- [24] Van Nies, *et al.* (2018). Self-replication of DNA by its encoded proteins in liposome-based synthetic cells. *Nature Communications*, 9, Article number: 1583.
- [25] Noireau, V. *et al.* (2004). A vesicle bioreactor as a step toward an artificial cell assembly. *PNAS*, 101 (51) 17669-17674; <https://doi.org/10.1073/pnas.0408236101>.
- [26] Oros, N. *et al.* (2007). Sexyloop: Self-Reproduction, Evolution and Sex in Cellular Automata. *The First IEEE Symposium on Artificial Life (Hawaii, USA)*. pp. 130–138.
- [27] Potrykus, M. *et al.* (2008). (p)ppGpp: still magical? *Annual Reviews Microbiology*, 62: 35-51.
- [28] Rasi, S.; Mavelli, F.; Luisi, P.L. (2003). Cooperative micelle binding and matrix effect in oleate vesicle formation. *J. Phys. Chem. B*, 107 (50), 14068-14076.
- [29] Rasi, S.; Mavelli, F.; Luisi, P.L. (2004). Matrix effect in oleate micelles-vesicles transformation. *Origins Life Evol. Biosph.*, 34 (1-2), 215-224.
- [30] Sayama, H. (1999). Toward the Realization of an Evolving Ecosystem on Cellular Automata. *Proceedings of the Fourth International Symposium on Artificial Life and Robotics (AROB 4th '99)*. Beppu, Oita, Japan. pp. 254–257.

- [31] Schrödinger, Erwin (1944). *What is Life?*. Cambridge University Press. ISBN 978-0-521-42708-1.
- [32] Shimizu, Y. *et al.* (2001). Cell-free translation reconstituted with purified components. *Nature Biotechnology* 19: 751–755.
- [33] Shimizu, Y., Kanamori, T., Ueda, T. (2005). Protein synthesis by pure translation systems. *Methods*, 36(3), 299-304.
- [34] Summerer, D. *et al.* (2006). A genetically encoded fluorescent amino acid. *PNAS*, 103 (26): 9785-9789.
- [35] Trifonov, Edward N. (2012). "Definition of Life: Navigation through Uncertainties". *Journal of Biomolecular Structure Dynamics*. 29 (4): 647–50. doi:10.1080/073911012010525017. ISSN 0739-1102. PMID 22208269. Archived from the original on 27 January 2012. Retrieved 12 January 2019.
- [36] Zhang, Y. –M. *et al.* (2008). Membrane lipid homeostasis in bacteria. *Nature Reviews Microbiology*, 6: 222–233.
- [37] Zhu, T.F. *et al.* (2009). Coupled Growth and Division of Model Protocell Membranes. *J. AM. CHEM. SOC.* 2009, 131, 5705–5713.

Part II

Review: Division in a Minimal Cell

Abstract

Division in cellular systems is an intricate and highly regulated task. *In vitro* division of liposomes has been demonstrated in a variety of ways. A minimal cell system requires a minimal amount of components to induce division events that allow for efficient and content-preserving multi-generational reproduction. In the present review, mechanisms deployed to induce division in liposomes are discussed in the context of membrane constituents as well as intracellular and extracellular environments. The factual compatibility of the techniques with liposome-based gene-expression remains subject of experimental investigation. Currently, electrical, osmotic and a minimal protein-based liposome division technique appear to hold especially high promises for the compatibility with a minimal cell.

Keywords: *Cell-free expression, In vitro transcription/translation, (Gene - Expressing) Liposomes, Division, Membrane (Electro)Deformation, Osmotic Membrane Deformation, Cholesterol Membrane Partitioning, Phase Transitions, FtsZ, Min system, Minimal Cell.*

1 Introduction

De novo engineering of living organisms has been a topic in focus for almost 60 years [Monod *et al.*, 1961]. Only 10 years after the discovery of the structure of DNA [Watson *et al.*, 1953], scientists started to give more and more importance to the biomolecular components that can be used towards the engineering of biology [Khalil *et al.*, 2010]. The reconstruction of life became a means to acquire broader understanding of how a minimal set of individual chemical and physical processes interact to underpin the complex interplay that we perceive as life. With the definition of life as an adapting autopoietic thermodynamically open system that maintains homeostasis and metabolism [Schrödinger, 1944; McKay *et al.*, 2004; Koshland *et al.*, 2002; Trifonov *et al.*, 2007], several pillars, such as growth [Ingolia *et al.*, 1978; Wilschut *et al.*, 1980; Ellens *et al.*, 1985; Bhattacharya *et al.*, 2019] and metabolism [Murtas *et al.*, 2007; Kuruma, Y. *et al.*, 2009; Scott *et al.*, 2016] need to be united in a single platform. One of the most well-known platforms for the reconstruction of life are phospholipid bilayer-enclosed liposomes, a highly abundant compartmentation technique in studied living systems [Szostak *et al.*, 2001]. The compartment specifically needs to allow for another essential pillar of life: **division**. In this review, we focus on the approaches that have been taken towards the establishment of division in liposomes and we will evaluate their compatibility with the reconstruction of many other pillars of life such as self-organisation, and the containment of information, as can be controlled by liposome-based gene-expression [Szostak *et al.*, 2001; Shimizu *et al.*, 2001]. In this context we specifically focus on Giant Unilamellar Liposomes (GUVs) in the lower size range ($1 - 20\mu\text{m}$) forming a platform for the reconstitution of life due to their size similarity to example given *Escherichia coli* bacteria.

2 Shaping Minimal Division

Reliable multi-generational reproduction of cellular information-containing compartments into subsequent generations, is at the essence of life and subject to current research [e.g. Sakuma *et al.*, 2011; Jimbo *et al.*, 2016; Urakami *et al.*, 2018]. Therein, questions can be raised on what division could, or should look like in a minimal cell.

In the construction of a minimal cell, systems originating from many different organisms may be combined to study their interplay, in the attempt to reach a minimalistic state. For the reconstitution of division, this implies a plethora of possible regulatory elements. From purely mechanical aspects associated with membrane constituents, to advanced encoded protein systems specifically constricting the cell at mid-plane.

The ubiquitous model organism *Escherichia coli* has had parts of its ingenious replication system mimicked [e.g. Martos *et al.*, 2012; Zieske *et al.*, 2013; Zieske *et al.*, 2014; Kretschmer *et al.*, 2014; Osawa *et al.*, 2008]. For a minimal system however, the exact reconstitution of the *E. coli* division machinery might

not be the preferred option as the division machinery consists of at least tens of proteins [Vicente *et al.*, 2006], which are in turn connected with the elongasome [Van der Ploeg *et al.*, 2013] that maintains the general elongated shape of the *E. coli* bacterium that consists of at least some ten more proteins [Bisson-Filho *et al.*, 2017; Hugonnet *et al.*, 2016]. In this light, attempts have been made at the construction of a minimal divisome [e.g. Nourian *et al.*, 2014; Ueda *et al.*, 2018].

Alternatively, more minimal bacteria as well as archaea have been studied in the light of a minimal cell reconstruction. An example is the focus on the Vps4/CdvA/ESCRT-III complex from the *Sulfolobus acidocaldarius* archaeon that has been demonstrated to support liposome deformation and to promote membrane interaction [Samson *et al.*, 2011; Härtel *et al.*, 2014]. Several *Mycoplasma* species in turn have their own system allowing for their reproduction [Miyata *et al.*, 1999]. *Mycoplasma* nevertheless, are also highly dependent on their environment for growth [Razin *et al.*, 1970], raising the philosophical debate on how dependent a living organism may be on its environment for executing and/or regulating its essential functions.

From an external influence point of view, external regulation such as temperature cycles and shear forces, as may have been important in the development of early life [Stüeken *et al.*, 2013; Hentrich *et al.*, 2014], may furthermore constitute a mechanism for division. In this light, liposome fission has been demonstrated achievable by amongst others thermal, mechanical, and osmotic means [e.g. Sakuma *et al.*, 2011; Deshpande *et al.*, 2018; Döbereiner *et al.*, 1993]. The compatibility of these external influences with liposomal content preservation, that is essential for homeostasis in a minimal cell, is variable. Content preservation facilitates multigenerational liposome-based gene-expression that is required for the reconstitution of some other pillars of life, such as metabolism and homeostasis. *The variation in compatibility of liposome division techniques with liposome-based gene-expression results in the necessity to analyse each technique for advantages and disadvantages.* The analysis should be based on a variety of criteria including division efficiency, controllability, reproducibility, lipid composition flexibility, compatibility with protein systems, compatibility with osmolarity, pH, temperature, viscosity and molecular crowding of gene-expressing systems.

The gene-expressing liposomes under consideration may contain a variety of membrane compounds. Throughout the bacterial kingdom membrane constituents vary, both regarding protein as well as lipid composition. While almost no bacteria contain compounds as cholesterol in their membrane, several *Mycoplasmas* have been described to contain the steroid that they can uptake from the environment [Razin *et al.*, 1970]. For the composition of the liposomes used as a prospective minimal cell, many different membrane compositions can be taken as a start and do not essentially have to mimic the environmental boundary of an existing organism. We may however learn from what is present in the environment and start from a lipid membrane composition such as found in the model organism *E. coli*.

In the following sections we will discuss the criteria for feasible liposome

division in gene-expressing systems. We will then elaborate upon the approaches taken to come to an overview and recommendation for future approaches in cell-free expressing liposome division for the construction of a minimal cell.

3 Morphology Associated Energy Considerations

Liposome shape deformation has amongst others been investigated through the development of models describing membrane energy [e.g. Helfrich *et al.*, 1973; Allain *et al.*, 2006]. In order to gain insight in the energy constraints necessary to achieve liposome deformation and division, we here analyse several models and experimental data to obtain a physical description of the constraints around liposome deformation and division. Herein, we relate membrane composition as well as internal and external conditions surrounding the liposomes, e.g. salt concentrations and protein systems, to preliminary division constraints.

3.1 Elongation as a Requirement for Intracellular-Content-Representative Division

Multiple mechanisms have been described to give rise to fission. Budding and birthing are well-described mechanisms that allow for some form of reproduction [Sakuma *et al.*, 2011]. Budding has been described as a consequence of domain formation due to changes in area-to-volume-ratios [Döbereiner *et al.*, 1993]. Pinching-off buds are often relatively small [Döbereiner *et al.*, 1993]. To achieve reproduction with a more reliable efficiency and to allow for daughter vesicles to both receive a representative amount of cytoplasmic content, a more spatially central division is required. A central form of division requires an increase in the membrane area-to-volume ratio. In correspondence with the Area Difference Elasticity (ADE) theory [Sakuma *et al.*, 2015], an increase of the area-to-volume ratio, through, most easily, a reduction in volume, imposes the stability of more elongated liposome shapes. Different liposome shapes are observed at all times in general samples as catalogued by Deuling *et al.* (1976), each representing different membrane energies as well as Gaussian curvatures, possibly related to inhomogeneous lipid distributions in the membrane.

Generally, to establish division, a controlled manner for liposomes elongation needs to be employed. We will further elaborate upon this in the course of this work (see experimental section). After the establishment of an elongated liposome shape with an increased area-to-volume ratio, a process of invagination needs to follow (see figure 3.1.1). The invagination is accompanied by a significant increase in the membrane free energy [Deserno, 2018] and therefore requires specific internally, or externally regulated forms of energy conveyance. The final step ensuring secure division without non-specific liposome rupturing is dependent on the formation of intermediate membrane structures.



Figure 3.1.1 Liposome fission is preceded by elongation, invagination and hemifission.

3.2 Membrane Dynamics and Fission

A generally accepted model for lipid bilayer membranes governing cells and liposomes has been proposed by Nicolson and Singer in 1972 [Singer *et al.*, 1972]. In their paper they describe the membrane as a two dimensional liquid that is restrictive to the lateral displacement of membrane components. With their fluid mosaic model that is compatible with thermodynamic considerations, they developed an early model for a mixed membrane structure containing lipids and proteins that are free to diffuse over the membrane. Within this system, phase separation of the membrane components in the fluid mosaic may occur due to e.g. temperature cycles [Sakuma *et al.*, 2011] for lipids mixtures possessing deviating melting temperatures [Shimshick *et al.*, 1973]. In liposome division, separation of membrane components into domains has been hypothesised to facilitate [Döbereiner *et al.*, 1993] division by inducing line tension [Lipowsky *et al.*, 1992], elucidating phase separation as one mechanism to confer local energy constraints initiating local fission.

During the addition of energy to the liposome environment - e.g. by applying temperature cycles or by changing the osmotic pressure - the observed liposome shapes may differ. Changing the shape of liposomes may constitute a first step in division as has been described by Sakuma *et al.* in 2011. In their work, a model for liposome division was deployed based on temperature cycling as they showed initial liposome deformation into pear-shaped objects. To better understand observed shape deformations in liposomes, Deuling *et al.* (1976) gave a physical description of liposome deformation. The description was based on an adapted version of the Helfrich energy function of the liposome membrane [Helfrich, 1973]. The equation is an extended version that includes osmotic pressure differences, induced line tension and the influence of an applied magnetic field (equation 1).

$$F = \frac{k_c}{2} \oint (2H - c_0)^2 dA + \bar{k}_c \oint K dA + \Delta P \oint dV + \lambda \oint dA - \frac{1}{2} \oint (\chi_n - \chi_t) * b * \cos^2 \psi * B^2 dx \quad (1)$$

Here, k_c is the bending modulus, H is the mean curvature at a point on the surface, c_0 is the spontaneous membrane curvature, P is the pressure difference over the liposome membrane, λ is the tensile strength on the surface, $\chi_n \cdot b$ and $\chi_t \cdot b$ are measures for the susceptibility to a magnetic field normal to the

surface area, where b is a measure for the thickness of the membrane, ψ is the angle made by a tangent to the point on the membrane with a line parallel to the symmetry axis x (see figure 3.2.1) and B is the magnetic field strength if applied.

The Helfrich free energy function as represented here does not take into account the membrane thickness, tilt, or entropic elasticity to account for multiple membrane components networks upon the incorporation of non-lipidic components. These factors can usually be seen as negligible however [Helfrich *et al.*, 1973].

The total energy function of the liposome as displayed in equation 1 tends to be minimised to an equilibrium state. Hence, the challenge in dividing liposomes is to supply enough energy to overcome the membrane tension barriers and to simultaneously provide a situation allowing the divided liposomes to obtain a steady state energy level of which the local minimum is constituted by the two daughter liposomes. To calculate this steady state, Euler-Lagrange equations can be used in a coordinate system defined by x and $\psi(x)$ as depicted in figure 3.2.1.

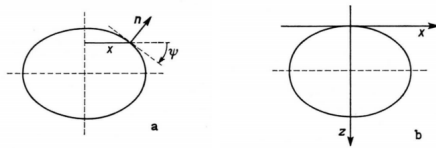


Figure 3.2.1 The coordinate system used to minimise the deformed membrane energy through the Euler-Lagrange method. Here x represents the distance from the polar axis and $\psi(x)$ is defined as the angle between the line normal to the polar axis and the contour [Helfrich, 1973].

The Euler-Lagrange equation that is to be solved in order to find the equilibrium shapes is then as represented in equation 2, the solutions of which yield a high amount of stable liposome topologies.

$$\frac{\partial f(x, \psi, \frac{d\psi}{dx})}{\partial \psi} - \frac{d}{dx} \frac{\partial f(x, \psi, \frac{d\psi}{dx})}{\partial \frac{d\psi}{dx}} = 0 \quad (2)$$

Deuling *et al.* (1976) used the Helfrich free energy function and the Newton-Raphson method for numerical optimisation to explain shape deformations in liposomes. The analysis concluded that the shape of fluid closed membranes is controlled exclusively by the curvature elasticity. Furthermore, in shapes with membrane closeness, of which some examples are depicted in figure 3.2.2, the opposite membranes do not significantly attract the other and thereby do not facilitate division from this point of reference. Hence, regardless of the amount of energy supplied to the environment, to achieve efficient and reproducible division there needs to be some form of directed constriction or induced line tension.

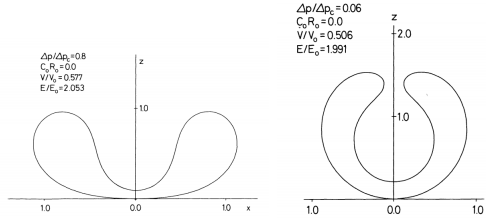


Figure 3.2.2 Liposome shape deformations as have amongst others been observed by Harbich *et al.* (1976) and Servuss *et al.* (1976) to which Deuling *et al.* fitted parameters giving a physical description of the systems. Left: deep cup-shaped vesicle, right: stomatocyte. [Deuling *et al.*, 1976].

The directed constriction may be applied either directly, e.g. through constricting proteins, or remotely, through actin polymerisation that generally initiates after bud formation in endocytosis, but reaches a maximum rate at the pinch off in mammalian endocytosis [Merrifield *et al.*, 2005]. Indirect constriction requires an order of magnitude higher constriction work rendering the mechanism of secondary importance in the context of this review, focusing mainly on a minimal division method [Bozic *et al.*, 2014].

The total process of invagination into the formation of two spheres attached through a narrow neck structure incurs an energy change of around $500 k_b T$, which could be achieved by proteins remodeling the membrane [Bassereau *et al.*, 2018; Jin and Baumgart, 2018; Kozlov *et al.*, 2018; Zeno and Stachowiak, 2018; Simon and Sykes, 2018; Voth, 2018], or through changes in environmental energy in combination with differing lipid behaviour in the membrane [Döbereiner *et al.*, 1993; Sakuma *et al.*, 2011]. When the membranes to be fused are brought significantly close in contact, intermediate membrane states may subsequently be formed that facilitate a fission event. These stalk structures [Markin *et al.*, 1984; Chernomordik *et al.*, 1985, 1987; Leikin *et al.*, 1987; Kozlov *et al.*, 1989; Siegel, 1993] are highly dependent on the membrane composition, on the neck radius and on intracellular and extracellular content [Siegel, 1999]. Recombining the leaflets of the separate membranes to render a different topological structure yields an initial decrease in overall membrane energy equal to $4\pi\kappa$, where κ is the Gaussian energy modulus ($\pm 250 k_b T$) [Deserno, 2018]. As a result, division is a favourable event after passage of the energy barrier.

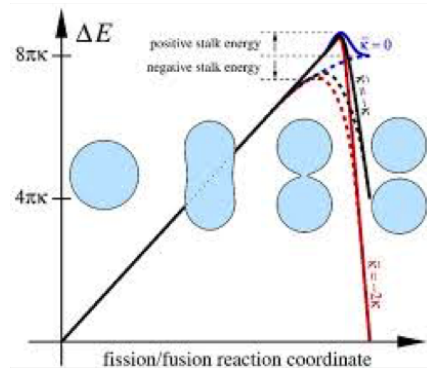


Figure 3.2.3 Simplified depiction of the energy barrier involved in vesicle fission and its dependence on stalk formation for division in liposomes. After an initial energy accumulation of $8\pi\kappa$ of bending energy, a topological change incurs upon the fission event. The exact maximum energy state is then determined by the membrane dependent transition state [Kozlovsky and Kozlov, 2002].

The exact energy barrier that is to overcome in the fission process is dependent on the bending modulus of the membrane. Phospholipid bilayers tend to have large bending moduli however that generally only allow for entropic stabilization within the context of significant negative Gaussian bending moduli that are largely determined by the membrane lipid composition [e.g. Siegel *et al.*, 2004]. For membranes with a flexibility given by a bending modulus around $10 k_b T$ such as in DOPC vesicles [Chen *et al.*, 1997], forces in the range of 0.1-1 pN are required for the invagination in vesicles around $10 \mu m$ in diameter, as modeled through the Helfrich-Canham Hamiltonian [Almendo-Vedia *et al.*, 2013]. As we describe later, FtsZ rings that constitute part of the *Escherichia coli* division mechanism may confer the forces for division. Alternatively, protein binding in itself may already confer enough membrane curvature to induce budding and fission [reviewed by Zimmerberg *et al.*, 2006]. An example of protein binding that is sufficient for fission induction, is the influenza virus A M2 protein that has been found to impose negative Gaussian membrane curvature as required for budding and subsequent fission [Schmidt *et al.*, 2013].

3.3 Intermediate Membrane Structures in Content-Preserving Division

The final state of invagination of the opposing membranes towards fission may result in rupturing of the neck followed by an act of resealing. The process of rupturing may be accompanied by leaking of the liposome content and is therefore most likely not compatible with the construction of a minimal cell. Alternatively, an intermediate structure may be formed that governs the highest membrane energy state, which is a state of hemifission [Deserno, 2018]. In hemifission, the two inner membrane leaflets fuse, while the outer leaflets remain in their initial continuous topological state. The energy of the hemifission

state is practically always higher than the energy associated with two separate closed membranes as obtained after the fission event, leading to mostly spontaneous division after crossing the energy barrier [Kozlovsky *et al.*, 2003]. Division through hemifission is thereby not accompanied by leakage, as the membrane maintains its relative impermeability throughout the process of fission.

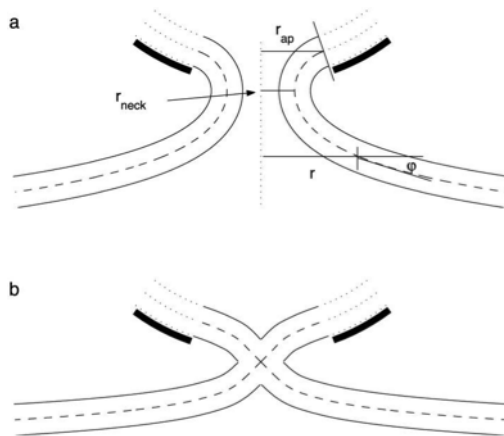


Figure 3.3.1. Schematic image of hemifission state in vesicles. Membrane invagination is (a) dependent on the neck radius and the membrane constituents. Dependent on the membrane constituents, membrane invagination may finally result in an intermediate state of hemifission (b) that generally allows for fission without intracellular content leakage [Kozlovsky *et al.*, 2003].

In addition to overall bending of the membrane [Hamm *et al.*, 2000] the hemifission state as described by Kozlovsky *et al.* (2003) requires the hydrocarbon chains of the membrane lipids to undergo tilt with respect to the membrane surface. The deformation is generated through structural packing of the hydrocarbon chains in the structural defect accompanied by the hemifission state, also known as the hydrophobic interstice [Siegel *et al.*, 1993]. In the model described by Kozlovsky *et al.* (2003), the free energy change that accompanies the transition towards the hemifission state is dependent on the neck radius and the bud size. The free energy associated with a constricted neck sharply increases for neck sizes below 5 nm , which is simultaneously the neck size for which the transition towards a hemifission state is accompanied with a change in free energy of around $50 k_bT$. This free energy is halfway a steep increase in free energy change that for somewhat larger buds ($> 50 \text{ nm}$) and larger neck radii ($\pm 20 \text{ nm}$) asymptotically approaches approximately $100 k_bT$. The transition towards the fission state in turn occurs spontaneously, it is slightly more favourable for larger buds and it is mainly dependent on the spontaneous membrane curvature. Highly negative spontaneous curvatures have not only been found to reduce the stalk transition bending energy [Kozlovsky, 2002], but also the topological bar-

rier [Deserno, 2018]. In fact, all transitions in the fission process are highly dependent on the spontaneous membrane curvature. Generally, the higher the spontaneous membrane curvature, the more favourable the hemifission and the final fission transitions are. Both of these transitions are in a lipid-intrinsic trade-off with the formation of a narrow neck that only becomes less favourable for high positive spontaneous curvatures and therefore might need either an externally invagination-inducing mechanism or a protein-induced invagination mechanism.

The intermediate states formed in membrane fusion are furthermore dependent on the saddle splay elastic modulus of the individual lipid monolayers constituting the membrane again showing the criticality of lipid compositions [Siegel *et al.*, 2004]. However, since the elastic modulus is generally significantly smaller than the bending rigidity [Ben-Shaul, 1995] it is often neglected.

The process of hemifission is one interpretation of the fission mechanism. The full fission event may occur through multiple structural transitions. The initial structure that has been described to form, the stalk [Markin *et al.*, 1984; Chernomordik *et al.*, 1985, 1987; Leikin *et al.*, 1987; Kozlov *et al.*, 1989; Siegel, 1993], is characterised by the fusion of the inner leaflets. Subsequently, the negative curvature of the still continuous outer membrane leaflets increases in the transmonolayer contact (TMC) state, after which the fusion pore establishes. If the latter transition only takes place relatively locally, an interlamellar attachment (ILA) structure [Siegel, 1986a,b] may arise that is accompanied by high negative curvature, and high stress topological pore formation in the liposome to undergo fission [Siegel, 1993]. As the free energy change furthermore decreases for larger ILA sizes ($< 5 \text{ nm}$), ILAs might increase in size to minimise the free energy along with local changes in lipid density and ILA shape [Siegel, 1999]. Multiple ILAs in proximity may then form an ILA lattice, which can rearrange to a QII phase [Siegel, 1986c; Siegel *et al.*, 1989c; Frederik *et al.*, 1991]. Cubic phases are relatively stable and can be a final intermediate for fission, as has been observed in e.g. fission induction through influenza virus A M2 proteins, depicted in figure 3.3.2 [Schmidt *et al.*, 2013].

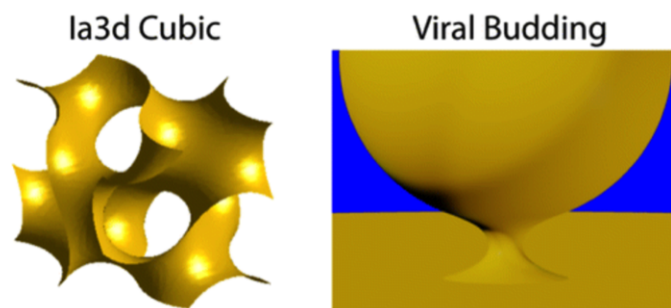


Figure 3.3.2 Depiction of the cubic phase intermediate membrane structure induced by influenza virus A M2 proteins and the subsequent budding event [Schmidt *et al.*, 2013].

An alternative membrane-rearranging pattern follows when rupturing of the outer membrane leaflets fails to occur. In this instance, the TMC structures build up to result in a hexagonal phase II (HII) state, that is less stable than the QII phase for a wide temperature range [Siegel, 1999]. For pure DOPE membranes relative instability of the QII phase with respect to the HII phase occurs at temperatures higher than 295 K [Siegel, 1999; Epanand, 1985]. DOPC addition increases membrane stability [Yang *et al.*, 2003]. The combination of DOPE and DOPC may in turn result in intracellular content-preserving fission due to composition-adjustable bilayer characteristics of the intermediate state. High molar fractions of e.g. DOPE may induce the system to lack a stably closed compartment for a reliable transfer of the intracellular content to the progeny as depicted in figure 3.3.3 [Jouhet, 2013].

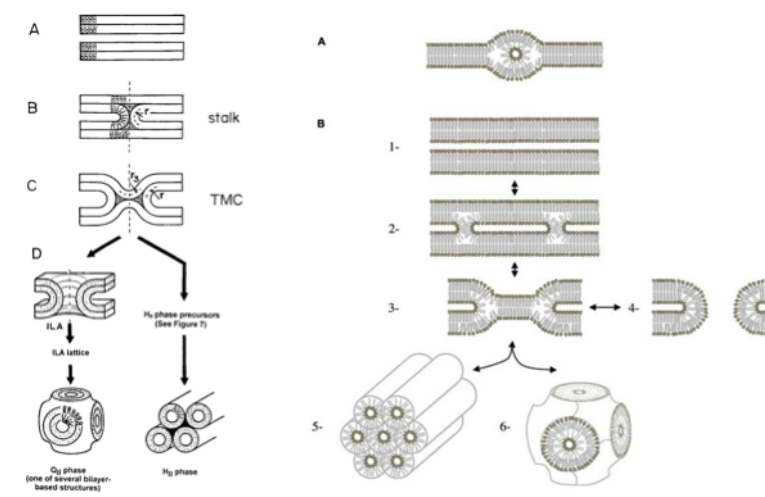


Figure 3.3.3 The intermediate stalk states in membrane fusion as an intermediate state in fission. Especially interesting in respect of fission are the cubic II and hexagonal II phases (depicted on the bottom) that have been described as advanced stages towards vesicle fission. [Siegel, 1999; Jouhet, 2013].

The preferred phase transition is dependent on both the temperature and on the lipid composition. While the cylindrical-shaped PC lipids favour the lamellar state in a membrane, addition of the inverse cone-shaped PE and PG lipids (see Appendix A) to the membrane destabilises the neck structure into either the hexagonal or cubic phase II state through their intrinsic curvature tendency [Jouhet, 2013]. Additional membrane constituents such as cholesterol may furthermore destabilise the lamellar phase into a more membrane fusion prone intermediate structure [Chen *et al.*, 1997].

Determining factors in the transitions in hemifission are not only the (Gaussian) curvature elastic energy, but also the bilayer rupture tension [Evans and Needham, 1986, 1987]. The rupture tension is the membrane composition-

dependent tension that needs to be applied to the bilayer to confer rupturing. Addition of PE to PC membranes has been found to increase this rupture tension [Evans and Needham, 1987], explaining the relative tendency of such PE-PC composite membranes to restructure in QII phases [Ellens *et al.*, 1989].

Molecular dynamics simulations and a free energy analysis have shown the coupling between lipid geometry and Gaussian rigidity to account for vesicle division [Urakami *et al.*, 2018].

The formation of favourable intermediate structures is essential for the compatibility of liposome-based gene-expression with the liposomes fission, as intermediate structures may prevent or induce content leakage. The larger the individual intermediate ILAs in the lattice, the less water content in the intermediate structure [Chen *et al.*, 1997], and the less content leakage occurs. Such optimised intermediate structures are largely influenced by the membrane composition as described.

In natural systems, the lamellar and the HII structure are not mutually exclusive and in fact often coexist [Jouhet, 2013], forming a scaffold essential for compartmentation as well as for the functionality of multiple enzymes such as an ATPase in mitochondria [Erand *et al.*, 1990; Li *et al.*, 1995; Latowski *et al.*, 2004]. Species as *E. coli* and *A. laidlawii* have even been found to actively adjust individual lipid properties through alteration of the polar head group or the acyl chains respectively [Lindblom *et al.*, 2002]. The homeostatic alteration of lipid membrane properties allows for local intrinsic curvature adjustments and has been hypothesised to be essential for the maintenance of spontaneous curvature in many biomembranes [Gruner, 1985].

For a minimal cell system such protein-induced alterations of the lipid membrane properties might be less relevant, but will be discussed in section 9. In the following sections we will encounter some intermediate structures formed along with the different division-inducing techniques to assess their inherent tendency towards intracellular content preservation.

3.4 Multigenerational Division and Membrane Growth Limitation

Apart from the membrane energy considerations, to allow for division, the membrane needs to be able to enclose the full volume of the two daughter cells, meaning that equation 3 and 4, relating the volume and membrane area changes respectively, need to be fulfilled.

$$\frac{4}{3}\pi R_0^3 - \text{volumeshrinkage} = \frac{4}{3}\pi R_1^3 + \frac{4}{3}\pi R_2^3 \quad (3)$$

$$4\pi R_0^2 + \text{membranegrowth} = 4\pi R_1^2 + 4\pi R_2^2 \quad (4)$$

The right membrane area to volume ratio can be achieved in several ways. Firstly, the osmotic pressure can be adjusted in order to create the right final volume for the daughter liposomes as can be predicted with the permeability model developed by Olbrich *et al.* in 2000. Secondly, the membrane could be

triggered to expand. The latter can be done either by lipid synthesis developed by liposome-based gene-expression [e.g. Scott *et al.*, 2016] or by the suppletion of lipids from the external environment, e.g. by fusion of the liposome with smaller liposomes from the external environment.

External fusion of micelles and small unilamellar vesicles (SUVs) with the vesicles under study is a promising technique to significantly increase the membrane area of the vesicles. The addition of fatty acid micelles has shown to allow for an incorporation rate up to 90% to induce vesicle growth [Berclaz *et al.*, 2001; Hanczyc *et al.*, 2003]. Although the high incorporation rates have mainly been achieved for fatty acid micelles [Berclaz *et al.*, 2001; Hanczyc *et al.*, 2003], the SUV induced growth is promising in this light. An alternative is liposome-based phospholipid synthesis that currently still suffers from a growth limitation to a few percent [e.g. Scott *et al.*, 2016].

With respect to liposome growth, Božič *et al.* (2004) described the relation between membrane properties and vesicle self-reproduction. They show that the budding shape that is necessary to achieve division requires the condition $T_d L_p \kappa C_0^4 \geq 1.85$ to be fulfilled, setting constraints based on the membrane area doubling time of the liposomes T_d , the hydraulic permeability L_p , the bending modulus κ and the spontaneous curvature C_0 .

The limitation of the currently implemented vesicle growth mechanisms is limiting all division approaches in the same way, although on the short term osmotically induced division or a coupling with differential osmotic pressures might facilitate division by a reduction in intracellular volume compared to the membrane area.

3.5 Comparing Approaches towards Division

Many attempts to reconstitute division in liposomes suffer from inefficiency, uncontrollability and/or limited flexibility. Several methods from physicochemical to mechanical methods have been demonstrated to facilitate liposome division. However, these methods may either lack in compatibility with gene-expressing systems (the PURE system [Shimizu *et al.*, 2001] example given). In order to have an overview of the most promising techniques, the following criteria have been chosen to compare on:

-Efficiency; How many liposomes in the sample are dividing after the induction and how frequent is the observed division?

-Controllability; How suitable is the technique to directly and reversibly alter membrane deformation for outward budding induction?

-Reproducibility; How often has liposome division been reconstituted with the particular technique?

-Lipid composition flexibility; How compatible is the technique with membranes of different lipid compositions?

-Compatibility with protein systems; How compatible is the technique with the incorporation of protein systems? Could the technique cause any form of interference with recruitment?

-Compatibility with osmolarity, pH, temperature, viscosity and molecular crowding of gene expressing systems; How compatible is the technique with PURE system?

-Functionality with multi generational divisions; Can the technique divide a liposome only once, or will the daughter liposomes possess the same division characteristics? How well does the technique preserve homeostasis and contain the intracellular content? How suitable is the technique to reproduce liposomes of sizes capable of containing a representative part of the cytoplasmic content?

The criteria are compared for each technique holding potential to reconstitute division in gene-expressing liposomes.

4 Thermal Division

Thermal cycles have been applied to liposomes to induce thermal deformation and division. In the process of thermal division, lipids are carefully chosen to possess melting temperatures (T_m) around which thermal cycles can be positioned to induce phase transitions from gel ($T < T_m$) to liquid crystalline ($T > T_m$) phase that are generally accompanied with membrane expansion as is necessary for division. Additionally, the shape of the lipids has to be carefully chosen to contain both cylinder and inverse cone shaped lipids [Sakuma *et al.*, 2011]. The method therefore can be seen as highly inflexible in terms of lipid membrane constituents.

For long it has been known that phospholipid membranes change their structure under thermal fluctuations, changing from the liquid-ordered ($L\beta'$) to the liquid-disordered ($L\alpha$) state upon an increase in the ambient temperature across the phase transition temperature [Chapman *et al.*, 1975]. In the transition, the bilayer expands upon transiting the lipid-characteristic transition temperature, decreasing its electrostatic free energy [Chapman *et al.*, 1975]. The transition temperature does not only depend on the type of lipid [Chapman *et al.*, 1975; Rowe *et al.*, 1983], but also on the ions present in the intra and extracellular solution. Divalent cations such as Ca^{2+} and Mg^{2+} have been found to increase the transition temperature through their charge neutralising effect [Träuble *et al.*, 1974]. Monovalent cations such as Na^+ , K^+ and Li^+ however, have been found to lower the transition temperature [Träuble *et al.*, 1974]. For the compatibility of the technique with the PURE system that contains a unique ion composition, it may therefore be recommendable to determine the transition temperature.

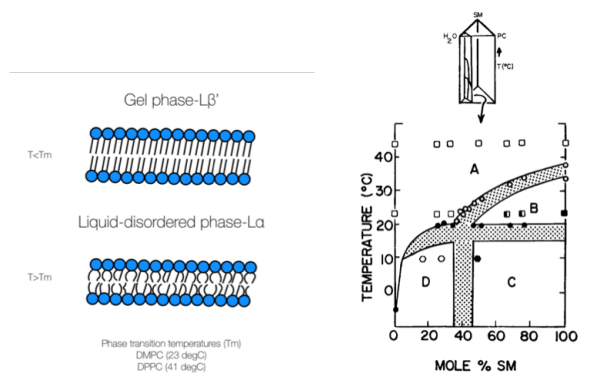


Figure 4.1 **Left:** Lipid phase transition effect on membrane properties. Above the melting temperature of the membrane lipids a transition is made from the compact liquid-ordered gel phase to the more expanded liquid-disordered phase. **Right:** Effect of molar percentage of sphingomyelin (SM) in a (Lecithin) PC membrane on the phase transition temperature in excess water. The striped areas correspond to the broad order-disorder transition range that

arises from the composite membrane. The (filled and open) round symbols here depict the Differential Scanning Calorimetry (DSC) peak temperatures for low and high temperatures respectively. The square symbols depict X-ray observations for a composite lamellar liquid crystal (open) and a composite lamellar liquid crystal mixed with SM/water gel phase (half open). The hexagonal symbols in turn represent a liquid crystal with intermediate phase (open), and a mixed gel with intermediate phase [Untracht *et al.*, 1977].

From the thermal energy considerations, in 2011, Sakuma *et al.* created a model for self-reproducing vesicles containing DLPE. Due to DLPE's induction of negative membrane curvature, as an inverse-cone shaped lipid, it is believed that DLPE can remodel the phospholipid bilayer membrane enhancing liposome tendency towards division. In this way Sakuma *et al.* (2011) applied temperature cycles with which they were able to induce pear shaped deformation as well as some division events.

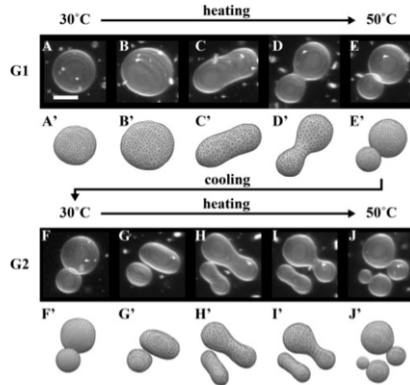


Figure 4.2 Temperature cycle induced deformation and division in DPPC/DLPE GUVs as observed by Jimbo *et al.* (2016). The scalebar in A represents $10\mu m$. The modeled shapes were obtained by a minimization of the bending energy for a constant volume and membrane area change. [Jimbo *et al.*, 2016].

Further research by Jimbo *et al.* (2016) focused on the exact role of DLPE in fission, elucidating the coupling between membrane curvature and PE lipid distribution as an explanation for the observed recurring fission behaviour.

For composite membranes, phase diagrams are significantly altered upon lipid-lipid interactions, generally resulting in a broader phase transition range (figure 4.1) for differing molar fractions of sphingomyelin in a lecithin PC membrane [Untracht *et al.*, 1977; Bagatolli *et al.*, 2009]. Practically all known living systems possess a multicomponent membrane separating their intracellular content from the environment, displaying intriguing physical and chemical characteristics that for example allow for budding upon temperature transitions induced phase separation [Li *et al.*, 2005].

The induced phase separation in composite membranes is dependent on the ambient temperature and on the characteristics of the membrane constituents. Differing carbon chain lengths and saturation, resulting in differences in attractive and repulsive forces within the membrane, often induce phase separation. Budding may occur through increasing dissipation compared to elastic forces on fluid-like domains in a gel phase membrane during temperature cycles around the phase transition temperature [Franke *et al.*, 2009]. It has been suggested that phase separation could be one of the driving factors in constricting the neck during budding [Lipowsky *et al.*, 1992]. In the model described by Sakuma *et al.* (2011) however, phase separation is believed not to be strictly necessary to break the relatively highly stable neck of a budding liposome.

In the process of thermal cycling, the heating and cooling rate necessary to induce the fission may be a limiting factor in many optical systems. Additionally, an increasing heat rate has just as an increased bulk viscosity been found to result in the formation of relatively smaller buds [Franke *et al.*, 2009], which might contain even less representative intracellular content although this has not posed a problem for Sakuma *et al.* (2011) and Jimbo *et al.* (2016).

To overcome the need for temperature cycling at high temperatures, Jurjen Wilschut *et al.* from the Danelon Lab at Delft University of Technology tested DMPC/DLPE liposomes for their fission induction properties in the presence of the PURE system [Shimizu *et al.*, 2001]. It was observed that the PURE system influences the deformation of DMPC/DLPE liposomes, and while elongation was achieved (see figure 4.3), fission was not observed in this system. A possible explanation for a lack of fission in DMPC/DLPE systems given by Wilschut (2018) is the hydrophobic mismatch between DMPC (14C) and DLPE (12C). The induced phase separation is consequently less strong than for DPPC (16C) and DLPE (12C), resulting in the absence of narrow neck formation as relatively less DLPE accumulates in the high curvature areas. Additionally, it was argued by Wilschut (2018) that the relative melting temperature of DLPE is different in the two systems. In the DMPC/DLPE system, DLPE ($T_m \approx 29^\circ\text{C}$) namely still adopts a solid phase upon crossing the melting temperature of DMPC ($T_m \approx 24^\circ\text{C}$). This might complicate curvature-induced membrane partitioning through decreased lateral diffusion rates [Wilschut *et al.*, 2018]. Additionally, the DMPC/DLPE liposomes were found to be of lower sample quality than DO liposomes and they were found not to be compatible with the binding of some membrane proteins as MinD, which is an essential protein in the establishment of *E. coli* division [Ferrer Castellà *et al.*, 2019].

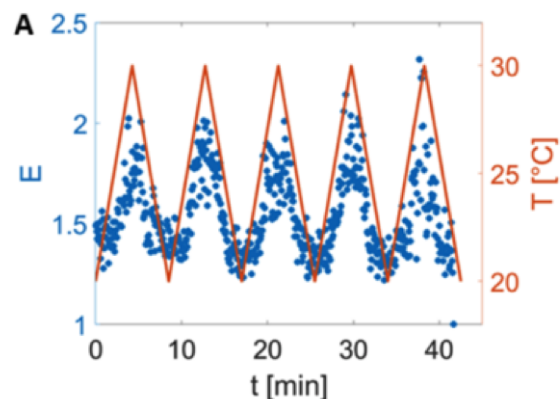


Figure 4.2 Elongation induced by temperature cycles around the lipid phase transition temperature as a function of time [Wilschut, 2018].

The efficiency of both composite lipid systems is limited. Even in the DP-PC/DLPE system described by Sakuma *et al.* (2011) with a sample population of 50 binary vesicles and an unspecified amount of fission events. The controllability of temperature mediated liposome division in turn is twofold. The study by Sakuma *et al.* (2011) showed highly controllable outward budding between 15-30% molar fractions of DLPE (in clear contrast to inward budding for molar DLPE fractions in the range 30-45%). Therefore, temperature mediated liposome division can be seen as a highly controllable division mechanism based on membrane constituting lipids. Nevertheless, only a small amount on the total observed liposomes in fact undergoes (a) fission event(s) each thermal cycle, and there is little possibility for predicting which ones will do.

In the same study by Sakuma *et al.* (2011), the daughter-mother liposome size ratio was found to be 0.4, which is considerably high compared to the often described buds pinching off membranes [e.g. Döbereiner *et al.*, 1993]. The described size ratio of 0.4 in itself provides for a possibly suitable platform for multigenerational reproduction, provided that the division technique is complemented with some form of growth [Ingolia *et al.*, 1978; Wilschut *et al.*, 1980; Ellens *et al.*, 1985; Bhattacharya *et al.*, 2019]. Nevertheless, the phase separation of the main lipid constituents that drives the fission is in principle exhaustible and does pose multigenerational limitation to the technique if the different lipids are not replenished over the generations where needed.

Thermal induced division has been achieved in multiple laboratories over the world [e.g. Li *et al.*, 2005; Sakuma *et al.*, 2011; Jimbo *et al.*, 2016]. Apart from possible technical difficulties, thermal division is a reproducible division technique. The technique knows limited flexibility when it comes to its application to membranes of different lipid compositions. Indeed, the membrane should be constituted by cylindrical and inverse cone shaped lipids, e.g. DPPC/DLPE.

However, if the fraction of the inverse cone shaped lipids becomes too high (50% for DPPC/DLPE), any form of reproduction is inhibited [Sakuma *et al.*, 2011].

For the compatibility of this thermal division technique with a prospective minimal cell, another restriction is the phase transition temperature of the cylindrical lipids used, as this temperature should preferably be compatible with enzyme activity (hence DO lipids, as found in *E. coli*, would not work with their transition temperatures below 0°C) and should not denature proteins. Hence, the DPPC/DLPE temperature cycles around the melting temperature of DPPC ($\sim 41^{\circ}\text{C}$), would not be compatible with a minimal cell. DMPC in turn is limited in the sample quality, has been observed not to be compatible with some membrane binding proteins such as MinD from *E. coli*. Furthermore, as described before [Wilschut *et al.*, 2018], it might not be possible to observe division in a system consisting of only DMPC/DLPE lipids with a thermal cycle around 24°C . This incompatibility might complicate further building up of a minimal cell and should be considered in the choice for fission inducing techniques.

Membrane permeability is also slightly increased during the phase transition cycle [Papahadjopoulos *et al.*, 1973]. This could allow for unwanted compounds to pass the membrane and interfere with gene-expression in the PURE system. However, the extend of the permeation is limited and the presence of equimolar amounts of cholesterol was found to remove this permeability change [Papahadjopoulos *et al.*, 1973].

When it comes to the initial step of elongation, temperature-mediated morphology changes are suitable, although the PURE system and possibly its viscosity has been described to influence the stages towards the fission process, to some extent inhibiting the elongation of the liposomes into a pear shape [Wilschut *et al.*, 2018].

5 Electrical Division

Electrical fields have been found to influence living cells as early as 1923 when Lund *et al.* found the orientation of the axis of symmetry of Fucus eggs to be influenced on the application of an electrical potential [Lund *et al.*, 1923]. The account of Lund *et al.* was the first that described control over cell polarity through electrical potentials in animal and plant cells. For bacteria, descriptions of their behaviour in electric fields would come a little later, an example being the account of electrolysis products inhibiting *E. coli* growth [Rosenberg *et al.*, 1965]. Since then, electric fields have been deployed to influence cells in various ways. Electric field strengths as low as 7 mV/mm have been observed to affect the directionality of embryonic cell growth of *Xenopus* [Hinkle *et al.*, 1981]. Similarly, physiological field strengths have been found to induce migration and reorientation of embryonic quail fibroblasts [Nuccitelli *et al.*, 1983; Erickson *et al.*, 1984].

In the construction of a minimal cell, the influence of electric fields on phospholipid membranes is of high interest. Electric fields could be a tool for cell shape deformation [Korlach *et al.*, 2005; Aranda *et al.*, 2008], as phospholipid membranes have the tendency to adopt different shape conformations upon different electric fields [Aranda *et al.*, 2008] in correspondence with the optimisation of the Helfrich energy function (equation 1). Possibly some shape deformations may result in division, although the latter has not been described in literature. The opposite effect, electrofusion, is relatively well-explored, for plant tissue cultures [Watts *et al.*, 1984; Zachrisson *et al.*, 1984; Gaff *et al.*, 1985] as well as amongst others mammalian cells [Blangero *et al.*, 1983 and 1984], and liposomes [Buschl *et al.*, 1982; Stoicheva *et al.*, 1994].

The observation of electrofusion under the application of electric fields may make electrodivision a questionable counter event, as division requires stimulation towards membrane aggregation and the formation of intermediate membrane structures [Markin *et al.*, 1984; Chernomordik *et al.*, 1985, 1987; Leikin *et al.*, 1987; Kozlov *et al.*, 1989; Siegel, 1993], while the prolate and oblate shapes are relatively stable structures [Stoicheva *et al.*, 1994; Aranda *et al.*, 2008]. The details of the applied electric field are determining for the behaviour, where low AC fields ($\pm 0.1\text{ kV/cm}$) are associated with dielectrophoretic movement, electrodeformation and electrorotation [Stoicheva *et al.*, 1994; Aranda *et al.*, 2008; Schwan *et al.*, 1969; Zimmermann *et al.*, 1982; Chan *et al.*, 1997; Voldman *et al.*, 2006], whilst high DC pulses are directly related to electroporation and electrofusion [Zimmermann *et al.*, 1982; Stoicheva *et al.*, 1994; Liu *et al.*, 2016]. In order to induce liposome fusion, block pulses of 1.7 kV/cm lasting several tens of microseconds have been used [Stoicheva *et al.*, 1994]. Similarly, accounts have been made of liposomes undergoing shape transitions upon the application of fields as low as 0.1 kV/cm minimising the total free energy [Aranda *et al.*, 2008; Vlahovska *et al.*, 2009]. In the transition, liposome shape is largely determined by the field frequency as well as by the conductivity ratio between the internal and external liposome solution, as depicted in figure 5.1 [Aranda *et al.*, 2008; Peterlin *et al.*, 2007]. In case of the PURE system used in a natural

swelling process, the conductivity ratio as depicted in figure 5.1 (A), may only be altered by adding e.g. sucrose to the external environment, yielding oblate shapes. Alternatively, using frequencies in the low range of the spectrum (i.e. $10^2 - 10^3$ Hz) prolate shapes may be achieved.

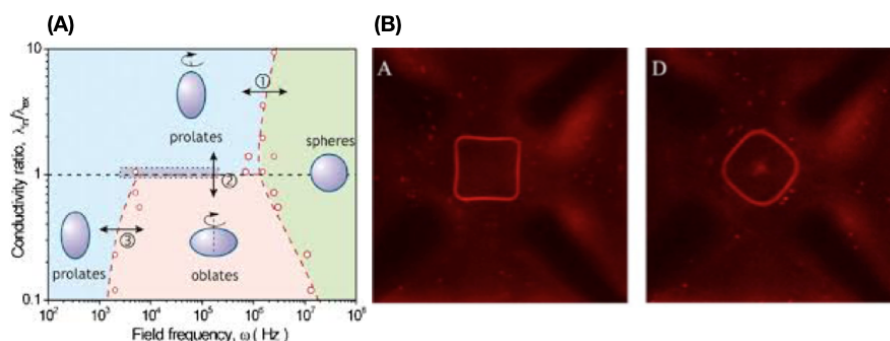


Figure 5.1. (A) The relationship between liposome shape transitions, frequency and the conductivity ratio between the internal and external liposome solutions [Aranda *et al.*, 2008]. (B) Liposome deformation upon capture in an electric octapole chamber [Korlach *et al.*, 2005].

In figure 5.1 (A) the shape transitions that liposomes undergo upon the application of a unidirectional AC electric field are described. Similarly, DC pulses of similar strengths around $0.1-0.2$ kV/cm have been shown to induce prolate shape transitions in DOPC vesicles upon 50 μ s application, given a higher external conductivity compared to the internal conductivity [Salipante *et al.*, 2014]. In both cases, the elongation achieved into oblate and prolate spheroids is limited to an aspect ratio of 1.10 and 1.25 respectively [Dimova *et al.*, 2007; Salipante *et al.*, 2014]. With more complex engineered systems such as a capturing octapole chamber [Korlach *et al.*, 2005], liposomes have been more specifically remodeled into custom shapes, as is depicted in figure 5.1b.

Individually, the electric field-modified shape transition does not appear highly promising for the onset of a fission event, as prolate and oblate shapes are highly limited in aspect ratio and thereby in bringing the opposing membranes together for aggregation. The octapole chamber as described by Korlach *et al.* (2005) in turn might be more flexible for shape deformations, but is also much more complex and requires individual trapping of liposomes. Therefore, the octapole chamber lacks on upscalability and would be a questionable approach towards division in the construction of a minimal cell.

Electrofusion in itself, in fact is the same process as is necessary for fission, although in electrofusion pore formation should occur through membrane fusion of nascent cells, whilst in fission this fusion should occur with the opposing membranes of a single cell/liposome. What complicates the fission induction is the size of the fusion pore that should be spanning the 3D membrane contact to allow for full disconnection of the membranes. Alternatively, a connected cubic structure that involves much higher curvatures may be necessary [Siegel, 1986].

Of primary importance in electrofusion is the membrane aggregation that will finally allow for membrane fusion upon application of an electric field and is not necessarily induced by the application of an electric field itself.

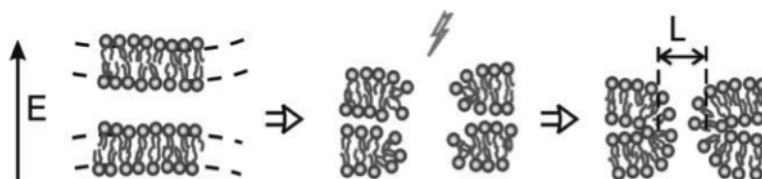


Figure 5.2 Membrane fusion occurs both in electrofusion as well as in a fission event, although in electrofusion the fusion pore connects the intracellular spaces of the cells/liposomes, whilst in a fission event the fusion pore connects external spaces through the intracellular space [Dimova *et al.*, 2007].

To allow for electrofission a different method may thus first be necessary to induce membrane aggregation, possibly through the application of differences in osmotic pressure as described in the experimental section of this work. The time scale on which the neck expansion occurs in electrofusion is in the order of tens of seconds, which is long compared to the approximate $100 \mu s$ of the electric pulse [Dimova *et al.*, 2007]. The neck expansion is therefore a separate process, independent of the electric field, and should not complicate fission by disaggregating the opposing membranes to undergo fusion. A pulsed electric field perpendicular to the aggregated membranes might then result in bilayer destabilization and a merging phase is required to establish the membrane fusion in fission as well, as described for electrofusion [Zimmermann *et al.*, 1982; Stoicheva *et al.*, 1994; Liu *et al.*, 2016]. The membrane fusion as required for the fission event represents a local minimum in the total free energy of the system as modeled with molecular dynamics simulations, depicted in figure 5.2 [Kawamoto *et al.*, 2014]. The transition is in need of external energy supply in division as could be conveyed through the electric field. The membrane tension needed to overcome the membrane fusion transition is near the rupture of $5-10 \text{ dyn/cm}$ [Needham *et al.*, 1989; Olbrich *et al.*, 2000]. AC fields generally convey tensions weaker than 0.1 dyn/cm , just enough for altering membrane undulations [Dimova *et al.*, 2007]. Therefore, DC pulses of several kV/cm might be most likely to achieve the required tension.

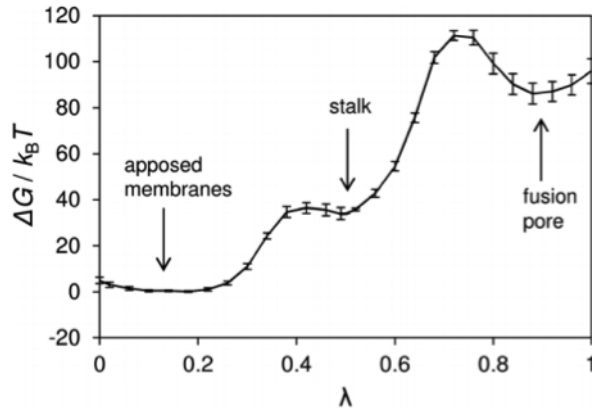


Figure 5.3 Quantification of the development of the total free energy of a membrane given the reaction coordinate λ based on molecular dynamics simulations. The figure shows that the fusion pore is a local minimum in the free energy spectrum. Compared to the apposed membranes and stalk structure, the fusion pore is significantly higher in free energy. The transition towards the fusion pore additionally involves an energy barrier between the stalk structure and the fusion pore formation [Kawamoto *et al.*, 2014].

These strong electric pulses do raise questions when it comes to accompanying membrane electroporation of the vesicles, which could render the method incompatible with containing compartmentalization, and therefore with homeostasis. Penetrating chloride anions as an example may already halt transcription. In the case of PE/PC liposomes electroporation has been found to occur significantly only for field strengths higher than 10 kV/cm [Liu *et al.*, 2016] as measured through 5(6)-carboxyfluorescein. This field strength is significantly higher than the $2\text{-}5 \text{ kV/cm}$ that would suffice for the establishment of membrane fusion [Dimova *et al.*, 2007]. Nevertheless, other values have been reported on in different systems. Field strengths of 0.6 kV/cm have been found to result in significant permeabilisation in Chinese Hamster Ovary (CHO) cells to propidium iodide [Teissie *et al.*, 1999]. Even electric field strengths as low as 0.02 kV/cm have been found to enhance plasmid transfection in *E. coli* [Xie *et al.*, 1990]. In the light of this research, ion permeability in field strengths required to induce fission events would be relatively high, although the membrane permeability only lasts for a few seconds [Kinosita *et al.*, 1988] generally resulting in little toxicity to cells. Therefore, membrane electrofusion is predicted to largely maintain its compatibility with gene-expression and homeostasis in liposomes.

The lipid composition strongly affects the electrofusion properties of the liposomes. For charged liquid droplets, fission events have been described when subject to the Rayleigh Limit, which dictates the maximum charge a liquid droplet can carry [Rayleigh, 1882; Taffin *et al.*, 1989; Gomez *et al.*, 1994]. An analysis of the Rayleigh criterion in the Debye-Huckel approximation for charged vesicles in the presence of counter ions reveals strong inward forces at

the vesicle equator due to an electric field in the presence of osmotic pressure, counteracting the outward surface tension forces [Thaokar *et al.*, 2010]. In this way, electro-osmotical destabilisation that might lead to fission has been described to occur in charged GUVs in a size range of 10-100 μm (vesicle charge limit: $Q = 8\pi\sqrt{(\gamma\epsilon_0r^3)}$) [Thaokar *et al.*, 2010]. Charged vesicles however have limited compatibility with living systems, since the negatively DNA should not be attached or strongly repulsed from the lipid compartment, which would complicate amongst others transcription.

There are indications that both DC as well as AC fields can induce fission events in largely neutral liposomes as well. POPC/POPG/Cholesterol GUVs in HEPES-KOH buffer with glucose have been found to undergo fission as a result of electric fields Sunami *et al.* (2018). In their study they quantified the amount of liposomes in the solution as well as the cytoplasmic fluorescent marker distribution. They found high vesicle destruction rates (quantified in figure 5.4) that increase for increasing numbers of DC pulses as well as for higher DC voltages, for longer initial AC application times and for increasing amounts of the negatively charged POPG in the membrane. At the same time, they found higher number DC pulses, as well as longer initial AC field application times and higher membrane POPG content to correlate with higher numbers of presumed fission events. Cholesterol in these POPC/POPG/Cholesterol membranes in turn appears to stabilise against fission events. Hence, both AC as well as DC fields might induce fission although both are accompanied with vesicle destruction, a lack of control over the resulting daughter liposome size, and possible leakage. Further analyses by Sunami *et al.* (2018), indicate that the application of a 0.45 kV/cm AC field for 15 s allows for the largest fission ratio of about 80%, with destruction ratios $< 10\%$ and about 30% leakage as quantified with TA647 red fluorescent protein. Almost no destruction and only 10% leakage were observed upon the application of a 0.15 kV/cm AC field for 45 s under the same conditions. These AC field conditions indicate that AC induced fission can be compatible with low leakage. However, the ion permeability and the extend to which this may complicate gene-expression in the PURE system remain a subject open to investigation.

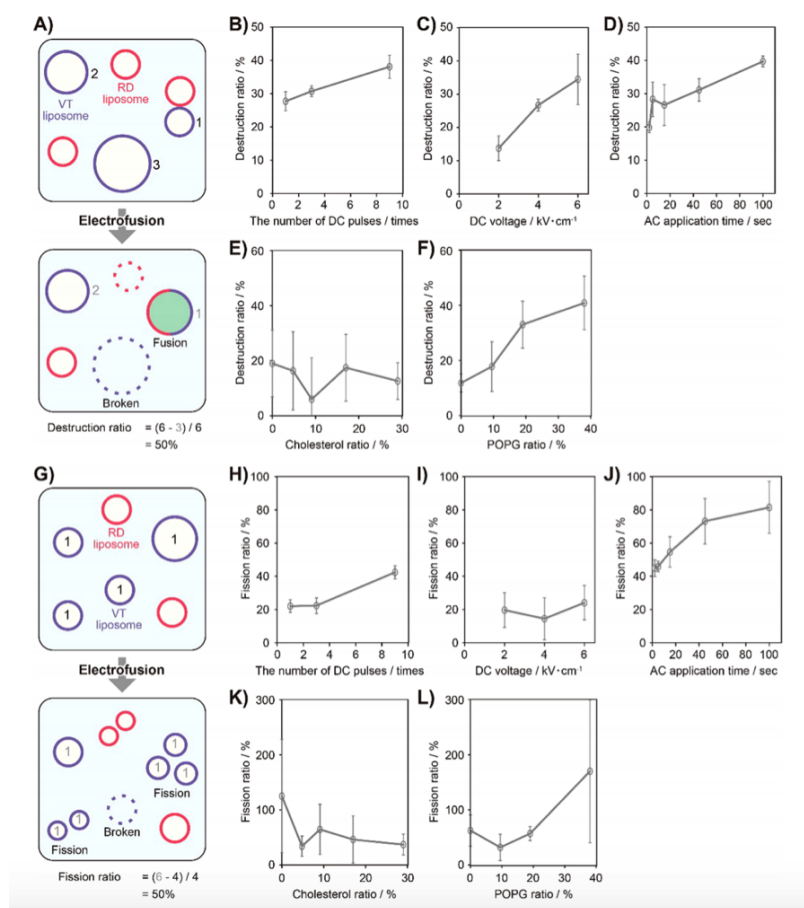


Figure 5.4 Destruction (A-F) and fission (G-L) ratios of POPC/POPG/Cholesterol vesicles quantified in terms of the number of applied DC pulses (B/H), the applied field strength (C/I), the initial AC application time used for alignment (D/J), the cholesterol ratio (E/K) and the POPG ratio (F/L) [Sunami *et al.*, 2018].

The integration of the use of electric fields to induce essential processes for life, such as division, is to be further discovered. It should therein be acknowledged that unforeseen complications might occur in several stages of the cell construction. It has for example been found that the application of electric fields may interfere with the implementation of growth processes, as observed for the bacterial species *S. Marcescens* and *E. coli* in fields as low as 0.94 kV/cm [Andersen *et al.*, 1965]. The same observation was made in the light of research on antibiotics in 2008 by Giladi *et al.* For pure lipid based growth, membrane electrofusion may facilitate multi generational growth, possibly through fusion with other vesicles [Ingolia *et al.*, 1978; Wilschut *et al.*, 1980; Ellens *et al.*, 1985].

Protein systems might be affected by the application of an electric field. In

a pulse field strength of 2 kV/cm, crystallization of hen egg-white lysozyme was observed in droplets [Taleb *et al.*, 1999]. In AC fields furthermore, the electric field conveys free energy to the output reaction, even for electrically neutral reactions [Dean Astumian *et al.*, 1989], thereby directly affecting a cell's metabolism. Also, the combination of AC fields with the Min system in *E. coli* division-site localisation is not promising due to presumed dislocalisation of MinD and MinE [Modchang *et al.*, 2004] and a supposed reduction in gradient effects for high Min protein concentrations [Modchang *et al.*, 2008] based on mathematical models.

All in all, electric fields may be used to convey energy for membrane fusion in a minimal cell. This method does however suffer from relatively low efficiency, controllability, and certain degrees of leakage. Also, in the incorporation of further cell functions such a growth and protein mediated compound exchange with the environment, electric fields may significantly influence the cell's behaviour. As long as researchers are aware of these properties, electric fields would be a valuable means towards the establishment of fission in prospective minimal cells that deserved further investigation. In this light, it should be noted however, that for the investigation of the fields described special high voltage generators are required to make the microscope chambers in which the liposomes are studied compatible with focusing on the sample.

6 Mechanical Division

Different mechanical approaches have been taken towards membrane deformation in GUVs that each rely on direct application of external mechanical force on the GUV-membrane. One technique may be the use of optical tweezers, possibly in combination with DNA origami. Alternatively, microfluidic splitting can result in controllable symmetric liposome splitting.

Optical tweezers have been used to measure forces required for the establishment of morphological transitions such as elongation in amongst others DOPC/-DOPG and DOPC/SM/Cholesterol vesicles indicating the need of forces of several piconewtons applied to the vesicle poles to establish elongation [Shitamichi *et al.*, 2009]. For the study of the behaviour of protein systems in different morphological states such as the elongated state, optical tweezers may thus facilitate this morphological transition. Division may in turn be established through controlled constriction using a DNA origami platform, although this has not been described feasible for actual division yet.

Optical tweezers do generally only focus on individual liposomes at a time however, and therefore lack upscalability towards the induction of morphological transitions in large amounts of GUVs. Up to several tens of optical tweezer traps have been described to be independently controllable in real time [Lafong *et al.*, 2006]. Another limiting factor is the necessity for liposome-incorporated silica beads necessary for the laser beams to focus on to induce the shape deformation, although any dielectric particle as small as 35 nm may be used for trapping [Neuman *et al.*, 2006].

For fission events, optical tweezers may be focused on dielectric beads attached to the membrane on either the internal or external side of the GUVs to induce membrane invagination and the onset of locally controlled division. To our knowledge this has not been described in literature. External DNA origami platforms could also be designed and controlled with magnetic tweezers to controllably transfer forces needed for the onset of division in GUVs. These methods would enable highly controllable and compatible division, although they lack on upscalability and on their multigenerational efficiency, as they are orientation dependent. Furthermore, they have not been well described in literature, leaving space for further research.

One deployed method for mechanical fission is extrusion, a process in which liposomes are forced through pores. Hanczyc *et al.* (2003) describe extrusion as a feasible method for content-preservative fission in fatty acid vesicles. Here, a decrease in average size from 100 nm to 88 nm is reported as evidence for the fission events. Consequently, any induced fission mostly results in relatively unequal and ruptured buds. Also, it needs to be remarked that the average vesicle size used is comparably small, which may influence the fission behaviour given the membrane component-determined bending energy. In the context of a content-preservative minimal cell, a more controllable method would be more favourable. In this light, a different approach towards mechanical fission induction has been developed on microfluidic chips. In 2003, a controlled microfluidic system was first used to induce fission in water-in-oil emulsion droplets for var-

ious flow rates and channel angles on PDMS chips [Tan *et al.*, 2003]. For GUVs a similar upscalable and controllable method for mechanical division has been developed on a microfluidic setup. Deshpande *et al.* (2018) showed a highly symmetric ($< 3\%$), low leakage ($< 10\%$) and reproducible mechanical division method for double-emulsion liposomes in 1-octanol. In this method double emulsion liposomes are formed in 1-octanol. Subsequently, a controlled hyperosmotic environment increases the area-to-volume ratio of the liposomes that allows for division, for which larger area-to-volume ratio's are critical. In the subsequent channel, the liposomes de-attach from the 1-octanol droplets before they encounter the splitter that ensures the formation of two daughter liposomes.

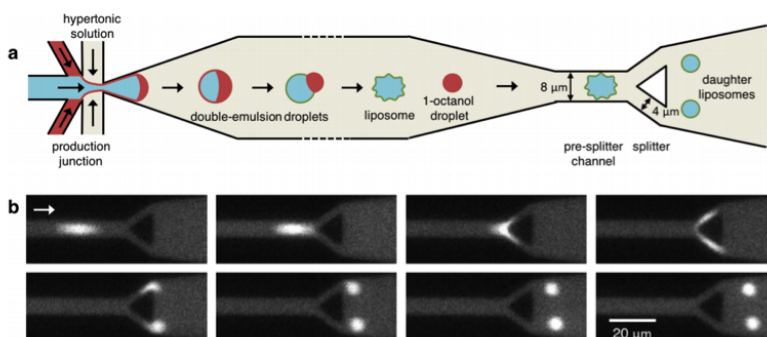


Figure 6.1 Mechanical liposome division (DOPC:Rh-PE = 99.9:0.1, molar ratio). (a) A schematic overview of the microfluidic setup for mechanical liposome division as designed by Deshpande *et al.* (2018). A double emulsion droplet is formed in 1-octanol, after which a hypertonic solution quickly increases the area-to-volume ratio to facilitate division at the splitter at the end of the microfluidic channel. (b) Visualisation of a liposome (encapsulated dye either Alexa Fluor 350 or Dextran-Alexa Fluor 647) that undergoes successful division at the splitter with little increase in background intensity indicating low leakage [Deshpande *et al.*, 2018].

The method described by Deshpande *et al.* (2018) also has its drawbacks. Some liposomes may burst upon encountering the splitter, others may evade the splitter by fully squeezing through one of the channels, also known as snaking events. Snaking events were observed to be especially prominent for the smallest liposomes (diameter = 4-6 μm), where 4 μm diameter mother liposomes almost always underwent snaking, and around 30% of the 6 μm diameter mother liposomes were observed to have the same destiny. For bursting an opposite size relation was discovered, where liposomes larger than 6 μm diameter would burst in more than half of the cases. The highest division frequency ($\pm 40\%$) was observed in mother liposomes of 6 μm diameter.

Furthermore, the liposomes are formed through octanol-assisted liposome assembly (OLA) [Deshpande *et al.*, 2015] that complicates the method for use in a minimal cell. In 2007, Jahn *et al.* gave the first description of liposome

formation in microfluidic devices. Jahn *et al.* used isopropyl alcohol (IPA) as a lipid-carrying organic (LO) phase for the formation of dimyristoylphosphatidylcholine (DMPC), cholesterol, dihexadecyl phosphate (DCP) liposomes. In general, the more hydrophobic the solvent, the better the liposome formation. The biocompatibility decreases however as the LO phase becomes more hydrophobic, since hydrophobic solvents denature proteins. Deshpande *et al.* (2015) argue that 1-octanol is a relatively well biocompatible organic solvent, since 10 volume% of 1-octanol had been shown to only result in a 2.5% loss of epoxide hydrolase enzymatic activity in yeast cells [Lotter *et al.*, 2004]. Based on the account by Lotter *et al.* (2004), the 0.05 volume% of 1-octanol in water, as a result of its natural water solubility, is not expected to be problematic. Deshpande *et al.* (2015) therefore tested OLA's compatibility with alpha-haemolysin and incorporated bacterial divisome proteins FtsZ and solubilised ZipA lacking the N-terminal domain, and possessing a His-tag instead to convey membrane recruitment to DGS-NTA(Ni). As depicted in figure 6.2 this indeed resulted in recruitment and bundle formation on the membrane, pointing at the relative compatibility of OLA with the FtsZ and sZipA proteins. Similarly, alpha-haemolysin was shown to be compatible with the OLA method for liposome production. It should be noted that many other proteins may not show similar compatibility and should be further investigated.

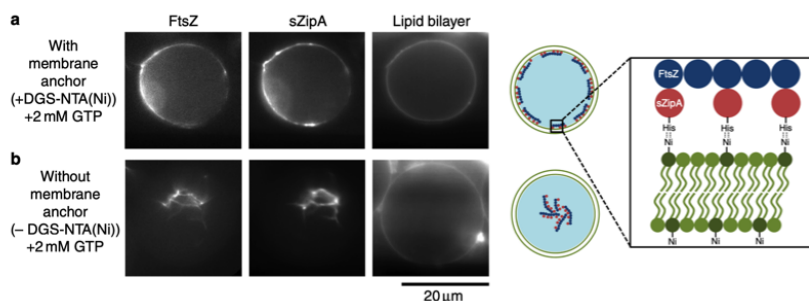


Figure 6.2 Compatibility of 1-octanol assisted liposome assembly (OLA) with the bacterial divisome proteins FtsZ and sZipA incorporated in the buffer phase inside the liposomes (DOPC, DOPG, DGS-NTA(Ni) and Liss Rhod PE (1,2-dioleoyl-sn-glycero-3-phosphoethanolamine-N-(lissamine rhodamine B sulfonyl) (ammonium salt))) [Deshpande *et al.*, 2015].

Mechanical division consists of a relatively broad set of tools. One of the most significant mechanical approaches is microfluidic division that demonstrates relatively reproducible and controllable. The protein compatibility and thereby the compatibility with the PURE system may be questionable in this microfluidic approach however, as can be said for its multigenerational reproducibility, since the microfluidic chamber needs to be adapted in size to the vesicles in subsequent generational splitting. Therefore, in the context of a minimal cell, this approach is promising, but certainly not without significant limitations.

7 Osmolarity Induced Division

Osmotic phenomena have been described as important in all the previously mentioned division inducing techniques. Osmosis may contribute to membrane fusion in at least four ways along the process. Firstly, osmotic pressures may induce membrane aggregation, bringing opposite membranes close together. Subsequently, a possible prerequisite for contact between the membranes is the dehydration of the lipid polar head groups [Parsegian *et al.*, 1989; Parsegian *et al.*, 1991]. Osmotic forces may induce the hemifused state, after which they may help remove intermediate membranous structures. Lastly, osmotic forces have been described to be at the core of the expansion of the fusion pore at the completion of the membrane fusion [O’Day, 1993].

The dependence on the type of osmotic agents has been reported to be critical in the establishment of liposome deformation and subsequent membrane fusion. Monovalent anions and cations, divalent cations, sugars and other compounds may all alter the osmotic pressure in and outside the liposomes under study. By largely decreasing the liposome volume, the addition of high osmolar concentrations to the external environment of the liposomes makes the membranes show apparent larger flexibility giving rise to initial membrane aggregation. Through micropipette manipulation, Vitkova *et al.* (2006) showed that the membrane elastic bending modulus of SOPC mono and bilayers is indeed decreased in the presence of sucrose concentrations near physiological level. Small angle neutron scattering (SANS) and thermodynamic analyses have furthermore been used to elucidate the membrane thinning effect of sucrose concentrations below 200 mM on (DODM)PC bilayers [Andersen *et al.*, 2011]. At low concentrations sugars appear to bind strongly to the membranes, resulting in the membrane thinning along with lateral expansion of the membrane that could allow for fusion of opposing membranes. This membrane thinning effect was observed to be about twice as strong for disaccharides such as sucrose compared to monosaccharides such as glucose [Andersen *et al.*, 2011]. Small angle X-ray and neutron scattering furthermore revealed that sucrose buffers decrease the average vesicle size [Kiselev *et al.*, 2001], allowing for speculation on fission induction based on pure osmotic forces.

According to a more recent study performed by Vitkova *et al.* (2018), the addition of sugars may also invoke a decrease in membrane rigidity along with an increase in the capacitance of the liposomes, which possibly increases the response of vesicles in an electric field as well. Similarly, lower pH has been found to increase the flexibility of membranes and a 20% decrease in bending elasticity modulus was found to result from a ten-fold increase in sodium chloride concentrations [Vitkova *et al.*, 2012], that may however show limited compatibility with liposome-based gene expression in the PURE system. In contrast, trace elements, such as iron, have been found to increase membrane rigidity [Garcia *et al.*, 2005], complicating division.

As Döbereiner *et al.* (1993) rightfully indicate in their paper, the performed calculations in many energy models consider fully fluid membranes rather than membranes containing solid patches as sometimes observed [Döbereiner *et al.*,

1993]. A finite shear elasticity would have to account for the solid patches, although the incorporation of a shear elasticity term will most likely not result in a qualitative behavioural change of the budding mechanism they describe. The formation of domains on the membrane along with bending energy might even be necessary to reconstitute fission in vesicles according to Döbereiner *et al.*. Energetically unfavourable line tension may occur at the domain boundaries facilitating the division as was proposed by Lipowsky *et al.* in 1992. Döbereiner *et al.* (1993) could reconstitute this same energetically directive fission in DMPC:Sphingomyelin(SPM):Cholesterol liposomes upon osmotic changes only. Due to coupling of the flip-flop rate to an osmotically induced water flow over the membrane, cholesterol redistributes over the membrane leaflets leading to domain formation and possibly line tension [Boroske *et al.*, 1981]. The dependency on osmotic changes in DMPC:SPM:Cholesterol liposomes therefore can be seen as a substantiation of the hypothesis that separation of liquid-ordered and liquid-disordered patches suffices to facilitate fission.

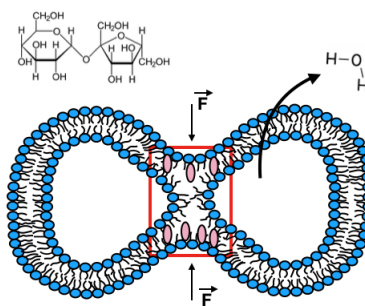


Figure 7.1 Schematic depiction of how cholesterol (pink) may redistribute over the membrane in invaginated liposomes, resulting in line tension that may facilitate fission as described by Lipowsky *et al.* in 1992.

Melatonin and progesteron can in turn also induce liquid disordered patches when present in low molar fractions in the membrane [Drolle *et al.*, 2013; Korkmaz *et al.*, 2005], which might account for some of their physiological functions, although their use in the context of a minimal cell will be limited, both being mammalian hormones. The same reasoning applies to cholesterol that requires a 37-step synthesis pathway mostly present in mammals [Russell *et al.*, 1992]. However, cholesterol synthesis has been found to be present in certain bacterial species [Hayami *et al.*, 1979] and several bacteria of the species *Mycoplasma* show a high dependency on cholesterol supplied by the external environment for their growth [Razin *et al.*, 1970].

The osmotic pressure approach has mainly been employed with DM lipids that tend to suffer from relatively lower liposome qualities compared to DO liposomes. Additionally, their compatibility with *E. coli* protein systems as the Min system and FtsZ are questionable. Therefore, it remains to be elucidated

to what extent the osmotic approach shows compatibility with DO liposomes.

Some other questions that remain regarding this osmolarity-based fission technique include the following. Is cholesterol essential for the onset of fission, or may the osmotic pressure difference suffice in itself? Although cholesterol is a frequently used compound to induce phase separation, the hypothesized basis for fission, i.e. phase separation along with osmotic pressures [Döbereiner *et al.*, 1993], may most likely be fulfilled with other lipidic compounds inducing phase separation as well. That raises the question: how critical is the role of sphingomyelin (see Appendix A), another compound frequently used in fission studies, for the onset of fission in GUVs? In 1995, Corver *et al.* observed that 1-2 mol% sphingolipids was required for the fusion of Semliki Forest virus with cholesterol containing liposomes [Corver *et al.*, 1995], suggesting an important role for sphingolipids in the membrane fusion process.

How compatible is the use of cholesterol with *E. coli* protein systems, especially membrane proteins such as FtsA and ZipA? Divisome proteins may not be necessary for division in a minimal cell however, if the osmotic division is feasible enough for division induction on itself. Other questions concern the efficiency of the method and whether the method may also result in fission around midplane instead of resulting in the pinch-off of submicrometer size buds only as described by Döbereiner *et al.* (1993).

Since osmosis appears to serve the most significant role in all of the described techniques, further investigation towards its compatibility with a minimal cell system in the light of the aforementioned questions is promising. We therefore elaborate on the questions mentioned in the experimental section of this work.

8 Lipid/Sterol Membrane Components and Division

Apart from the externally influencing techniques, intrinsic membrane characteristics are critical in determining vesicle morphology and possibly in facilitating division. Lipid shapes, i.e. cylindrical, cone or inverse-cone shapes, as well as their relative chain lengths, are critical in determining their collective behaviour. Composite membranes in this respect show fascinating behaviour both in terms of phase separation and in terms of possibly resulting tension generation. On the one hand, tail saturation and tail length can drive preferential inter leaflet interactions underlying phase separation facilitating the build up of line tension [Lipowsky *et al.*, 1992; Sanchez-Migallon *et al.*, 1995]. On the other hand, lipid shapes can facilitate local changes in membrane curvature that may facilitate division, as described for the inverse cone shaped DLPE [Sakama *et al.*, 2011]. Many PE lipids furthermore have a dehydrating effect due to a comparably small head group, which might be more important than their tendency to stabilise the HII phase in promoting membrane fusion [Ellens *et al.*, 1986a; Kinnunen *et al.*, 2000].

In the final stages of division, the vesicle lipid composition is determining as well for the formation of intermediate structures, which in natural membranes is dictated by the complex interplay between peptides, membrane lipids, and possibly sterols. From a lipid intrinsic perspective, negatively charged lipids such as cardiolipin, phosphatidylserine (PS), phosphatidic acid (PA) and phosphatidylglycerol (PG) (see Appendix A for their structures) have been found to directly induce fission upon contact with divalent cations such as Ca^{2+} or Mg^{2+} [Kinnunen *et al.*, 2000; Sunami *et al.*, 2018]. The latter is an important component of the PURE system that may be used for the reconstitution of gene-expression in liposomes. It has furthermore been raised that these divalent cations may induce the formation of the HII phase in cardiolipin containing membranes [Rand *et al.*, 1972]. Therefore, the PURE system in combination with relatively high DOPG/cardiolipin membrane content may facilitate membrane fusion, although leakage is not excluded.

Polyethylene glycol (PEG) in turn has been found to facilitate lipid mixing without membrane fusion in (DO/DP)PC GUVs [Burgess *et al.*, 1991]. Above 40 w% PEG, a dramatic increase in membrane fusion was observed through an increase in average vesicle size however. Based on these findings Burgess *et al.* (1991) hypothesised that the membranes only come in critical contact for larger dehydration of the lipid heads at the high PEG concentrations.

8.1 Cholesterol

As briefly described in the context of osmotic fission induction, cholesterol is a steroid that is rarely present in bacteria and requires a 37-step synthesis pathway [Russell *et al.*, 1992]. Several Mycoplasmas do possess the ability to take up cholesterol from the environment however, showing a cholesterol dependency

for growth [Razin *et al.*, 1970]. As a largely hydrophobic compound, cholesterol partitions within the inner and outer leaflets of the membrane, where it continuously redistributes between the leaflets through so-called flip-flopping that may happen within 73 ns [Choubey *et al.*, 2013]. The effect cholesterol has on the membrane properties is dependent on the membrane composition and the molar fraction of cholesterol. Cholesterol’s main partitioning in the hydrophobic leaflets is accompanied by its preference for high curvature areas [Wang *et al.*, 2008]. Therefore, cholesterol usually stabilises the formation of the HII phase. The La-HII transition is counteracted however in the presence of most PE lipids [Noordam *et al.*, 1980]. For molar percentages higher than 40 mol% cholesterol has furthermore been observed to preferentially stabilise the lamellar phase [Epanand *et al.*, 1987]. For PE/PC mixtures, cholesterol is believed to either induce the HII phase for non-saturated PC constituents, or the lamellar phase for saturated PC lipids in the membrane [Cullis *et al.*, 1978; Cullis *et al.*, 1979; Tilcock *et al.*, 1982]. Further research on PE/PC vesicles resulted in the hypothesis that rather than inducing the HII phase, cholesterol addition only destabilises the lamellar bilayer structure [Cheng *et al.*, 1986]. Hence, dependent on the membrane composition, cholesterol may induce completely different membrane properties that may either facilitate or counteract a fission process. Nevertheless, whether it is the induction of line tension due to phase separation [Lipowsky *et al.*, 1992; Baumgart *et al.*, 2003], or the increase in membrane rigidity that results in a morphological transition [Nomura *et al.*, 2005; experimental section] and decreased membrane permeability [Papahadjopoulos, D. *et al.*, 1971; Yeagle *et al.*, 1977; Demel *et al.*, 1972], cholesterol has diverse effects that may all contribute to the formation of a homeostatically stable minimal cell (see experimental section).

8.2 Sphingolipids

As indicated in section 7, sphingolipids such as sphingomyelin are often used in the context of membrane fusion facilitation [e.g. Döbereiner *et al.*, 1993]. Sphingolipids are mostly known in eukaryotes, especially in neurons. Sphingolipids tend to undergo interactions with cholesterol, giving rise to enhanced nano and microdomain formation [e.g. Barenholz *et al.*, 2004] that may facilitate fission. In bacteria only rare species such as *Flectobacillus major* [Batrakov *et al.*, 2000] contain a pathway to synthesise sphingolipids. Nevertheless, some bacterial species can uptake sphingolipids from the environment [Heung *et al.*, 2005], allowing sphingolipids to possibly form a part of a minimal cell.

8.3 Excess Membrane Synthesis

A slightly different method that may facilitate cell proliferation is the synthesis of excess cell membrane [Mercier *et al.*, 2012; Mercier *et al.*, 2013]. The cell-wall lacking bacterial L-forms have been shown to proliferate in a manner independent from cytoskeletal elements [Mercier *et al.*, 2012; Mercier *et al.*, 2013]. Mercier *et al.* (2012) showed branched-chain fatty acid (BCFA) synthesis

to be essential for membrane growth and deformation in *Bacillus subtilis* mutant L-forms [P. Domínguez-Cuevas *et al.*, 2012]. In the same system, Mercier *et al.* (2012) observed a halt in proliferation in branched-chain alpha-keto acid dehydrogenase (BKD) mutants that lack the bkd enzyme complex involved in the synthesis of BCFAs. Without BCFAs, especially membrane scission was observed to fail to occur after growth and deformation. Mercier *et al.* (2012) attribute the failing membrane scission to an increase in membrane rigidity, pointing at the crucial importance of membrane composition. In 2013, Mercier *et al.* found the proliferation to be especially induced by an AccDA fatty acid mutant overexpression, showing that membrane intrinsic parameters suffice to induce division. The membrane synthesis induced fission effect has only been shown as such in a top-down approach however, leaving a promising opportunity for the minimal cell. Membrane synthesis has been shown in the context of a minimal cell. Limitations are set however, by the synthesis and incorporation efficiency that currently only allow for a membrane area increase of a few percent [e.g. Scott *et al.*, 2016]. Alternatively, membrane area could be increased from an external perspective through including fusion of SUVs and/or micelles with the vesicles under study, which is a technique that has been demonstrated more efficient [Berclaz *et al.*, 2001; Hanczyc *et al.*, 2003]. The excess membrane synthesis method is especially interesting due to the membrane intrinsic forces that may enable fission.

9 Protein-based Fission

Proteins play a paramount role in almost all living systems. Hemagglutinin (HA) is only a single example of a (glyco)protein that may position in the membrane leaflets [Durrer *et al.*, 1996], whilst isolated peptides show fusogenic behaviour that has also been demonstrated in liposomes [reviewed by Martin and Ruyschaert 2000, Tamm and Han 2000]. Soluble N-ethylmaleimide-sensitive factor (NSF) Attachment Receptor (SNARE) proteins are another example of proteins that assist in membrane fusion, although mainly during endocytosis [Chen *et al.*, 2001; Jahn *et al.*, 2006]. Both are part of mostly locally membrane fusion systems in viruses or eukaryotes respectively and involve relatively complex mechanisms. In the context of a minimal cell a more centrally controlled system would be favourable, to establish a relatively more symmetric division, or at least a division in which both daughter cells have a good chance of encapsulating a representative fraction of the mother's cytoplasmic content.

9.1 Reproduction in Mycoplasmas

Unlike many bacterial species, Mycoplasmas do not possess a rigid cell wall structure consisting of e.g. peptidoglycan. As a consequence, Mycoplasmas generally adopt a variety of morphologies [Razin *et al.*, 1998]. Several distinct reproduction pathways have been hypothesised for Mycoplasmas [Miyata, M. *et al.*, 1999]. Of these reproduction pathways, binary fission that occurs mainly in species possessing a polarized structure is the most well-described [Freundt *et al.*, 1969; Seto *et al.*, 1999]. What drives the binary fission process in Mycoplasma however? In 1994, a submembranous tubulin-like filament network was discovered to be present in *M. gallisepticum* that may contribute to the species' morphology changes during reproduction [Korolev *et al.*, 1994]. Furthermore, the FtsZ protein that is essential for the midplane constriction of bacteria with cell wall was found to be synthesised in several Mycoplasmas, lacking however many other genes for the divisome proteins (see section 9.2) [Lutkenhaus *et al.*, 1997]. Therefore, a still not fully elucidated mechanism different from the mechanism in most cell walled bacteria - although most likely still protein-dependent - will enable the binary fission in Mycoplasmas. For the reconstitution of a minimal cell the exact mechanism underlying Mycoplasmas' binary fission and a possible relation with cholesterol and lipidic components are of high interest. Craig Venter and his team have elucidated minimal Mycoplasma genomes that suggest the indispensability of FtsA for Mycoplasma division, whilst FtsZ appears non-essential [Hutchison *et al.*, 2016]. Many efforts have furthermore gone out towards the reconstruction of essential parts of the *E. coli* model system [Martos *et al.*, 2012; Zieske *et al.*, 2013; Zieske *et al.*, 2014; Kretschmer *et al.*, 2014] to study the minimal set of components necessary for the onset of fission events. The exact essential components and their mechanisms of acting in Mycoplasma division are still to be elucidated.

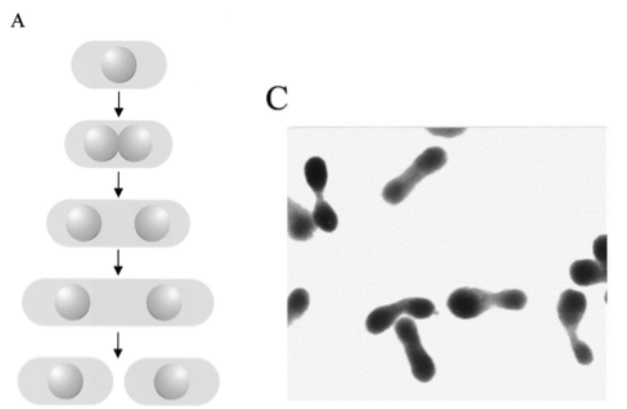


Figure 9.1. Binary fission in *M. capricolum*. A. In a rich medium *M. capricolum* elongates after which it undergoes binary fission (schematic drawing) C. Electron microscopic image of *M. capricolum* in elongated shape to undergo binary fission [Miyata *et al.*, 1999].

9.2 *E. coli* division system

E. coli bacteria possess a highly regulated division mechanism that controllably divides the bacterium at mid-plane and is sensitive to external cues such as nutrient availability and UV-induced DNA damage as well as to its own growth [Burton *et al.*, 1983; Persson *et al.*, 2007; Wang *et al.*, 2009; Osella *et al.*, 2014]. The division machinery of *E. coli* consists of many components as depicted in figure 10.2. and some essential parts may even to be discovered. *E. coli* amongst others uses the Min system, nucleoid occlusion and the Ter macrodomain assisted by either ZapA, ZapB or MatP [Bailey *et al.*, 2014] to control the spatial organisation of membrane-associated FtsA-FtsZ bundles [Chen *et al.*, 2005; Szwedziak *et al.*, 2014].

The Min system is one of the most well known systems influencing the FtsA-FtsZ bundle positioning. MinD binds to phospholipid membranes with its conserved C terminal domain in an ATP-dependent manner [Hu *et al.*, 2003]. When bound to the membrane, MinD polymerises after which it is able to recruit and activate MinC proteins that subsequently inhibit FtsZ polymerisation [e.g. Pichoff *et al.*, 2001]. MinE proteins in turn form circularised structures in the lumen around mid-plane of the bacterium and detach MinD from the membrane due to their ATP-hydrolysing effect [e.g. Meinhardt *et al.*, 2001]. As the FtsZ polymerisation inhibiting MinD-MinC complex consequently is only located at the cell poles, the FtsZ ring formation may only occur at mid-plane, allowing for localised positioning of the division machinery.

After the assembly of FtsZ rings at mid-plane, constriction follows assisted by remodeling of the peptidoglycan layer [Bisson-Filho *et al.*, 2018]. In this process, peptidoglycan synthases associate with the FtsA-FtsZ complex to cir-

cle and form concentric rings of peptidoglycan inducing the eventual division [Bisson-Filho *et al.*, 2018].

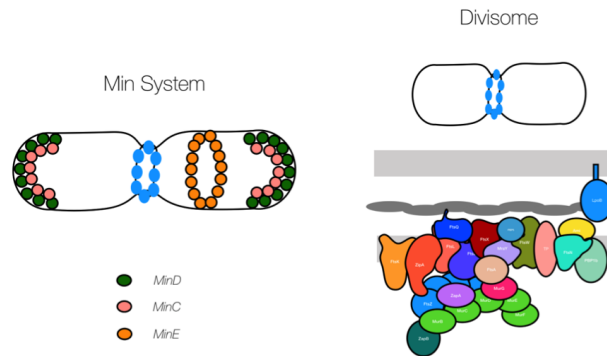


Figure 9.2 *E. coli* divisome positioning system (Min system) and the *E. coli* divisome respectively.

As depicted in figure 9.2, a plethora of membrane proteins are generally present in *E. coli*. Only relatively little may be essential for division however [Nourian *et al.*, 2014; Ueda *et al.*, 2018]. Other proteins, but certainly also the essential proteins, may facilitate the coupling of division with other processes. In times of starvation or UV-induced DNA damage for example, *E. coli* slows down reproduction. One manner of regulation used in this context is through low concentrations of UDP-glucose that result in low intracellular UgtP concentrations giving rise to localized UgtP patches that may inhibit division through directly binding FtsZ, preventing FtsZ bundle formation, although the exact mechanisms underlying this pathway remain to be elucidated [Wang *et al.*, 2009].

Together with the plethora of other molecular interactions, *E. coli* division constitutes an elegant, highly controlled and robust process of which several parts have been reconstituted *in vitro* [Martos *et al.*, 2012; Zieske *et al.*, 2013; Zieske *et al.*, 2014; Kretschmer *et al.*, 2014; Osawa *et al.*, 2008]. A good example of the reconstitution of the *E. coli* division system is the observation of contractile FtsZ rings in liposomes as observed by Osawa *et al.* (2008). By modifying the C-terminal domain of FtsZ to include a YFP with an amphipathic helix, Osawa *et al.* (2008) evaded the need for the incorporation of FtsA and showed contractile Z-rings forming within multilamellar liposomes as depicted in figure 9.3 Current investigations go out to reconstituting contractile Z-rings in unilamellar vesicles instead, in combination with the use of FtsA for the membrane recruitment (see experimental section). The objective of the research field is thereby mainly to reconstruct a minimal divisome allowing for controllable division as reviewed by Nourian *et al.* (2014). Nourian *et al.* (2014) additionally found the N-terminal amphipathic helix and Bin-amphysin-Rvs (BAR) domain of rat amphiphysin 1 to generate tubular structures in dioleoyl phospholipid

liposomes after its liposomal synthesis in the PURE $_{flex}$ system [Shimizu *et al.*, 2014]. Apart from the tubular structures in this instance, no specific membrane invaginations were observed.

In the same pursuit of the establishment of a minimal divisome, Ueda *et al.* (2018) recently demonstrated membrane deformation through liposomal de novo synthesis of FtsZ, ZipA and FtsA. The deformations presented by Ueda *et al.* (2018) show high irregularity, but show a promising step towards a minimal genetically-encoded divisome.

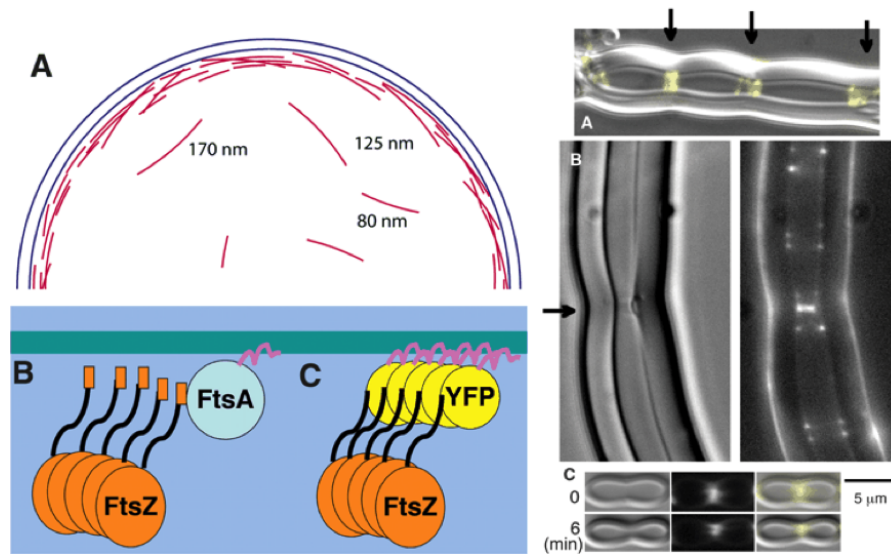


Figure 9.3 **Left:** Schematic drawings of FtsZ bundle formation at the membrane. (A) FtsZ bundle formation at the membrane. (B) Usually, FtsZ is anchored to the membrane for polymerization through binding the membrane binding protein FtsA. In this experiment, the FtsA binding domain was replaced by YFP that would make the bundles attach to the membrane via an amphipathic helix. **Right:** Images of constricting Z-rings formed after FtsZ-mts and GTP were added externally to multilamellar Egg PC and DOPG (2-40%) liposomes. Some tubular, multilamellar liposomes were found to encapsulate FtsZ-mts and GTP. For these cases FtsZ was found to assemble into Z rings. (A) Three yellow Z-rings indicated with the arrows colocalized with membrane invaginations in a multilamellar liposome. (B) Z-ring formed near the liposome mid-plane (arrow). (C) Liposome with visible constriction around mid-plane 5-10 minutes after preparation of the sample. In a timespan of 6 minutes the constriction narrowed significantly [Osawa *et al.*, 2008].

Alternatively, bacteria such as *E. coli* and *B. subtilis* has been shown to be able to reproduce through membrane blebbing and tubulation in its wall-free L-form [Mercier *et al.*, 2013]. This mechanism has been regarded as crucial in bacterial evolution and directly links to several mechanisms described to facilitate division without protein systems [Zhu and Szostak *et al.*, 2009; Hanczyc

et al., 2003; Peterlin *et al.*, 2009; Terasawa *et al.*, 2012]. Although it has been raised that the L form in itself already facilitates division, GUVs mimicking cell wall-free organisms tend to be relatively stable. Protein-induced membrane deformations in such systems have been described under the influence of MinD and MinE [Litschel *et al.*, 2018], although the deformations observed until now seem highly limited.

9.3 Archaeal Division

The protein systems in Archaea are another well-studied topic in the light of division establishment *in vitro*. The archaeal division system relies on CdvB proteins that are recruited by CdvA proteins to the membrane. The Cdv proteins play a critical role in neck constriction [Samson *et al.* 2008; Lindas *et al.* 2008; Peel *et al.*, 2011], comparable to the eukaryotic endosomal sorting complex required for transport (ESCRT). Liposome fission has been demonstrated through reconstituting minimal ESCRT-complexes with as little as six components [Saksena *et al.* 2009; Wollert *et al.* 2009; Wollert and Hurley 2010]. This system is however relatively uncontrollable in that the membrane constriction has, up until now, mainly given rise to endocytosis-like events [Wollert *et al.*, 2009; Härtel *et al.*, 2014].

9.4 Virally Induced Fission

A different perspective on inducing fission in a minimal cell is infecting liposomes with a virus. Although many viruses depend on the host cells' Endosomal Sorting Complexes Required for Transport (ESCRT proteins), some viruses such as influenza A confer their own mechanism for budding induction. The 17-amino acid long amphipathic cytoplasmic tail of the M2 proteins [Rossman *et al.*, 2010] provides a controllable method of fission on the one hand. On the other hand, the type of fission induced by these specific proteins is limited in size extend and limited in internal and external budding controllability. Furthermore, for virus infection of liposomes to be possible, the liposomes should contain receptors in their membrane, which do impose an extra load on a minimal cell. Nevertheless, initially the amphipathic M2 helix has also been added directly to POPC:POPG:(Cholesterol) GUVs demonstrating subsequent budding and fission. In figure 9.4 phase separation, budding and fission events are shown as a result of the M2 amphipathic helix in combination with high and low levels of cholesterol in the vesicle membranes. In low cholesterol content GUVs ($\pm 5\%$), the M2AH-TMR peptide is sufficient to cause budding and fission in vesicles. The M2AH-TMR peptide induced fission may be expected to work in DO-liposomes as well, although this is a subject open to research.

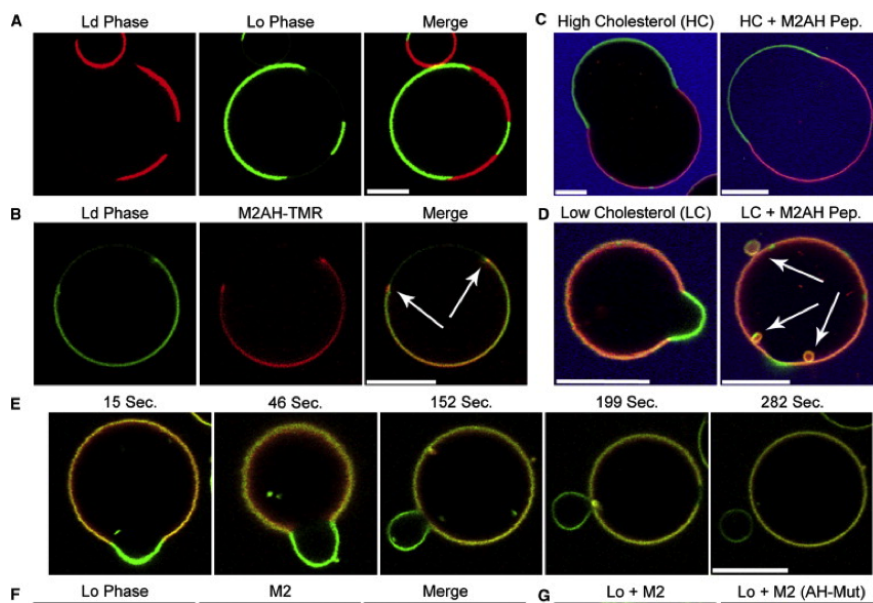


Figure 9.4 Budding and fission occurring at phase boundaries induced by the M2 amphipathic helix from the influenza A virus in GUVs formed by electroformation and imaged within 1 hour [Rossman *et al.*, 2010]. (A) Phase separation in POPC: POPG: Cholesterol(20%). (B) Clustering of M2AH-TMR peptide at the phase boundaries. (C,D) Budding as a result of M2AH-TMR peptide clustering at the phase boundaries in (C) high cholesterol GUVs (20%), and (D) low cholesterol GUVs (5%). (E) Budding and fission in 5% cholesterol GUV timelapse.

All in all, the protein-based division mechanisms show relatively high reproducibility, controllability and efficiency, are highly compatible, and are therefore the most well-known mechanisms present in life as we know it today. Albeit the advantages that come with protein-based division, the complete protein-based mechanisms entail a high complexity and may therefore not be the most suitable in the case of a minimal cell, compared to example given the osmotic pressure induced division. Virally induced division therefore may be an interesting alternative, although this process is again less controllable and efficient. Investigations towards a facilitating combination of internally controlled (lipid and) protein-based division with externally controlled division may lead to both a minimal and controllably and efficiently reproducing cell.

10 Conclusion

All mechanisms discussed show their own advantages and disadvantages in the light of a minimal cell. While thermal cycles show limited compatibility with the PURE system and limited size control for binary fission, the application of an electric field appears less dependent on membrane composition. The electrically induced fission suffers from the same uncontrollability when it comes to vesicle size, and additionally displays uncontrollability over simultaneous bursting and cell fusion events, along with some liposome leakage that complicates the liposomal preservation of the PURE system. In contrast to the thermal and electrical approach, the microfluidic mechanical approach appears more promising for controlled symmetric division events with relatively low leakage. However, the technique used for liposome formation in this context is dependent on a lipid phase carrier that allows for the most robust liposome formation the more hydrophobic the organic solvent used. The hydrophobicity of the organic solvent is in trade off, with its protein compatibility, that is a limiting factor to the mechanical division in relation to the PURE system. Osmotic pressure induced division has also been observed, although the control over size and onset of fission in this case is again limiting. In all cases, osmotic phenomena together with intrinsic membrane properties play a critical role in establishing fission, pointing at a promising future for these characteristics, possibly in combination with a minimal protein system.

Phase separation oftentimes plays a critical role in establishing actual budding and fission. When it comes to division based on phase separation, the cholesterol/osmotic approach is of better interest than example given temperature cycling, since the cholesterol approach does not necessarily involve a two-fold lipid phase separation. Lipid phase separation might namely lead to uneven partitioning of the membrane constituents over the daughter cells, which in turn imposes a limitation in multigenerational reproduction. Externally imposed virally induced proliferation such as through the M2 amphipathic helix, is another highly interesting mechanism as the viral infection may induce temporally controlled liposome proliferation that is independent of liposomally encoded proteins. In essence, as Mercier *et al.* (2013) argue, even membrane intrinsic properties themselves may be enough for proliferation, allowing for an even more minimal cell, although the optimal membrane composition remains to be elucidated.

In table 10.1, a schematic overview is presented of the feasibility of the described techniques in the context of essential criteria for a minimal cell (section 3.5). It should be noted that the scaling is arbitrary, and that the scaling represents an average of the different techniques within the categories. Some criteria are more essential than others in the light of a minimal cell. The compatibility with a system like the PURE system is e.g. essential, whilst the efficiency is of relatively less imminent importance. Consequently, especially the electrical, osmotic, and membrane based (lipid/sterol/protein) methods are promising.

Table 10.1 Overview of the approaches that have been described in relation to liposome division and their feasibility for use in the context of a minimal cell. Here the approaches are judged on the criteria introduced in section 3.5 on an arbitrary scale from - - for absolutely not compatible to ++ for highly compatible.

	Thermal	Electrical	Mechanical	Osmotical	(Lipid/ Sterol) Membrane Components	Protein based
Efficiency	-	-	+	-	-	-
Controllability	--	--	++	--	--	+
Reproducibility	+	-/+	++	-/+	-	-
Lipid composition flexibility	--	-	+	-/+	-/+	-/+
Protein Compatibility	-	-/+	-	+	-/+	++
PURE system Compatibility	--	+	-	++	++	++
Multi- generational feasibility	-/+	-	-/+	-	-/+	++

Given the most critical role of osmotic influences on division in relation to all techniques, the following part will concern the experimental compatibility of osmotical influences on gene-expressing liposomes together with the influence of the frequently used membrane component cholesterol on liposome morphology. Furthermore, we will elaborate on the relatively unexplored electrical fission in experimental context to determine the factual interplay with the PURE system.

References

- [1] Allain, J.-M. *et al.* (2006). Budding and fission of a multiphase vesicle. *Eur. Phys. J. E* 20: 409-420.
- [2] Almendro-Vedia, V.G. (2013). Mechanics of Constriction during Cell Division: A Variational Approach. *PLoS ONE* 8(8): e69750. doi:10.1371/journal.pone.0069750.
- [3] Andersen, I. *et al.* (1965). The influence of electric fields on bacterial growth. *International Journal of Biometeorology*, 9(3): 211-218.
- [4] Andersen, H.D. *et al.* (2011). Reconciliation of opposing views on membrane-sugar interactions. *Proc. Natl. Acad. Sci. U.S.A.*, 108: 1874-1878.
- [5] Aranda, S. *et al.* (2008). Morphological Transitions of Vesicles Induced by Alternating Electric Fields. *Biophysical Journal: Biophysical Letters*, L19-L21. doi: 10.1529/biophysj.108.132548.
- [6] Bagatolli, L. *et al.* (2009). Phase behaviour of multicomponent membranes: Experimental and computational techniques. *Soft Matter*, 5 (17), 3234-3248.
- [7] Bailey MW, Bisicchia P, Warren BT, Sherratt DJ, Männik J (2014) Evidence for Divisome Localization Mechanisms Independent of the Min System and SlmA in *Escherichia coli*. *PLoS Genet* 10(8): e1004504. <https://doi.org/10.1371/journal.pgen.1004504>.
- [8] Barenholz, Y. *et al.* (2004). Sphingomyelin and Cholesterol: From Membrane Biophysics and Rafts to Potential Medical Applications. *Subcellular Biochemistry, Volume 37: Membrane Dynamics and Domains*. Edited by Peter J. Quinn. Kluwer Academic/Plenum Publishers, New York.
- [9] Basanez, G., *et al.* (2002). Membrane fusion: the process and its energy suppliers, *Cell Mol. Life Sci.*, 59, 1478.
- [10] Bassereau, P., *et al.* (2018). Membrane curvature and BAR-domain proteins. *J. Phys. D: Appl. Phys.* 51 343001.
- [11] Batrakov, S.G. *et al.* (2000). The polar-lipid composition of the sphingolipid-producing bacterium *Flectobacillus major*. *Biochimica et Biophysica Acta (BBA) - Molecular and Cell Biology of Lipids*, 1484 (2-3): 225-240.
- [12] Baumgart *et al.* (2003). Imaging coexisting fluid domains in biomembrane models coupling curvature and line tension. *Nature*, 425: 821-824.

- [13] Ben-Shaul, A. (1995). Molecular theory of chain packing, elasticity and lipid-protein interaction in lipid bilayers. In *Structure and Dynamics of Membranes*. R. Lipowsky, and E. Sackmann, editors. Elsevier, Amsterdam, the Netherlands. pp.359–401.
- [14] Bentz, J, Ellens, H, LaL M-Z and Szoka FC (1985). On the correlation between HII phase and the contact-induced destabilization of phosphatidylethanolamine-containing membranes. *Proc Natl Acad Sci USA* 82 5742-5745.
- [15] Bentz J Ellens, H and Szoka, F C (1987). Destabilization of phosphatidylethanolamine-containing liposomes: hexagonal phase and asymmetric membranes. *Biochemistry*, 26: 2105-2116.
- [16] Bentz, J. *et al.* (1988). Membrane fusion: kinetics and mechanisms. *Colloids Surfaces*, 30: 65-112.
- [17] Berclaz, N., Muller, M., Walde, P., Luisi., P.L. (2001). Growth and transformation of vesicles studied by ferritin labeling and cryotransmission electron microscopy. *J Phys Chem*, 105, pp. 1056-1064.
- [18] Bhattacharya, A. *et al.* (2019). A minimal biochemical route towards de novo formation of synthetic phospholipid membranes. *Nature Communications*, volume 10, Article number: 300.
- [19] Bisson-Filho, A.W. *et al.* (2017). Treadmilling by FtsZ filaments drives peptidoglycan synthesis and bacterial cell division. *Science*; Vol. 355, Issue 6326, pp. 739-743.DOI: 10.1126/science.aak9973.
- [20] Bisson-Filho *et al.* (2018).MreB filaments align along greatest principal membrane curvature to orient cell wall synthesis, 7:e32471. DOI: <https://doi.org/10.7554/eLife.32471>.
- [21] Blangero C. and Teissie J. (1983). Homokaryon production by electrofusion: A convenient way to produce a large number of viable mammalian fused cells. *Biochem. Biophys. Res. Communications* 114: 663–669.
- [22] Blangero C. and Teissie J. (1984). Ionic control of mammalian cell electrofusion. 8th International Biophysics Congress, July/August 1984, Bristol.
- [23] Boroske, E.M. *et al.* (1981). Osmotic shrinkage of giant egg-lecithin vesicles. *Biophys. J.* 34:95-109.
- [24] Božič, B. Svetina, S. (2004). A relationship between membrane properties forms the basis of a selectivity mechanism for vesicle self-reproduction. *Eur Biophys J*, 33: 565. <https://doi.org/10.1007/s00249-004-0404-5>.
- [25] Božič, B. *et al.* (2014). Direct and remote constriction of membrane necks. *Physical Review E* 89, 052701.

- [26] Burgess, S.W. *et al.* (1991). Polyethylene glycol-induced lipid mixing but not fusion between synthetic phosphatidylcholine large unilamellar vesicles. *Biochemistry*, 30(17): 4193-4200.
- [27] Burton, P. *et al.* (1983). Two pathways of division inhibition in UV-irradiated *E. coli*. *Molecular and General Genetics MGG*, 190(2): 309-314.
- [28] Buschl R., Ringsdorf H., and Zimmermann U.: 1982. Electric field-induced fusion of large liposomes from natural and polymerizable lipids. *FEBS Lett.* 150: 38-42.
- [29] Chan K.L., Gascoyne P.R.C., Becker F.F., Pethig R. (1997). Electrorotation of liposomes: verification of dielectric multi-shell model for cells. *Bba-Lipid Lipid Met*; 1349: 182-96.
- [30] Chapman, D. *et al.* (1975). Phase transitions and fluidity characteristics of lipids and cell membranes. *Quarterly Reviews of Biophysics*, 8(2): 185-235.
- [31] Chen, Z., and Rand, R.P. (1997). The influence of cholesterol on phospholipid membrane curvature and bending elasticity. *Biophys. J.* 73: 267-276.
- [32] Chen, Y.A. *et al.* (2001). SNARE-mediated membrane fusion. *Nature Reviews Molecular Cell Biology*, 2: 98-106.
- [33] Chen, Y. *et al.* (2005). Rapid in vitro assembly dynamics and subunit turnover of FtsZ demonstrated by fluorescence resonance energy transfer. *J. Biol. Chem.* 280, 22549-22554. doi:10.1074/jbc.M500895200pmid:15826938.
- [34] Cheng. K. H., *et al.* (1986). The role of cholesterol in the activity of reconstituted Ca-ATPase vesicles containing unsaturated phosphatidylethanolamine. *J Biol Chem* 261, 5081-5087.
- [35] Chernomordik, L. *et al.* (1995). Lipids in biological membrane fusion. *J. Membr. Biol.* 146: 1-14.
- [36] Chernomordik, L. *et al.* (1995). The hemifusion intermediate and its conversion to complete fusion: regulation by membrane composition. *Biophys J.* 69: 922-929.
- [37] Chernomordik, L. *et al.* (1995). Bending membranes to the task: structural intermediates in bilayer fusion. *Curr Opin Struct Biol.* 5: 541-547.
- [38] Chernomordik, L. *et al.* (1997). An early stage of membrane fusion mediated by the low pH conformation of influenza hemagglutinin depends upon membrane lipids. *Journal of Cell Biology*, 136(1), 81-93.
- [39] Choubey, A. *et al.* (2013). Cholesterol Translocation in a Phospholipid Membrane. *Biophysical Journal*, 104(11): 2429-2436.

- [40] Corver, J., Moesby, L., Erukulla, R. K., Reddy, K. C., Bittman, R., and Wilschut, J. (1995). Sphingolipid-dependent fusion of Semliki Forest virus with cholesterol-containing liposomes requires both the 3-hydroxyl group and the double bond of the sphingolipid backbone. *Virology* 69:3220.
- [41] Cullis, P.R., and De Kruijff, B. (1978). The polymorphic phase behavior of phosphatidyl-ethanolamines of natural and synthetic origin, *biochim. Biophys. Acta* 513: 31-42.
- [42] Cullis, P.R. *et al.* (1978). Polymorphic phase behaviour of lipid mixtures as detected by ³¹P NMR. Evidence that cholesterol may destabilize bilayer structure in membrane systems containing phosphatidylethanolamine. *Biochem Biophys Acta* 507, 207-218.
- [43] Cullis, P.R. *et al.* (1979). Lipid polymorphism and the functional roles of lipids in biological membranes. *Biochem Biophys Acta* 513, 21-30.
- [44] Cullis, P.R., *et al.* (1986). Lipid polymorphism and membrane fusion. *Biochem Soc Trans*, 14: 242-245.
- [45] Dean Astumian, R. *et al.* (1989). Nonlinear effect of an oscillating electric field on membrane proteins. *J. Chem. Phys.* 91, 4891. <https://doi.org/10.1063/1.456728>.
- [46] Demel, R.A. *et al.* (1972). THE EFFECT OF STEROL STRUCTURE ON THE PERMEABILITY OF LIPOMES TO GLUCOSE, GLYCEROL AND Rb . *Biochim. Biophys. Acta*, 255: 321-330.
- [47] Deshpande, S. *et al.* (2015). Octanol-assisted liposome assembly on chip. *Nature Communications*, 7:10447. DOI: 10.1038/ncomms10447.
- [48] Deuling, H.J., Helfrich, W. (1976). The curvature elasticity of fluid membranes : A catalogue of vesicle shapes.
- [49] Dimova, R. *et al.* (2007). Giant vesicles in electric fields. *Soft Matter*, 3: 817-827.
- [50] Döbereiner H.-G., *et al.* (1993) Budding and Fission of Vesicles. *Biophysical Journal*, 65: 1396-1403.
- [51] P. Domínguez-Cuevas, R. Mercier, M. Leaver, Y.Kawai, J. Errington The rod to L-form transition of *Bacillus subtilis* is limited by a requirement for the protoplast to escape from the cell wall sacculus. *Mol. Microbiol.*, 83 (2012), pp. 52-66.
- [52] Drolle, E. *et al.* (2013). Effect of melatonin and cholesterol on the structure of DOPC and DPPC membranes. *Biochimica et Biophysica Acta (BBA) - Biomembranes*; Volume 1828, Issue 9, Pages 2247-2254.

- [53] Durrer, P. *et al.* (1996). H⁺-induced membrane insertion of influenza virus hemagglutinin involves the HA2 amino-terminal fusion peptide but not the coiled-coil region. *J. Biol. Chem.*, 271: 13417-13421.
- [54] Eeman, M. *et al.* (2010). From biological membranes to biomimetic model membranes. *BASE* 14 (4).
- [55] Ellens, H., Bentz, J. Szoka, F. C. (1985). H⁺- and Ca²⁺-induced fusion and destabilization of liposomes. *Biochemistry* 24, 3099–3106.
- [56] Ellens, H. Bentz, J and Szoka, F C (1986). Fusion of phosphatidylethanolamine-containing liposomes and mechanism of L. alpha. HII phase transition. *Biochemistry*, 25: 4141-4147.
- [57] Epanand, R. M. (1985). High sensitivity differential scanning calorimetry of the bilayer to hexagonal phase transitions of diacylphosphatidylethanolamines. *Chem. Phys. Lipids.* 36:387–393.
- [58] Epanand, R.M., and Bottega, R. (1987). Modulation of the phase transition behavior of phosphatidylethanolamine by cholesterol and oxysterols. *Biochemistry* 26, 1820-1825.
- [59] Epanand, R.M. *et al.* (1990). The role of membrane biophysical properties in the regulation of protein kinase C activity. *Trends in Pharmacological Sciences*, 11(8): 317-320.
- [60] Erickson, C.A. *et al.* (1984). Embryonic fibroblast motility and orientation can be influenced by physiological electric fields. *J. Cell Biol.* 98: 296-307.
- [61] Evans, E.A., and Needham, D. (1987). Physical properties of surfactant bilayer membranes: Thermal transitions, elasticity, rigidity, cohesion, and colloidal interactions. *J. Phys. Chem.* 91, 4219-4228.
- [62] Evans, E.A., and Rawicz, W. (1990). Entropy-driven tension and bending elasticity in condensed-fluid membranes. *Phys. Rev. Lett.*, 64: 2094-2097.
- [63] Ferrer Castellà, C. *et al.* (2019). Master Thesis Christophe Danelon Lab.
- [64] Franke, T. *et al.* (2009). Phase-Transition- and Dissipation-Driven Budding in Lipid Vesicles. *Chem Phys Chem*, 10(16): 2852-2857.
- [65] Freundt, E.A. *et al.* (1969). Cellular morphology and mode of replication of the mycoplasmas. L. Hayflick (Ed.), *The Mycoplasmatales and the L-phase of bacteria*, Appleton-Century-Crofts, New York.
- [66] Gaff D. F., Ziegler H., and Zimmermann U.(1985). Electrofusion of protoplasts from desiccation tolerant grass species with desiccation sensitive grass protoplasts. *J. Plant Physiol.* 120: 375–380.

- [67] Gallay, J., and De Kruijff, B. (1982). Correlation between molecular shape and hexagonal HII phase promoting ability of sterols, *FEBS Lett.* 143: 133.
- [68] Garcia, J.J. *et al.* (2005). Effects of trace elements on membrane fluidity. *Journal of Trace Elements in Medicine and Biology*, 19(1): 19-22.
- [69] Gawrisch, K. *et al.* (1992). Membrane dipole potentials, hydration forces, and the ordering of water at membrane surfaces. *Biophys J.*, 61(5): 1213-1223. doi: 10.1016/S0006-3495(92)81931-8.
- [70] Gomez, A. *et al.* (1994). Charge and fission of droplets in electrostatic sprays. *Physics of Fluids*, 6(1): 404-414.
- [71] Gingell, D and Glnsberg, L (1978) in *Membrane Fusion* (Poste, G and Nicolson, G L, eds), pp 791-833, Elsevier, Amsterdam.
- [72] Gruner S.M. (1985). Intrinsic curvature hypothesis for biomembrane lipid composition: a role for nonbilayer lipids. *Proc Natl Acad Sci U S A.*, 82(11):3665-9.
- [73] Hamm, M., and M. Kozlov. 2000. Elastic energy of tilt and bending of fluid membranes. *Eur. Phys. J. E.* 3:323-335.
- [74] Hanczyc, M.M., Fujikawa, S.M., and Szostak, J.W. (2003). Experimental models of primitive cellular compartments: encapsulation, growth, and division. *Science* 302, 618-622.
- [75] Harbich, W., Servuss, R. M. and Helfrich, W. (1976). Optical studies of lecithin-membrane melting. *Phys. Lett.* 57A; 294.
- [76] Härtel T and Schwille P (2014) ESCRT-III mediated cell division in *Sulfolobus acidocaldarius* – a reconstitution perspective. *Front. Microbiol.* 5:257. doi: 10.3389/fmicb.2014.00257.
- [77] Hayami, M. *et al.* (1979). Presence and Synthesis of Cholesterol in Stable Staphylococcal L-Forms. *Journal of Bacteriology*, 140(3): 859-863.
- [78] Helfrich, W. (1973). Elastic Properties of Lipid Bilayers: Theory and Possible Experiments. *Z. Naturforsch.* 28c, 693-703.
- [79] Hentrich, C. *et al.* (2014). Controlled Growth of Filamentous Fatty Acid Vesicles under Flow. *Langmuir*, 30, 14916-14925.
- [80] Heung, L.J. *et al.* (2005). Role of Sphingolipids in Microbial Pathogenesis. *Infection and Immunity*, 74 (1): 28-39. DOI: 10.1128/IAI.74.1.28-39.2006.
- [81] Hinkle, L. *et al.* (1981). The direction of growth of differentiating neurones and myoblasts from frog embryos in an applied electric field. *J. Physiol. (Lond.)*. 314: 121-135.

- [82] Hope, M.J. *et al.* (1981). The role of nonbilayer lipid structures in the fusion of human erythrocytes induced by lipid fusogens. *Biochem Biophys Acta*, 640: 82-90.
- [83] Hu, Z. *et al.* (2003). A conserved sequence at the C-terminus of MinD is required for binding to the membrane and targeting MinC to the septum. *Molecular Microbiology*, 47 (2): 345-355.
- [84] Hutchison, C.A. *et al.* (2016). Design and synthesis of a minimal bacterial genome. *Science* 351 (6280), aad6253. DOI: 10.1126/science.aad6253.
- [85] Ingolia, T. D. Koshland, D. E. Jr *J. Biol. Chem.* 253, 3821–3829 (1978).
- [86] Jahn, R. *et al.* (2006). SNAREs-engines for membrane fusion. *Nature Reviews Molecular Cell Biology*, 7: 631-643.
- [87] Jahn, A. *et al.* (2007). Microfluidic Directed Formation of Liposomes of Controlled Size. *Langmuir*, 23(11): 6289-6293.
- [88] Jimbo, T. *et al.* (2016). Role of inverse-cone shape lipids in temperature controlled self-reproduction of binary vesicles. *Biophysical Journal*, 110 (7): 1551-1562.
- [89] Jin, R. *et al.* (2018). Amphipathic helices coupling with membrane curvature. *J. Phys. D: Appl. Phys.* 51, 343001.
- [90] Kawamoto, S. *et al.* (2014). Free energy analysis along the stalk mechanism of membrane fusion. *Soft Matter*, 10, 3048.
- [91] Khalil, A.S. *et al.* (2010). Synthetic biology: applications come of age. *Nature Reviews Genetics* 11, 367-379.
- [92] Kinoshita *et al.* (1988). Electroporation of cell membrane visualized under a pulsed-laser fluorescence microscope. *Biophysical Journal*, 53(6): 1015-1019.
- [93] Kinnunen, P.K.J. *et al.* (2000). Mechanisms of Initiation of Membrane Fusion: Role of Lipids. *Bioscience Reports*, 20(6): 465-482.
- [94] Kiselev, M.A. *et al.* (2001). A sucrose solutions application to the study of model biological membranes. *Nuclear Instruments and Methods in Physics Research Section A: Accelerators, Spectrometers, Detectors and Associated Equipment*, 470(1-2): 409-416.
- [95] Korkmaz, F. *et al.* (2005). Effect of progesterone on DPPC membrane: Evidence for lateral phase separation and inverse action in lipid dynamics. *Archives of Biochemistry and Biophysics*; Volume 440, Issue 2, Pages 141-147.

- [96] Korolev, E.V. *et al.* (1994). Tubular structures of *Mycoplasma gallisepticum* and their possible participation in cell motility. *Microbiology*, 140: 671-681.
- [97] Koshland, Jr., Daniel E. (22 March 2002). The Seven Pillars of Life. *Science*. 295 (5563):221516. doi:10.1126/science.1068489. Retrieved on 12 January 2019.
- [98] Kozlov, M.M. (2018). Continuum elasticity models of membrane shaping and remodeling. *J. Phys. D: Appl. Phys.* 51, 343001.
- [99] Kozlovsky Y and Kozlov M M (2002). Stalk model of membrane fusion: solution of energy crisis *Biophys. J.* 82 882.
- [100] Koslovsky, Y. *et al.* (2003). Membrane Fission: Model for Intermediate Structures. *Biophysical Journal*, 85(1): 85-96.
- [101] Kretschmer, S. *et al.* (2014). Toward spatially regulated division of protocells: insights into the *E. coli* Min system from in vitro studies. *Life*, 4(4), 915-928.
- [102] De Kruijff, B. *et al.* (1981). *Membranes and Intracellular Communication* (Bahan. R, *et al.*, eds), pp 79-91, North-Holland, Amsterdam.
- [103] De Kruijff, B. *et al.* (1985). *Progress in Protein-Lipid Interactions* (Watts, A and De Pont, J J H M. eds), pp 89-142, Elsevier, Amsterdam.
- [104] De Kruijff, B., *et al.* (1985). *The Enzymes of Biological Membranes* (2nd Edn) (Martmosl. AN, ed), pp 131-204, Plenum Press, New York.
- [105] Lafong, A. *et al.* (2006). Time-Multiplexed Laguerre-Gaussian holographic optical tweezers for biological applications. *Optics Express*, 14(7): 3065-3072.
- [106] Latowski *et al.* (2004). Violaxanthin De-Epoxidase, the Xanthophyll Cycle Enzyme, Requires Lipid Inverted Hexagonal Structures for Its Activity. *American Chemical Society Publications, Biochemistry*, 43(15), pp 4417-4420.
- [107] Li *et al.* (1995). Effect of propensity of hexagonal II phase formation on the activity of mitochondrial ubiquinol-cytochrome c reductase and H⁺-ATPase. *Chemistry and Physics of Lipids*, 76(2): 135-144.
- [108] Li, L. *et al.* (2005). Budding Dynamics of Multicomponent Tubular Vesicles. *J. AM. CHEM. SOC.*, 127, 17996-17997.
- [109] Lindas, A. C., Karlsson, E. A., Lindgren, M. T., Ettema, T. J., and Bernander, R. (2008). A unique cell division machinery in the Archaea. *Proc. Natl. Acad. Sci. U.S.A.* 105, 18942–18946. doi: 10.1073/pnas.0809467105.

- [110] Lindblom G, Orädd G, Rilfors L, Morein S. (2002). Regulation of lipid composition in *Acholeplasma laidlawii* and *Escherichia coli* membranes: NMR studies of lipid lateral diffusion at different growth temperatures. *Biochemistry*, 41(38):11512-5.
- [111] Lipowsky, R. *et al.* (1992). Budding of membranes induced by intramembrane domains. *J. Phys. II* 2:1825-1840.
- [112] Litschel, T. *et al.* (2018). Beating Vesicles: Encapsulated Protein Oscillations Cause Dynamic Membrane Deformations. *Angewandte Chemie*, 57 (50): 16286-16290.
- [113] Liu, Z. *et al.* (2016). Effects of vesicle components on the electropermeability of lipid bilayers of vesicles induced by pulsed electric fields (PEF) treatment. *Journal of Food Engineering*, 179: 88-97.
- [114] Lotter, J., Botes, A. L., Van Dyk, M. S. Breytenbach, J. C. (2004). Correlation between the physicochemical properties of organic solvents and their biocompatibility toward epoxide hydrolase activity in whole-cells of a yeast, *Rhodotorula sp.* *Biotechnol. Lett.* 26, 1191–1195.
- [115] Lowther J Charmier G Raman MC, *et al.* (2011). Role of a conserved arginine residue during catalysis in serine palmitoyltransferase *FEBS Lett*, 585 172934.
- [116] Lowther J Naismith JH Dunn TM, *et al.* (2012). Structural, mechanistic and regulatory studies of serine palmitoyltransferase *Biochem Soc T*, 40 54754.
- [117] Lund, E. J. *et al.* (1923). Electrical Control of Organic Polarity in the Egg of *Fucus*. *Botanical Gazette* 76 (3): 288-301.
- [118] Lutkenhaus, J. *et al.* (1997). Bacterial cell division and the Z ring. *Annu. Rev. Biochem.*, 66: 93-116.
- [119] Martin, I. *et al.* (2000). Common properties of fusion peptides from diverse systems. *Biosci. Rep.*, 20: 483-500.
- [120] Martos, A. *et al.* (2012). Towards a bottom-up reconstitution of bacterial cell division. *Trends in cell biology*, 22(12): 634-643.
- [121] McKay, Chris P. (14 September 2004). "What Is Life—and How Do We Search for It in Other Worlds?". *PLoS Biology*. 2 (2(9)): 302. doi:10.1371/journal.pbio.0020302.
- [122] Meinhardt, H. *et al.* (2001). Pattern formation in *Escherichia coli*: A model for the pole-to-pole oscillations of Min proteins and the localization of the division site. *PNAS*, 98 (25): 14202-14207. <https://doi.org/10.1073/pnas.251216598>.

- [123] Mercier, R. *et al.* (2012). Crucial Role for Membrane Fluidity in Proliferation of Primitive Cells. *Cell Reports*, 1 (5): 417-423.
- [124] Mercier, R. *et al.* (2013). Excess Membrane Synthesis Drives a Primitive Mode of Cell Proliferation. *Cell* 152, 997–1007.
- [125] Merrifield, C. J., Perrais, D., and Zenisek, D. (2005). Coupling between clathrin-coated-pit invagination, cortactin recruitment, and membrane scission observed in live cells. *Cell* 121, 593.
- [126] Miyata, M. *et al.* (1999). Cell reproduction cycle of mycoplasma. *Biochimie*, 81(8-9): 873-878.
- [127] Modchang, C. *et al.* (2004). Modeling of the dynamic pole-to-pole oscillations of the min proteins in bacterial cell division: The effect of an external field. arXiv:physics/0412110 [physics.bio-ph].
- [128] Modchang, C. *et al.* (2008). Stochastic modeling of external electric field effect on Escherichia coli Min protein dynamics. *Journal of the Korean Physical Society*. Vol.53, No.2 (2008), 851-862.
- [129] Monod, J. Jacob, F. (1961). General conclusions: telenomic mechanisms in cellular metabolism, growth, and differentiation. *Cold Spring Harb. Symp. Quant. Biol.* 26, 389–401.
- [130] Murtas, G. *et al.* (2007). Protein synthesis in liposomes with a minimal set of enzymes. *Biochemical and Biophysical Research Communications*, Vol. 363 (1): 12-17.
- [131] Needham, D., and Hochmuth, R. M. (1989). Electro-mechanical permeabilization of lipid vesicles. Role of membrane tension and compressibility. *Biophys. J.*, 55, 1001.
- [132] Needham, D., and Nunn, R.S. (1990). Elastic deformation and failure of lipid bilayer membranes containing cholesterol. *Biophysical Journal* 58: 997-1009.
- [133] Neuman, K.C. *et al.* (2006). Optical trapping. *Rev. Sci. Instrum.*, 75(9): 2787-2809.
- [134] Nomura, S.M. *et al.* (2005). Changes in the morphology of cell-size liposomes in the presence of cholesterol: Formation of neuron-like tubes and liposome networks. *Biochimica et Biophysica Acta (BBA) - Biomembranes*. 1669 (2): 164-169.
- [135] Noordam, P.C., *et al.* (1980). Barrier characteristics of membrane model systems containing unsaturated phosphatidylethanolamines, *Chem. Phys. Lipids* 27:221-232.
- [136] Nourian, Z. *et al.* (2014). Toward the assembly of a minimal divisome. *Syst Synth Biol.*, 8(3): 237–247.

- [137] Nuccitelli, R. *et al.* (1983). Embryonic cell motility can be guided by physiological electric fields. *Exp. Cell Res.* 147: 195-201.
- [138] O'Day, D.H. (1993). *Signal Transduction during Biomembrane Fusion*. Academic Press Inc., Toronto.
- [139] Olbrich, K., Rawicz, W., Needham, D., and Evans, E. (2000). Water permeability and mechanical strength of polyunsaturated lipid bilayers. *Biophys. J.*, 79, 321.
- [140] Osawa, M. *et al.* (2008). Reconstitution of Contractile FtsZ Rings in Liposomes. *Science*, 320 (5877): 792-794.
- [141] Osella, M. (2014). Concerted control of *Escherichia coli* cell division. *PNAS*, 111(9): 3431-3435; <https://doi.org/10.1073/pnas.1313715111>.
- [142] Papahadjopoulos, D. *et al.* (1971). Permeability properties of phospholipid membranes: effect of cholesterol and temperature. *Biochimica et Biophysica Acta*, 266: 561-583.
- [143] Papahadjopoulos, D. *et al.* (1973). Phase transitions in phospholipid vesicles. Fluorescence polarization and permeability measurements concerning the effect of temperature and cholesterol. *Biochimica et Biophysica Acta (BBA) – Biomembranes*, 311(3): 330-348.
- [144] Parsegian, V.A. *et al.* (1991). Direct osmotic stress measurements of hydration and electrostatic double-layer forces between bilayers of double-chained ammonium acetate surfactants. *J. Phys. Chem.*, 95: 4777-4782.
- [145] Peel, S., Macheboeuf, P., Martinelli, N., and Weissenhorn, W. (2011). Divergent pathways lead to ESCRT-III-catalyzed membrane fission. *Trends Biochem. Sci.* 36, 199–210. doi: 10.1016/j.tibs.2010.09.004.
- [146] Perrier, D.L. *et al.* (2017). Lipid vesicles in pulsed electric fields: Fundamental principles of the membrane response and its biomedical applications. *Advances in Colloid and Interface Science*, 249, 248-271.
- [147] Persson, O. *et al.* (2007). Metabolic control of the *Escherichia coli* universal stress protein response through fructose-6-phosphate. *Molecular Microbiology*, 65(4): 968-978.
- [148] Peterlin, P. *et al.* (2007). The prolate-to-oblate shape transition of phospholipid vesicles in response to frequency variation of an AC electric field can be explained by the dielectric anisotropy of a phospholipid bilayer. *J. Phys.: Condens. Matter* 19. 136220 (15pp). DOI: 10.1088/0953-8984/19/13/136220.
- [149] Pichoff S, Lutkenhaus J (2001). *Escherichia coli* division inhibitor MinCD blocks septation by preventing Z-ring formation. *J Bacteriol*, 183(22):6630-5.

- [150] Van der Ploeg *et al.* (2013). Colocalization and interaction between elongasome and divisome during a preparative cell division phase in *Escherichia coli*. *Molecular Microbiology*, 87(5): 1074-1087.
- [151] Prestegard, J.H. and O'Brien, M.P. (1987). Membrane and vesicle fusion. *Annu Rev Phys Chem*, 38: 383-411.
- [152] Rand, R.P., and Sengupta, S. (1972). Cardiolipin forms hexagonal structures with divalent cations. *Biochem Biophys Acta* 255, 484-492.
- [153] Rand, R.P. (1981). Interacting phospholipid bilayers: measured forces and induced structural changes. *Annu Rev Biophys Bioeng*, 10: 277-314.
- [154] Rand, R.P. and Parsegian, V.A. (1986). Mimicry and mechanism in phospholipid models of membrane fusion. *Annu Rev Physiol* 48: 201-212.
- [155] Rand, R. P., and V. A. Parsegian. (1989). Hydration forces between phospholipid bilayers. *Biochim. Biophys. Acta.* 988:351–376.
- [156] Rayleigh, L. (1882). "On the Equilibrium of Liquid Conducting Masses charged with Electricity". *Philosophical Magazine*. 14 (1): 184–186. doi:10.1080/14786448208628425.
- [157] Razin S, Tully JG (1970). Cholesterol Requirement of Mycoplasmas. *Journal of Bacteriology*. 102 (2): 306–310. PMC 247552. PMID 4911537.
- [158] Razin, S. *et al.* (1998). Molecular biology and pathogenicity of mycoplasmas. *Microbiology Molecular Biology Reviews*, 62: 1094-1156.
- [159] Rosenberg, B., L. Vancamp, and T. Krigas. 1965. Inhibition of cell division in *Escherichia coli* by electrolysis products from a platinum electrode. *Nature* 205:698–699.
- [160] Rossman, J.S. (2010). Influenza Virus M2 Protein Mediates ESCRT-Independent Membrane Scission. *Vol. 142 (6): 902-913.*
- [161] Rowe, E.S. (1983). Lipid chain length and temperature dependence of ethanolphosphatidylcholine interactions. *Biochemistry – ACS Publications*, 22(14): 3299-3305.
- [162] Russell, D.W. (1992). Cholesterol Biosynthesis and Metabolism. *Cardiovascular Drugs and Therapy*, 6(2): 103-110.
- [163] Saksena, S., Sun, J., Chu, T., and Emr, S. D. (2007). Emr, ESCRTing proteins in the endocytic pathway. *Trends Biochem. Sci.* 32, 561–573. doi: 10.1016/j.tibs.2007.09.010.
- [164] Sakuma, Y., Imai, M. (2011). Model system of self-reproducing vesicles. *Physical review letters*, 107(19), 198101.

- [165] Salipante, P.F. *et al.* (2014). Vesicle deformation in DC electric pulses. *Soft Matter*, 10, 3386.
- [166] Samson, R. Y., Obita, T., Freund, S. M., Williams, R. L., and Bell, S. D. (2008). A role for the ESCRT system in cell division in archaea. *Science* 322, 1710–1713. doi: 10.1126/science.1165322.
- [167] Samson, R. Y., Obita, T., Hodgson, B., Shaw, M. K., Chong, P. L., Williams, R. L., *et al.* (2011). Molecular and structural basis of ESCRT-III recruitment to membranes during archaeal cell division. *Mol. Cell* 41, 186–196. doi: 10.1016/j.molcel.2010.12.018.
- [168] Sanchez-Migallon, M. P., Aranda, F. J., and Gomez-Fernandez, J. C. (1995). The dissimilar effect of diacylglycerols on Ca (2+)-induced phosphatidylserine vesicle fusion. *Biophys. J.* 68:558.
- [169] Schmidt, N.W. *et al.* (2013). Influenza Virus A M2 Protein Generates Negative Gaussian Membrane Curvature Necessary for Budding and Scission. *J. Am. Chem. Soc.*, 2013, 135 (37), pp 13710–13719. DOI: 10.1021/ja400146z.
- [170] Schrödinger, Erwin (1944). *What is Life?*. Cambridge University Press. ISBN 978-0-521-42708-1.
- [171] Schwan H.P., Sher L.D. (1969). Alternative-current field-induced forces and their biological implications. *J. Electrochem. Soc.* 1969;116:22C–6C.
- [172] Scott, A., Noga, M.J., De Graaf, P., Westerlaken, I., Yildirim, E. and Danelon, C.. Cell-free phospholipid biosynthesis by gene-encoded enzymes reconstituted in liposomes. *PLoS One*. 2016 Oct 6;11(10):e0163058.
- [173] Seddon, J.M. (1990). Structure of the inverted hexagonal (HII) phase, and non-lamellar phase transitions of lipids. *Biochimica et Biophysica Acta* 1031, 1-69.
- [174] Servuss, R. M., Harbich, W. and Helfrich, W. (1976). Measurement of the curvature-elastic modulus of egg lecithin bilayers. *Biochim. Biophys. Acta* 436; 900.
- [175] Seto, S. *et al.* (1999). Partitioning, movement and positioning of nucleoids in *Mycoplasma capricolum*. *Journal of Bacteriology*, 181.
- [176] Shimizu, Y. *et al.* (2001). Cell-free translation reconstituted with purified components. *Nat. Biotechnol.* 19: 751–755.
- [177] Shimizu Y, Kuruma Y, Kanamori T, Ueda T (2014) The PURE system for protein production. *Methods Mol Biol* 1118:275–284.
- [178] Shimshick, E.J. *et al.* (1973). Lateral Phase Separation in Phospholipid Membranes. *Biochemistry*, Vol. 12 (12), 2351-2360.

- [179] Shitamichi, Y. *et al.* (2009). Mechanical properties of a giant liposome studied using optical tweezers. *Chemical Physics Letters*, 479(4-6), 274-278.
- [180] Siegel, D.P. (1984). Inverted micellar structures in bilayer membranes. Formation rates and half-lives. *Biophys J*, 45: 399-420.
- [181] Siegel, D.P. (1986). Inverted micellar intermediates and the transitions between lamellar, cubic, and inverted hexagonal lipid phases. II. Implications for membrane-membrane interactions and membrane fusion. *Biophys J*, 49: 1171-1183.
- [182] Siegel, D.P. *et al.* (1986). Inverted micellar intermediates and the transition between lamellar, cubic, and inverted hexagonal lipid phases. II. Implications for membrane-membrane interactions and membrane fusion. *Biophysical Journal*, 49(6): 1171-1183.
- [183] Siegel, D.P. *et al.* (1993). Energetics of intermediates in membrane fusion: comparison of stalk and inverted micellar intermediate mechanisms. *Biophys J.*, 65(5):2124-40.
- [184] Siegel, D.P. *et al.* (2004). The Gaussian Curvature Elastic Modulus of N-Monomethylated Dioleoylphosphatidylethanolamine: Relevance to Membrane Fusion and Lipid Phase Behavior. *Biophysical Journal*, Vol. 87 (1): 366-374.
- [185] Simon, S.A. *et al.* (1982). Influence of cholesterol on water penetration into bilayers. *Science* 216, 65-67.
- [186] Simon, C. *et al.* (2018). Cytoskeleton-mediated membrane reshaping in endocytosis. *J. Phys. D: Appl. Phys.* 51, 343001.
- [187] Singer, S.J. and Nicolson, G.L. (1972). The Fluid Mosaic Model of the Structure of Cell Membranes. *Science*, Vol. 175, 720-731.
- [188] Stoicheva, N.G. *et al.* (1994). Electrofusion of cell-size liposomes. *Biochimica et Biophysica Acta (BBA)- Biomembranes*, 1195(1): 31-38.
- [189] Stüeken, E.E. *et al.* (2013). Did life originate from a global chemical reactor? *Geobiology*, 11(2): 101-126.
- [190] Sunami, T. *et al.* (2018). Flow Cytometric Analysis To Evaluate Morphological Changes in Giant Liposomes As Observed in Electrofusion Experiments. *Langmuir*, 34: 88-96.
- [191] Szostak, J.W., Bartel, D.P. and Luisi, P.L. (2001). Synthesizing Life. *Nature*, 409, 387-390. <http://dx.doi.org/10.1038/35053176>.
- [192] Szwedziak, P. *et al.* (2014). Architecture of the ring formed by the tubulin homologue FtsZ in bacterial cell division. *eLife* 3, e04601. doi:10.7554/eLife.04601pmid:25490152

- [193] Taffin, D.C. *et al.* (1989). Electrified Droplet Fission and the Rayleigh Limit. *Langmuir*, 5(2): 376-384.
- [194] Taleb, M. *et al.* (1999). Crystallization of proteins under an external electric field. *Journal of Crystal Growth*, 200(3-4): 575-582.
- [195] Tamm, L.K. *et al.* (2000). Viral fusion peptides: a tool set to disrupt and connect biological membranes. *Biosci. Rep.*, 20: 501-518.
- [196] Tan, Y.-C. *et al.* (2003). Controlled fission of droplet emulsion in bifurcating microfluidic channels. TRANSDUCERS '03. 12th International Conference on Solid-State Sensors, Actuators and Microsystems. Digest of Technical Papers (Cat. No.03TH8664). DOI: 10.1109/SENSOR.2003.1215245.
- [197] Teissie, J. *et al.* (1999). Electroporabilisation of cell membranes. *Advanced Drug Delivery Reviews*, 35(1): 3-19.
- [198] Terasawa, H., Nishimura, K., Suzuki, H., Matsuura, T., and Yomo, T. (2012). Coupling of the fusion and budding of giant phospholipid vesicles containing macromolecules. *Proc. Natl. Acad. Sci. USA* 109, 5942–5947.
- [199] Thaokar, R.M. *et al.* (2010). Rayleigh instability of charged drops and vesicles in the presence of counterions. *Phys. Fluids* 22, 034107.
- [200] Tilcock, C.P.S. *et al.* (1982). Influence of cholesterol on the structural preferences of dioleoylphosphatidylethanolamine-dioleoylphosphatidylcholine systems: A phosphorus 31 and deuterium nuclear magnetic resonance study. *Biochemistry* 21, 4596-4601.
- [201] Tilcock, C.P.A., *et al.* (1984). Influence of cholesterol esters of varying unsaturation on the polymorphic phase preferences of egg phosphatidylethanolamine, *Chem. Phys. Lipids* 35: 363-370.
- [202] Träuble, H. *et al.* (1974). Electrostatic Effects on Lipid Phase Transitions: Membrane Structure and Ionic Environment. *PNAS*, 71(1) 214-219. <https://doi.org/10.1073/pnas.71.1.214>.
- [203] Trifonov, Edward N. (2012). "Definition of Life: Navigation through Uncertainties". *Journal of Biomolecular Structure Dynamics*. 29 (4): 64750. doi:10.1080/073911012010525017. Retrieved on 12 January 2019.
- [204] Untracht, S.H. *et al.* (1977). Molecular Interactions between Lecithin and Sphingomyelin. *The Journal of Biological Chemistry*, 252(13): 449-4457.
- [205] Urakami, N. *et al.* (2018). Molecular mechanism of vesicle division induced by coupling between lipid geometry and membrane curvatures. *Soft Matter*, 14(16): 3018-3027.
- [206] Verkleij, A.J. (1984). Lipidic Intramembranous Particles. *Biochem Biophys Acta*, 779: 43-63.

- [207] Verkleij, A. (1986). Phospholipid Research and the Nervous System (Horrocks, L A, Freysz. L and Toffano, G, eds), pp 207-216. Livlma Press, Padova.
- [208] Vicente, M. *et al.* (2006). The order of the ring: assembly of Escherichia coli cell division components. *Molecular Microbiology*, 61(1): 5-8.
- [209] Vitkova, V. *et al.* (2006). Sugars in the Aqueous Phase Change the Mechanical Properties of Lipid Mono- and Bilayers, 449(1): 95-106.
- [210] Vitkova, V. *et al.* (2012). BENDING RIGIDITY OF LIPID MEMBRANES AND THE pH OF AQUEOUS SURROUNDINGS. Tome 65, No 3.
- [211] Vlahovska, P.M. *et al.* (2009). Electrohydrodynamic Model of Vesicle Deformation in Alternating Electric Fields. *Biophysical Journal*, 96 (12): 4789-4803.
- [212] Voldman J. (2006). Electrical forces for microscale cell manipulation. *Annu. Rev. Biomed. Eng.*; 8: 425–54.
- [213] Voth, G.A. *et al.* (2018). Simulations of N-BAR protein interactions with membranes. *J. Phys. D: Appl. Phys.* 51, 343001.
- [214] Walter, K.S., Fricker, E.J., and Fricker, C.R. (1994). Observations on the use of a medium detecting β -glucuronidase activity and lactose fermentation for the simultaneous detection of Escherichia coli and coliforms. *Lett. Appl. Microbiology*, 19, 47-49.
- [215] Wang, W. *et al.* (2008). Evidence of Cholesterol Accumulated in High Curvature Regions: Implication to the Curvature Elastic Energy for Lipid Mixtures. *Biophysical Journal*, 94(11): 4577.
- [216] Wang, J.D. *et al.* (2009). Metabolism, cell growth and the bacterial cell cycle. *Nature Reviews Microbiology*, 7: 822-827.
- [217] Watson, J.W. *et al.* (1953). Molecular Structure of Nucleic Acids: A Structure for Deoxyribose Nucleic Acid. *Nature* volume 171, pages 737–738.
- [218] Watts J. W. and King J. M. (1984). A simple method for large-scale electrofusion and culture of plant protoplasts. *Biosci. Rep.* 4: 335–342.
- [219] Wilschut, J., Düzgünes, N., Fraley, R. Papahadjopoulos, D. *Biochemistry* 19, 6011–6021 (1980).
- [220] Wilschut, J. (2018). Thermal deformation and division of gene-expressing liposomes. Master thesis Danelon Lab.
- [221] Wollert, T., Wunder, C., Lippincott-Schwartz, J., and Hurley, J. H. (2009). Membrane scission by the ESCRT-III complex. *Nature* 458, 172–177. doi: 10.1038/nature07836.

- [222] Wollert, T., and Hurley, J. H. (2010). Molecular mechanism of multivesicular body biogenesis by ESCRT complexes. *Nature* 464, 864–869. doi: 10.1038/nature08849.
- [223] Xie, T.D., and T. Y. Tsong. 1990. Study of mechanisms of electric field-induced DNA transfection II. Transfection by lowamplitude, low-frequency alternating electric fields. *Biophys. J.* 58:897-903.
- [224] Xu, W. *et al.* (2016). A Programmable DNA Origami Platform to Organize SNAREs for Membrane Fusion. *J. Am. Chem. Soc.*, 138(13), 4439-4447.
- [225] Yang L, Huang HW. A rhombohedral phase of lipid containing a membrane fusion intermediate structure. *Biophys. J.* 2003; 84:1808-1817.
- [226] Yeagle, P.L. *et al.* (1977). Differential effects of cholesterol and lanosterol on artificial membranes. *Proc. Natl. Acad. Sci. USA*, 74: 4924-4926.
- [227] Zachrisson A. and Bornman C. H. (1984). Application of electric field fusion in plant tissue culture. *Physiol. Plant* 61: 314–320.
- [228] Zeno, W.F. *et al.* (2018). Membrane remodeling by protein crowding. *J. Phys. D: Appl. Phys.* 51, 343001.
- [229] Zhu, T.F., and Szostak, J.W. (2009). Coupled growth and division of model protocell membranes. *J. Am. Chem. Soc.* 131, 5705–5713.
- [230] Zieske, K. *et al.* (2013). Reconstitution of Pole-to-Pole Oscillations of Min Proteins in Microengineered Polydimethylsiloxane Compartments. *Angewandte Chemie International*, 52(1): 459-462.
- [231] Zieske, K. *et al.* (2014). Reconstitution of self-organising protein gradients as spatial cues in cell-free systems. *Elife*, 03949.
- [232] Zimmerberg, J. *et al.* (2006). How proteins produce cellular membrane curvature. *Nature Reviews Molecular Cell Biology*, 7, 9-19.
- [233] Zimmermann, U. (1982). Electric field-mediated fusion and related electrical phenomena. *Biochimica et Biophysica Acta (BBA) - Reviews on Biomembranes*; 694: 227–77.
- [234] Zong, W. *et al.* (2018). Deformation of giant unilamellar vesicles under osmotic stress. *Colloids and Surfaces B: Biointerfaces*, 172, 459-463.

Part III

Experimental Approach towards Division in Gene-Expressing Liposomes

Abstract

In respect of the reconstitution of division in a prospective minimal cell, we created a protocol for the elongation of DO-liposomes (DOPC, DOPE, DOPG, 18:1 Cardiolipin, PEG-biotin, Texas Red) as a first step towards liposome division, and as a means to facilitate the study of a minimal division. We observed that cholesterol and extra-liposomal sucrose may affect this *E. coli*-based lipid composition in its morphological stability in the presence of gene expression (eYFP) through the PURE $_{frex2.0}$ system. To assess the stability in terms of elongation of the liposomes as well as their expression, we conducted a triplicate study consisting of counting liposomes in confocal microscopy images for cholesterol (30%) and non-cholesterol containing liposomes in an external sucrose concentration range from 0 to 200 mM. Additionally, we showed that the addition of sucrose from the beginning of expression initiation does not inhibit expression. The results were further validated by imaging flow cytometry. We found cholesterol to be an important factor in the establishment of liposome elongation that may be compatible with and facilitating the *in vitro* study of amongst others the bacterial Min system. Further experiments on the compatibility of cholesterol in DO-liposomes with FtsZ bundle formation appear to be promising.

Keywords: *(Gene-Expressing) Liposomes, Division, Membrane (Electro) Deformation, Osmotical Coupling, Cholesterol Membrane Partitioning, Imaging flow cytometry, Confocal microscopy, FtsZ, Min system, Minimal Cell.*

11 Introduction

As has been described in the review part, liposome division has been observed by several groups [e.g. Döbereiner *et al.*, 1993; Sakuma *et al.* 1993]. However, for the establishment of gene-expression-compatible and controlled binary fission, a combination of several externally and/or internally fission inducing techniques may be necessary. One initial step towards binary fission is elongation as requirement to increase the relative area-to-volume ratio. Elongation is also present in bacteria such as *E. coli*, where a protein complex, the elongasome, that is closely related to the division machinery complex, ensures a controlled morphology facilitating division. In the reconstitution of division in a (prospective) minimal cell however, the full elongasome and divisome complexes as present in *E. coli* might not be the preferred solution. In the attempt to establish division therefore, it would be an advantage to establish these properties of elongation and/or division in a different way, as described in the review part.

In reviewing the several mechanisms for division (part II), some promising techniques for division induction were found to be electrodivision and osmotic division. Hence, we chose to further experimentally investigate these techniques and their compatibility with gene-expressing DO-liposomes (DOPC, DOPE, DOPG, 18:1 Cardiolipin, PEG-biotin, Texas Red).

Since osmotic division has usually been described in combination with cholesterol in the membrane [e.g. Döbereiner *et al.*, 1993], we chose to incorporate cholesterol in the DO-liposomes. For both the cholesterol/osmotic approach as well as for the electrical approach we studied changes in membrane properties concerning morphology and how these morphologies may facilitate, or counteract the study of the *E. coli* division system to allow for possible coupling of externally division stimulating techniques with some form of internal regulation that is in turn a little less complex than occurring in the natural situation. The morphology changes were initially assessed with confocal microscopy that allows for relatively high-resolution imaging, but lacks on more quantitative aspects. Additionally, imaging flow cytometry was employed to assess morphological changes more quantitatively.

In respect of the externally controlled facilitation of division, elongation of gene-expressing liposomes (DOPC, DOPE, DOPG, 18:1 Cardiolipin, PEG-biotin, Texas Red) is expected to aid the study of *E. coli* division protein systems, such as the Min system and FtsZ ring formation, concerning the similarly elongated shape that is imposed on *E. coli* through the elongasome protein complex. In this way, the present study would provide a platform for division in a minimal cell and/or for further study towards the reconstitution of more complexly regulated and encoded division systems in liposomes.

The experimental questions we try to answer are the following:

-Can we experimentally establish controllable liposome elongation that is compatible with gene expression in the PURE system [Shimizu *et al.*, 2001] through electrical stimuli and/or the addition of cholesterol and/or sucrose to the liposomes? (see figure 11.1)

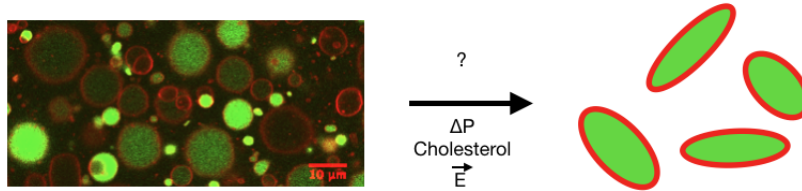


Figure 11.1 Schematic drawing of the initial (mostly spherical) liposome situation and the desired more elongated situation.

-Can we experimentally establish controllable liposome elongation that is compatible with the organisation of membrane proteins essential for *E. coli* division (e.g. FtsA and MinD)?

-Can we experimentally establish liposome division that is compatible with gene expression in the PURE system?

12 Material and Methods

12.1 Preparing GUVs

GUVs were prepared in a 3-step method containing an adapted process of natural swelling [Kumazawa *et al.*, 1996]. In the liposome formation process firstly, lipid-coated silica beads (212-300 μm , acid-washed, Sigma Aldrich) are produced that we find to be stable for several months stored under argon at $-20\text{ }^{\circ}\text{C}$. Subsequently, the lipid-coated beads are used in a 2 hour natural swelling process on ice with amongst others the PURE system, more specifically PURE_{free}2.0 to allow for the incorporation of the essential components for transcription and translation. Lastly, four freeze-thaw cycles are applied to destroy multilamellar vesicles [Kersbergen *et al.*, 2017], before they are added to the chamber with a cut pipet tip for imaging, or to the reaction tube in case of imaging flow cytometry, with a constant fraction of DNase to inhibit extraliposomal gene-expression.

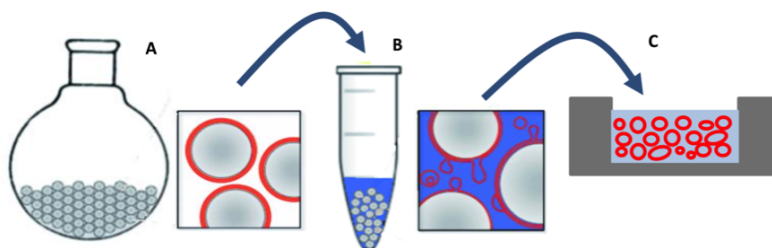


Figure 12.1.1 Schematic representation of GUV preparation. (A) Silica beads in a round bottom flask are first coated with a lipid film by drying a lipid mixture in the rotary evaporator. (B) Subsequently, a 2 hour natural swelling process is initiated that allows for the incorporation of amongst others DNA and essential components from the PURE system. After this process, four subsequent freeze-thaw cycles are applied to destroy multilamellar structures and the liposome mixture is transferred to a glass chamber for imaging with added DNase to prevent extraliposomal gene-expression [Figure adapted by Wilschut *et al.*, 2018 from Nourian *et al.*, 2013].

12.2 Preparing Lipid-Coated Silica Beads (\pm cholesterol)

The lipid-coated silica beads were prepared by adding the components in table 12.2.1 to a round bottom flask along with twice the amount of chloroform to enhance the lipid release from the pipet tips. Subsequently, a 2.5 chloroform:1 Rhamnose-methanol (100 mM) addition was made after which 600 mg of 212-300 μm acid-washed silica beads (Sigma Aldrich) were added. The round bottom flask was then placed in the rotary evaporator where the pressure was slowly regulated to 200 mbar at which the evaporation was completed in 2 hours. With a clean spatula the lipid-coated beads were then transferred to 1.5 mL tubes that were put on vacuum overnight, after which they were stored under argon at -20

$^{\circ}\text{C}$ for at least one night before use. This was carried out for both lipid-coated beads with cholesterol (30%) and without cholesterol as separately represented in table 12.2.1. For the lipid/sterol nomenclature see Appendix A.

Table 12.2.1 Lipid mixtures used for the preparation of lipid-coated silica beads (-/+ cholesterol respectively). See Appendix A for the lipid/sterol nomenclature.

Lipid (/sterol)	Fraction (mol%) -cholesterol	Fraction (mol%) + 30% cholesterol
DOPC	50	35
DOPE	36	25.2
DOPG	12	8.4
18:1 Cardiolipin	2	1.4
Cholesterol	0	30
Total	100	100
Lipid	Fraction (mass%)	Fraction (mass%)
Texas Red	0.5	0.5
PEG-biotin	1	0.5

12.3 Swelling and Freeze-Thaw cycles

The samples were generally prepared either on the day of imaging, or (rarely) on the day before. The lipid beads were first placed in the dessicator for at least 30 min to ensure dry beads giving optimal sample quality. Subsequently, the swelling solution was prepared in a 0.5 μL tube according to table 12.3.1.

Table 12.3.1. Swelling solution composition YFP-expression.

Reactant	Volume (μL)
PURE <i>flex</i> 2.0 Buffer (Solution I)	10
PURE <i>flex</i> 2.0 Enzymes (Solution II)	1
PURE <i>flex</i> 2.0 Ribosomes (Solution III)	2
MilliQ (fresh, RNase free)	to a final volume of 20 μL
DNA construct: pUC57-T7-eYFP-LL-Spinach, or T7-eYFP-LL-Spinach	to a final concentration of 15 ng/ μL to a final concentration of 5 ng/ μL

The pUC57-T7-eYFP-LL-Spinach plasmid was used in all YFP expression experiments that were imaged with confocal microscopy, except for the kinetic studies, where YFP expression was only used to access relative membrane and

expression stability, and imaging flow cytometry experiments that used their own reference. For all imaging flow cytometry experiments the T7-eYFP-LL-Spinach construct was used.

In some cases, when the only subject of interest was the deformation of the liposomes, irrespective of gene-expression, the swelling solution consisted of homemade pure buffer only (potassium glutamate, magnesium acetate, HEPES; pH 7.6). Similarly, the swelling solution differed for FtsZ and Min experiments, as described in their respective sections. The rest of the process is identical in each case.

Upon mixing the swelling solution by carefully pipetting up and down once, 10 mg of lipid-coated beads were added to the solution. Every time it was made sure that all beads were fully hydrated on the bottom of the swelling solution. Subsequently, the beads were slowly rotated to the edges of the solution several times every 30 minutes over a course of 2 hours (see figure 12.3.1). The process was then finalised by applying four freeze-thaw cycles, meaning that the samples were instantly frozen in liquid nitrogen four times in order to destroy multilamellar structures [Kersbergen *et al.*, 2017].

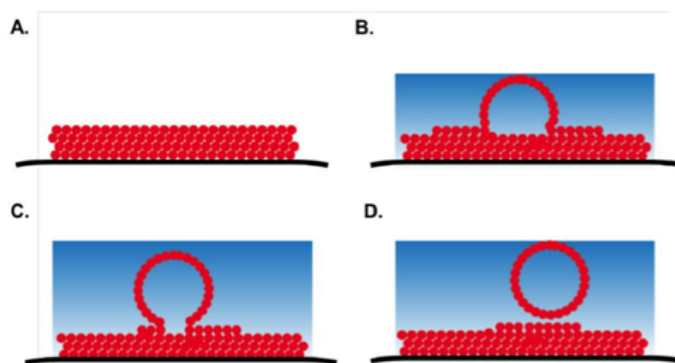


Figure 12.3.1 Natural swelling as occurring on the silica beads. (A) Multiple lipidic layers form on the solid surface on the beads during bead preparation. (B, C, D) During swelling and rotation the lipid films become hydrated and may dissociate from the lipid-coated beads under the formation of liposomes. [Figure adapted by Wilschut *et al.*, 2018 from Kockelkoren *et al.*, 2018].

The supernatant (generally 7.5 μL of this solution) in the tubes was then transferred to a hand-drilled glass chamber with a reaction volume of several tens of microlitres (or tube for imaging flow cytometry). In pipetting the liposome solution, consistently a cut pipet tip was used to reduce shear forces rupturing the liposomes. DNase (15 μL liposome solution: 1 μL DNase; generally 0.5 μL) was then immediately added to the solution to reduce extraliposomal DNA expression.

In case of direct imaging, the chamber was then placed at the confocal microscope at around 35 $^{\circ}\text{C}$, or rarely first in an incubator at 37 $^{\circ}\text{C}$ in case the

microscope was in use, to induce gene-expression for 3 hours before the start of imaging. Since the liposomes were generally not attached to the surface, although the lower temperature, the former method at the microscope was preferred to allow liposomes to precipitate a little.

For these experiments, the glass chamber was closed by a coverslip to limit evaporation causing an uncontrollable increase in external osmolarity as well as a possible dry-out of the sample.

12.4 Osmolarity assays

An external osmolarity range of 0-200 mM sucrose was chosen on top of the internal osmolarity provided by the external PURE $flex$ 2.0 system [Shimizu *et al.*, 2001]. Sucrose was chosen instead of e.g. LiCl, KCl or glucose based on results presented by Zong *et al.* (2018) that showed higher permeabilities for DMPC liposomes with other osmotically active agents. Higher permeabilities might induce larger shape deformations, however too large molar water fluxes might complicate gene expression. Additionally, chloride ions might inhibit gene expression, leading to our choice for sucrose. The choice for 30% cholesterol was furthermore based around the maximal shape deformation as observed by Zong *et al.* (2018).

The osmolarity range was applied through consecutive additions of a 1 M sucrose solution in milliQ, on an 8 μ L liposome solution, this meant the addition of 0 μ L (0 mM), 0.9 μ L (100 mM), 1.1 μ L (200 mM) consecutively up to a total of 2 μ L 1 M sucrose solution on the total sample (200 mM sucrose). In order to have approximately the exact same sample as control, the sucrose additions were chosen to be applied during imaging.

When sucrose is added only during imaging however, one cannot be sure that the addition of sucrose does not directly or indirectly inhibit the YFP-expression as the YFP observed may be a sole result of what had already been synthesised before the sucrose addition. Therefore, alternatively, a single experiment was conducted to observe whether the addition of 200 mM sucrose before the initiation of YFP-expression would complicate the expression. In this case the sucrose was added immediately upon loading the liposome solution in the chamber, before incubation. In all osmolarity assays the preparation followed the guidelines as indicated in section 12.4, with beads that were at maximum 1.5 months old.

12.5 Kinetics

In order to study the morphological stability of the liposomes in time, two kinetic studies were carried out of 55 and 15 hours respectively for the YFP-expressing 30% cholesterol liposomes. In these experiments, a separate channel in the closed chamber was filled with 20 μ L milliQ to limit evaporation of the sample under study on these comparably long time scales. The imaging is in general complicated through the precipitation of larger GUVs in time on top of the objects of study. This is one of the reasons for the change of approach

towards imaging flow cytometry along the course of the research.

In all kinetic assays the preparation followed the guidelines as indicated in section 12.3, with beads that were at maximum 1.5 months old.

12.5.1 Surface functionalisation

In order to allow for the more long term stable study of individual liposomes and their morphology as necessary in these kinetic studies, the glass chambers were functionalized by initial washing with milliQ (10 μL), after which 10 minute incubation with BSA:BSA-biotin (1 mg/mL;10 μL) and Neutravidin (1 mg/mL; 10 μL) respectively followed, with intermediate double washing with milliQ (10 μL). Finally, the channels were washed three times with home made pure buffer (potassium glutamate, magnesium acetate, HEPES; pH 7.6; 10 μL) that was only removed just before adding the liposome solution.

12.6 Electrodeformation Approach

In literature, electrodeformation has been described for AC field strengths as low as 0.1 kV/cm [Aranda *et al.*, 2008]. In order to reconstitute such fields, we constructed two different chambers with copper electrodes that we connected to a wave generator producing 25 Vpp (max.) at 20 kHz (for a prolate shape [Aranda *et al.*, 2008]). For the initial 4.5 mm gap chamber, the applied potential resulted in an electric field strength of 0.03 kV/cm through the sample. To observe a possible increase in effect, a second chamber was constructed with a 1.5 mm gap, providing a field strength of up to 0.08 kV/cm given the limited application potential of the wave generator. More on the construction of the electrochambers can be found in Appendix B.

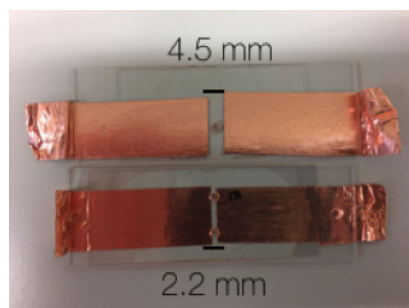


Figure 12.6.1. Electrodeformation chambers constructed with Dr. Roland Kieffer. A smaller electrode gap increases the field strength achievable with limited application potential. The electrodeformation approach was tested with pUC57-T7-eYFP-LL-Spinach expressing liposomes as described in section 12.3.

12.7 FtsZ bundle formation

FtsZ bundle and/or ring formation was studied in both 30% cholesterol containing and non-cholesterol containing liposomes as given by table 12.7.1. The rest of the reaction conditions was identical to what was described in section 12.3.

Table 12.7.1. Swelling solution composition for FtsA, ZapA coexpressing liposomes under the addition of purified FtsZ protein.

Reactant	Volume (μL)
PURE _{flex} 2.0 Buffer (Solution I)	10
PURE _{flex} 2.0 Enzymes (Solution II)	1
PURE _{flex} 2.0 Ribosomes (Solution III)	2
DNAk mix	1
FtsZ (45 μM)	1.33
rGTP (100 mM)	0.5
rATP (100 mM)	0.5
FtsA construct: 2018-01-05-C-ftsA-opt (≈ 43 nM)	2
ZapA construct: 2017-01-03-Pd-pUC57-zapA-opt (20 ng/ μL) (for +chol)/	2
2018-01-05-C-zapA-opt (≈ 100 nM) (for -chol)	2

In all experiments the preparation followed the guidelines as indicated in section 12.3, with beads that were at maximum 1.5 months old.

12.8 Min System

The Min system was studied in both 30% cholesterol containing and non-cholesterol containing liposomes under the reaction conditions as given by table 12.8.1. The rest of the reaction conditions was identical to what was described in section 12.3. We tested wave development for two different DNA concentrations to study the effect of total protein concentration on any observed wave.

Table 12.8.1. Swelling solution composition for MinD and MinE coexpressing liposomes under the addition of purified MinC protein.

Reactant	Volume (μL)
PURE <i>flex</i> 2.0 Buffer (Solution I)	10
PURE <i>flex</i> 2.0 Enzymes (Solution II)	1
PURE <i>flex</i> 2.0 Ribosomes (Solution III)	2
MilliQ (fresh, RNase free)	2.42
eGFP-MinC (20 μM)*	1.5
ATP (50 mM)**	1.5
MinEopt1 (356 nM)	1.68 (10)
MinD2 (158 nM)	1.9 (5)
DNAk mix	1.5

* eGFP-MinC was freshly diluted by taking 0.5 μL eGFP-MinC and 2.68 μL 1x home made PURE buffer (potassium glutamate, magnesium acetate, HEPES; pH 7.6)

** ATP was freshly diluted by mixing 1 μL ATP (100 mM) and 1 μL milliQ.

12.9 Cholesterol titrations

Non-expressing liposomes without cholesterol were synthesised according to the protocol described in section 12.3.

A 5 mg/mL cholesterol in chloroform solution was used for titration. The solution was vortexed before use every time and finally sonicated for 10 minutes to ensure even cholesterol distribution. Of this solution volumes between 0.5 and 3 μL were added to the liposome solution (8 μL). Finally, the resulting changes in morphology of the liposomes were assessed.

12.10 Laser Scanning Confocal Microscopy Imaging

The imaging was carried out with laser scanning confocal microscopy, using an A1R Nikon Confocal Microscope with a 100x oil immersion objective. Laser scanning confocal microscopy entails the projection of laser light on fluorescently labelled samples through a dichroic mirror and a rotating scan mirror. The light emitted by the sample is subsequently collected and passed through a pinhole to only detect in-focus light (see figure 12.10.1).

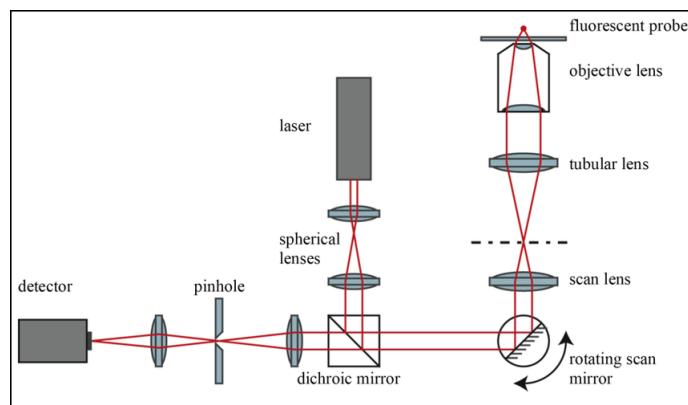


Figure 12.10.1. Schematic Image of a Confocal Microscope. During laser scanning confocal imaging, laser light is passed through a set of lenses and reflected on the the sample through a combination of a dichroic mirror and a rotating scan mirror. Fluorescent light coming from the sample after excitation is in turn passed through the dichroic mirror and detected by the detector through a pinhole that is important in determining the contrast and resolution as it blocks out-of-focus light [Ghoushchi *et al.*, 2015].

In confocal imaging, the 561, 488 and 640 nm lasers were used to visualise the Texas Red (liposome membrane), expressed YFP, and FtsZ (dye-Atto647) respectively. For visualising YFP, one would generally use the 514 nm laser. However, as in our set-up the 514 nm laser is coupled to the 561 nm laser, the lasers could not be used for imaging simultaneously, which is an inhibiting factor in the imaging of moving liposomes. As the overlap in filter spectrum of YFP with the 488 nm laser also allows for its visualisation, this setting was preferred and used in all cases. The exact laser settings used are indicated below each image individually, but were chosen to be reference compatible within the separate studies.

For the image acquisition, the NIS Elements Viewer Software accompanying the Nikon Microscope was used. To maintain constant sample temperature during acquisition, the temperature controller present at the microscope was furthermore employed.

12.10.1 Image Analysis

The image analysis was carried out in using the FIJI software [Schindelin *et al.*, 2012]. FIJI [Schindelin *et al.*, 2012] and its Adjust Brightness/contrast option (that allows for the adjustment of the upper and lower limits of the display through adjustment of the pixel value settings) has been used for viewing and analysing the acquired confocal microscopy images. In the more quantitative cases, the Regions of Interests (ROIs) were saved using the ROI Manager option in FIJI [Schindelin *et al.*, 2012], allowing for a reviewing process in the assessment of liposome morphology.

For 3D viewing, instead the NIS Elements Viewer was used as this software allowed for an apparent higher image contrast in these cases.

12.11 Cleaning Chambers

Cleaning the glass chambers happened in a 5-step sonication process as soon as possible after using the chambers to ensure the removal of amphiphilic components. The chambers were sonicated in a Sonerix digitec bath sonicator (Bandelin) for 10 minutes in a glass beaker that consecutively contained chloroform:methanol (1:1), Hellmanex (2%), KOH (1M), ethanol (70%) and milliQ. Afterwards the chambers were stored on milliQ in a closed environment, e.g. in falcon tubes.

The electrodeformation chambers were cleaned in the same step process, only by pipetting 3 times about 20 μL of the solutions described, instead of sonication to prevent contact of the copper electrodes with corroding agents.

12.12 Imaging Flow Cytometry

For the imaging flow cytometry experiments, the ImageStream®X Mark II Imaging Flow Cytometer was operated at Sanquin in Amsterdam. Here, the background solution in the flow cell was PBS and between the samples, the flow cell was flushed with milliQ. The liposomes were diluted 200 times for analysable liposome concentrations (< 300 million in 200 μL ; minimal reaction volume: 50 μL). Sometimes the liposomes were resuspended during the measurement by pipetting with a cut pipet tip.

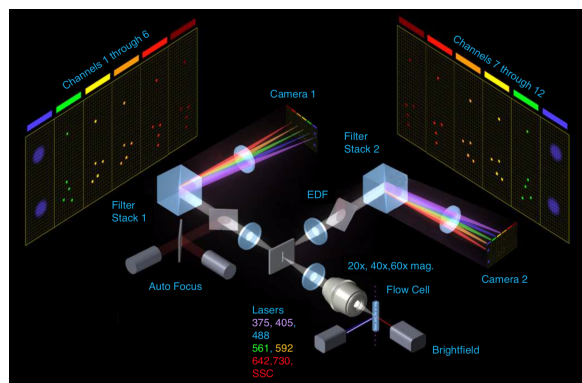


Figure 12.12.1. The optical layout of the ImageStream®X Mark II Imaging Flow Cytometer. The liposomes are transferred in a flow cell that confers a flow velocity 10 times lower than for regular flow cytometry, i.e. several centimeters per second. In the current settings a maximal objective magnification of 60 times can be achieved, allowing for enough magnification to identify the liposomes.

Over a course of two days, a triplicate study was carried out towards quantification of the morphological influence of (30%) cholesterol incorporation in a DO-lipid composition as given in table 12.2.1. The liposome formation was carried out according to section 12.3 (with the T7-eYFP-LL-Spinach construct), either on the day before (1st day, 1 experiment; to prevent expression on the day before, the liposomes were stored in the 4 ° fridge) or on the same day (2nd day, 2 experiments). Both times the liposome formation process was carried out at Delft University of Technology, where the samples had a 2-hour incubation at 37 ° C. After the incubation, the samples were carefully transferred in a polystyrene box by train and bus towards Amsterdam at ambient temperature, allowing for further incubation.

Apart from the samples under study, two reference samples were made each time. One for the Texas Red control, which was made with the liposome lipid beads from table 12.2.1 (without cholesterol) and a swelling solution consisting of home made PURE buffer (potassium glutamate, magnesium acetate, HEPES; pH 7.6) for cost efficiency. The other reference sample was for the YFP control and was made with lipid beads with the same lipid content as in table 12.2.1, lacking cholesterol and Texas Red.

Before the flow cytometry, the samples were each diluted 200 times (1:199 μL ; with cut pipet tip) in home made PURE buffer (potassium glutamate, magnesium acetate, HEPES; pH 7.6) to allow for analysis (i.e. the samples generated by natural swelling with a total reaction volume of 20 μL yield >300 million liposomes).

The operation was done on instrument ISX163 with 7 %-beads, 60x objective magnification, core tracking and focus tracking, along with the following laser settings:

- 488nm Laser: 100mW
- 561nm Laser: 20mW
- 642nm Power: 0mW
- 785nm Power: 22.38mW

In channel 2 (Ch02), the 488 nm laser was used to excite YFP. Texas Red was in turn excited by the 561 nm laser in channel 4 (Ch04). The 785 nm laser was used to generate side-scatter signal in channel 6 (Ch06), and a LED was used to generate bright-field images (Ch01).

12.12.1 PBS addition during initiation of expression

In the process of imaging flow cytometry, for a few seconds, the liposome solution is generally brought in contact with PBS buffer in a laminar flow. Ion exchange may in this respect alter the external conditions the liposomes are experiencing.

To study the possible effect of the PBS contact on the liposome shapes as compared to the other analyses made by laser scanning confocal microscopy, a single-time experiment was conducted to analyse the effects of PBS on liposome morphology of both 30% cholesterol and non-cholesterol containing liposomes prepared according to the protocol described in section 12.3, expressing the T77-eYFP-LL-Spinach construct. For this experiment 5 μL of the liposome solution was mixed with 2.5 μL (1x) PBS buffer and 0.5 μL DNase. Subsequently, the liposome morphology was again manually assessed, knowing that in the imaging flow cytometry the PBS contact is significantly less pronounced.

12.12.2 Imaging Flow Cytometry Analysis

The imaging flow cytometry data analysis was carried out with the IDEAS software® from Luminex corporation. Firstly, a selection was done to distinguish any type of liposome from the so-called speed beads that are running in the background of the flow. This can be done based on the Texas Red intensity that is characteristic for liposomes (and liposomal aggregates), along with a difference in refractive index in SSC (Side Scatter Imaging) that makes speed beads easy to distinguish.

Secondly, the brightfield image was analysed on contrast versus root mean square gradient and a threshold for contrast values was empirically selected (> 0.15). In this way, liposomes can be distinguished from dye precipitates.

Subsequently, the YFP intensity was determined, as in regular flow cytometry, by a dot plot of YFP intensity versus Texas Red intensity. Again, based on individual images, empirical thresholds were set.

Lastly, the elongation factors were determined, plotted, and further analysed for the different populations, giving further insight in differentiated morphological vesicle behaviour. For the total analyses steps, see Appendix F.

Later this year, Luminex Corporation ® will release a deep learning tool to better distinguish morphological phenotypes. For now, as an alternative we used the feature finder that recognises phenotypes and selects them in the populations based on the Fischer Linear Discriminant (see Appendix E). With the feature finder finally, the invagination patterns of the liposomes were analysed.

13 Results

The principle aim of all studies conducted was to develop a method that (stably and robustly) elongates gene-expressing liposomes. Furthermore, we sought for an elongation method that would either induce division of gene-expressing liposomes on itself, or demonstrate compatibility with the expressed Min system and FtsZ bundle/ring formation to allow for *E. coli*-like division reconstitution. In this respect, we focussed on electric fields, osmolarity, cholesterol, and, amongst others, tested compatibility with the membrane binding proteins FtsA and MinD.

13.1 Membrane cholesterol (30%) and increased external sucrose concentrations appear to independently elongate DO-liposomes, while showing compatible with YFP expression in the PURE system

Counting liposomes manually from confocal images gave initial insight in the morphological behaviour of cholesterol (30%) vesicles in comparison to their non-cholesterol containing counter parts. During the same experiments the vesicle morphology was traced under the addition of sucrose during imaging. In figure 13.1.1 characteristic images are depicted for liposome (no cholesterol) morphology under the addition of sucrose, resulting in more elongated shapes by eye. For the higher sucrose concentrations (i.e. 200 mM) several initial fission events were even observed in these samples without cholesterol that were not observed to this extend in the samples without cholesterol (see white arrows in the right image in figure 13.1.1). In as far these events constitute fission, it should be noted that the observed events do not equally pass the protein content to both daughter liposomes, as most are only relatively small buds.

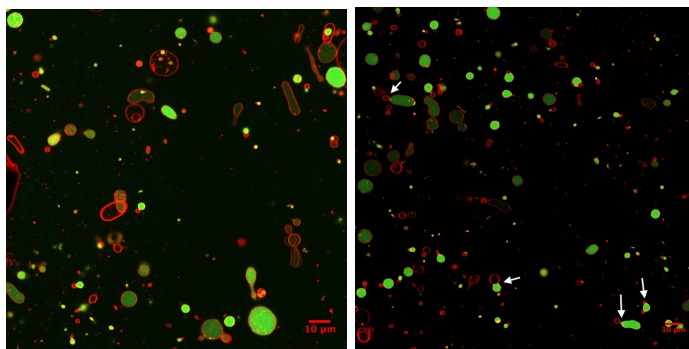


Figure 13.1.1 Liposome morphology for externally added sucrose concentrations of 100 mM and 200 mM respectively during imaging (no cholesterol, $t > 3$ hours). In the right image, white arrows indicate some of the most prominent expected fission events. Red: Texas Red Membrane, Green: expressed eYFP. (K-drive: 14-12-003/002 respectively; settings: 488nm-25%, and 561nm-10%).

For (30%) cholesterol liposomes, similar shape deformations occur under sucrose addition. Nevertheless, even without the addition of sucrose, the (30%) cholesterol liposomes appeared to behave more elongated as depicted in figure 13.1.2. For higher sucrose concentrations (200 mM), additionally relatively more invagination appeared as can be observed from figure 13.1.2. The invagination behaviour has not been quantified however, as the amount of liposomes in the 200 mM sucrose samples was generally reduced and highly variable. The elongation observed furthermore shows compatibility with liposomal gene-expression studies due to observable conserved lumen, and conserved numbers of YFP-expressing liposomes (see figures 14.1.2 and 14.1.3, right).

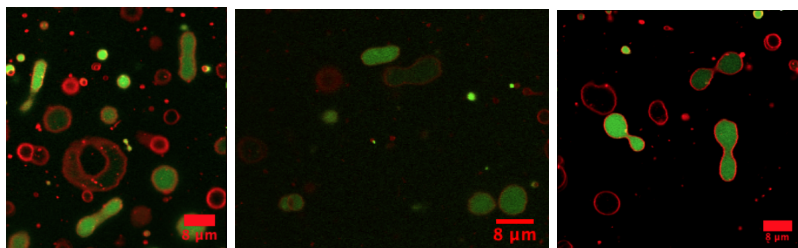


Figure 13.1.2 (30%) cholesterol liposomes under increasing sucrose concentrations (0, 100, 200 mM respectively) appear more elongated. Some more overview pictures are provided in Appendix C. Red: Texas Red Membrane, Green: expressed eYFP. (K-drive: 18-12-001; settings: 488nm-25%, and 561nm-10%).

Upon observing the apparent shape transitions invoked by sucrose and cholesterol, the morphology was quantified. The initial morphology quantification was carried out by manual selection and counting of all (regular, elongated and/or expressing) unilamellar liposomes of a triplicate study. For every data point on average 1000 liposomes have been counted that are representative for populations of thousands of liposomes. Here, the selection and counting was done based on visual appearance, meaning that in order to be quantified as elongated the aspect ratio's would have to exceed approximate values of 1.2. The results of the triplicate study are depicted in figure 13.1.3.

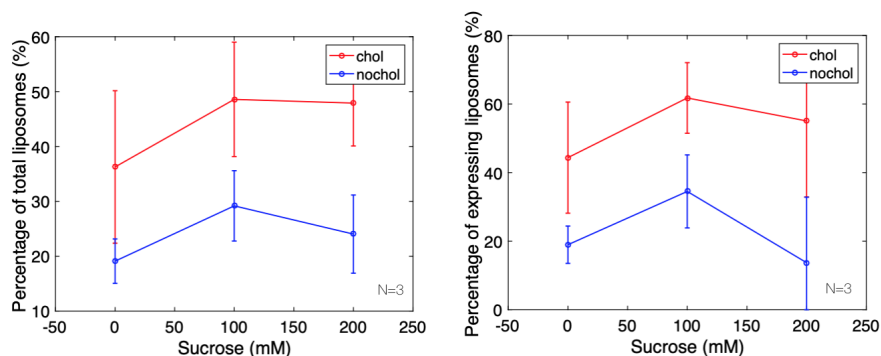


Figure 13.1.3 Membrane cholesterol (30%) and external sucrose concentrations (0-200 mM) independently affect liposome morphology in terms of elongation as determined by manual counting of confocal microscopy images ($N=3$). Here on average ± 1000 liposomes have been counted for each data point in different representative fields of view, and minimally 350 liposomes, if low abundant, such as in the case of higher sucrose concentrations (i.e. 200 mM). Note also that in the 2D confocal plane the elongation may be underestimated. **Left:** percentage of elongated liposomes on the total population; **Right:** percentage of elongated expressing liposomes on the total population of expressing liposomes.

From figure 13.1.3 it becomes apparent that cholesterol in itself does significantly increase the elongation rate from 19% to 36% (almost a 100% increase in elongation observed), and therefore on its own has a more pronounced effect on elongation than sucrose in the external environment that in itself only increases the elongation to 29%. Careful notion needs to be taken of the large error bars obtained that are partly inherent to the population heterogeneity obtained through the process of natural swelling.

Further notions include the stabilisation and even decrease in elongation in both expressing and non-expressing liposomes. The decrease in elongation for higher sucrose concentration may be twofold. On the one hand, elongated liposomes may preferentially divide, resulting in more spherical daughter liposomes. On the other hand, elongated liposomes may preferentially rupture and/or be more porous due to e.g. larger netto membrane areas.

In figure 13.1.3, the difference between cholesterol and non-cholesterol containing liposomes is especially interesting, indicating a stabilising effect of cholesterol, both in terms of liposome containment as well as in terms of membrane permeability of elongated liposomes. The percentage of expressing liposomes on the full population has thereby found to be largely independent of cholesterol and only decrease relatively marginally over the tested external sucrose range as depicted in Appendix C. Consequently, the decrease in elongation in the expressing population is not purely due to a decrease in the total amount of expressing liposomes. Instead, especially for the non-cholesterol liposomes, the amount of elongated expressing liposomes decreases.

With 2D confocal imaging however, it remains a challenge to observe division events (3D), if division even happens. During imaging we did observe some fission candidates (see Appendix D). No clear protocol for division has been established however, as more quantitative methods would be necessary to assess the liposome behaviour. Therefore, we further quantified liposome morphology with imaging flow cytometry as described in section 13.3.

13.1.1 The addition sucrose (200 mM) at transcription initiation shows uninhibited YFP expression, especially in cholesterol liposomes

To assess whether sucrose does not inhibit expression initiation and continuation on time scales relevant to expression and usual system analysis, 200 mM sucrose was added to the external environment of the liposomes from the initiation of expression. After 3 hours, as usual, the samples with and without cholesterol were imaged as depicted in figure 13.1.1.1.

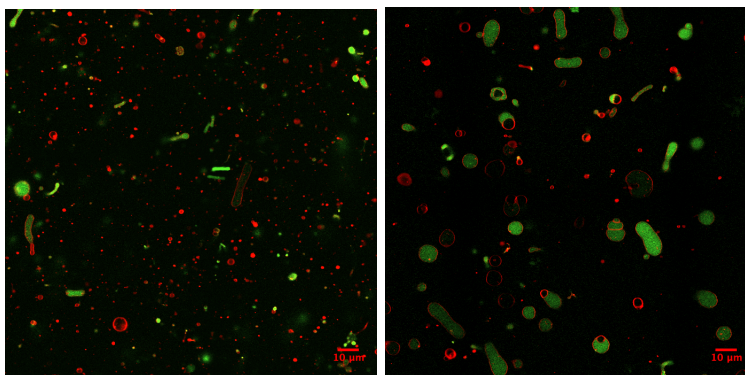


Figure 13.1.1.1 No-cholesterol and cholesterol liposomes (30 %) respectively in 200 mM sucrose from the initiation of expression after 3 hours. The liposome expression was not inhibited by the high sucrose exposure from the start of expression. Red: Texas Red Membrane, Green: expressed eYFP. (K-drive: 19-12-001; settings: 488nm-25%, and 561nm-10%)

As becomes apparent from figure 13.1.1.1, even with high concentrations of sucrose present in the liposome environment from transcription initiation, significant populations of expressing liposomes were observed. In line with earlier morphology behaviour observed, long presence of high sucrose concentrations decreases the amount of liposomes, which is an effect most pronounced for no-cholesterol liposomes in accordance with the results from figure 13.1.3.

13.2 Cholesterol (30%) liposomes may be stable for 5 hours in elongated shape

Two kinetic studies (55 and 15 hours respectively) were performed on eYFP expressing liposomes. In both cases, surface functionalisation was carried out

through the procedure described in section 12.5.1. The aim of the studies was to quantify the temporal stability of the elongated morphologies observed in earlier experiments. After 1 hour, $44\% \pm 17\%$ elongation was counted, compared to $17\% \pm 5\%$ after 5 hours and only a single liposome after 30 hours (N=2; 200 representative liposomes per data point counted). Two factors complicated the study, resulting in little temporal data. Firstly, the surface functionalisation in both cases did not appear to be highly efficient. Secondly, in time more and more (bigger) liposomes precipitated upon the liposomes under study, complicating the morphological temporal tracing of individual liposomes as well. Additionally, since all experiments for morphological quantification were carried out without surface functionalisation, the surface interaction may also have influenced the observed morphologies. We were still able to observe significant proportions of elongated liposomes up to five hours after expression initiation.

To circumvent the complications encountered in the kinetic studies, imaging flow cytometry was used to assess the liposome morphology after ± 24 hours, see section 12.12. Here it needs to be taken into account however that the liposomes have been transported to Amsterdam with the involved vibrations.

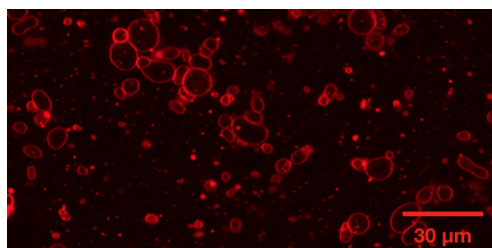


Figure 13.2.1 Kinetic morphology study on (30%) cholesterol liposomes after 1 hour (Texas Red Channel shown only). (K-drive: 09-01-001 and 14-01-001 respectively; settings: 488nm-25%, and 561nm-10%)

13.3 Imaging flow cytometry (IFC) studies corroborate that membrane cholesterol (30%) induces elongation and confirm cholesterol liposome stability over 24 hours

In total three imaging flow cytometry (IFC) runs were executed at Sanquin in Amsterdam. For the first run, the liposomes were prepared the day before the analysis, after which they were kept in the fridge to prevent YFP-expression initiation. From the first analysis that started 24 hours after the liposome formation, especially in the size category 7-10 μm (the sizes mostly observed with confocal microscopy), a stable 17% of cholesterol liposomes were found to still be elongated, compared to 8% in the non-cholesterol liposomes. Therefore, the stability kinetics are suspected to have been affected by either the surface functionalisation or the liposome precipitation.

For further quantitative studies, freshly prepared liposomes were analysed by IFC as described in Appendix F. From these IFC analyses we found that cholesterol indeed does appear to significantly elongate liposomes about 1.5 times more frequently than the non-cholesterol vesicles. Herein, vesicles of sizes below 1 and above 10 μm were not taken into consideration in this context as they are more likely not to be feasible liposomes.

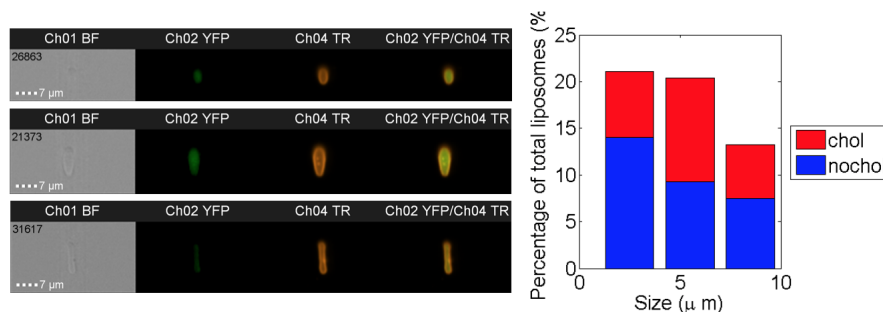


Figure 13.3.1 Elongation in cholesterol and non-cholesterol vesicles was quantified by imaging flow cytometry (see Appendix F). **Left:** Examples of expressing elongated cholesterol liposomes as imaged by IFC (60x magnification; bright field, 488 nm (expressed eYFP), 561 nm (Texas Red Membrane), and 488/561 nm channels respectively), **Right:** Cholesterol appears to elongate liposomes by a factor of 1.5 more frequently compared to vesicles without cholesterol (elongation criterion: $1.4 < \text{aspect ratio} < 5$; $N=1$).

Based on earlier flow cytometry quantifications by Dr. Zhanar Abil, the expected YFP-expression frequency amongst the liposomes, given the amount of DNA added, would be less than 10%. During the imaging flow cytometry studies performed however, lower expression percentages were found, which may be primarily attributed to a lacking maximum laser power for the 488 nm laser. Additionally, the expression percentages appeared to be significantly more affected by pipetting resuspension in the cholesterol vesicles than in the non-cholesterol vesicles as was observed by comparing the expression in subsequent IFC runs after additional resuspension. This observation may either be due to cholesterol inducing non-content preservative division, or due to a higher susceptibility to shear forces for the cholesterol-containing membranes. Overall, a steady 2% of expressing liposomes was observed in both populations.

Looking at figure 13.3.1 on the right, it appears that there may be a slight vesicle size dependence for elongation induced by membrane cholesterol. The elongation effects in intermediate liposomes may be a consequence of different factors. Firstly, its larger membrane areas may allow for more flexibility, especially if e.g. due to a certain minor degree of evaporation some osmotic pressure is build up. In these cases, cholesterol, which favours negative curvatures may

preferentially redistribute along the less curved areas, conferring a locally higher rigidity to the accumulation sides, thereby elongating the vesicle. Alternatively, the smaller vesicles may already be products of division events, after which elongation for these smaller vesicles is complicated due to the increased volume-to-area ratio compared to before the division. Up until now however, it remains hard to tell whether division is taking place.

13.3.1 PBS induces liposome morphology changes similar to sucrose and is compatible with the PURE system and liposomal YFP-expression

In the flow cell of the imaging flow cytometer, the liposomes are brought in contact with a PBS solution for a few microseconds in a laminar flow. To ensure that the ions in PBS do not interfere with expression or liposome stability, some confocal imaging data was gathered to confirm that PBS does not negatively affect expression or stability. Some images of the influence of PBS on the liposomes are depicted in figure 13.3.1.1. It should be noted that here the liposomes have been surrounded in PBS solution since expression initiation (> 3 hours), which is incomparable with the short term laminar flow after expression in the imaging flow cytometer. Therefore, the PBS is not expected to significantly influence the morphology, or expression.

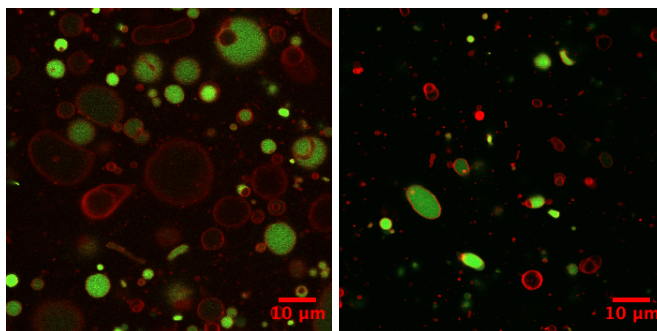


Figure 13.3.1.1 Liposomes in 1x PBS buffer since the onset of expression (> 3 hours). **Left:** no cholesterol, **Right:** 30% cholesterol (N=1). Differing liposome amounts may have been due to different sample quality. The YFP-expression does not appear to be inhibited by the PBS. Red: Texas Red Membrane, Green: expressed eYFP. (K-drive:29-01-PBS-cho1-002 and 29-01-PBS-+chol-001 respectively; settings: 488nm-25%, and 561nm-10%)

13.4 Electrodeformation requires specialised high voltage equipment

The electrodeformation approach has been attempted twice on cholesterol liposomes with different chambers. The first chamber with the wide 4.5 mm gap, did not result in visible liposome reorientation at the maximum supplied voltage of the oscilloscope (and $f=20$ kHz), see figure 13.4.1.

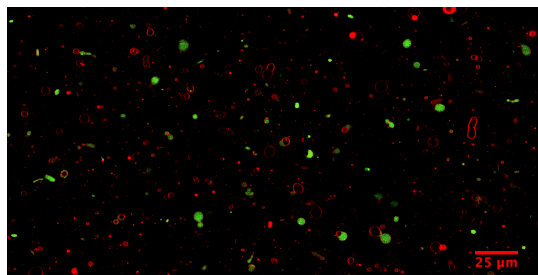


Figure 13.4.1 Liposomes in the first chamber with gap width 4.5 mm and maximum voltage supply at 20 kHz. The poles were located on the left and right respectively. At the given frequency (minor) prolate shape deformations would generally be observed, given high enough field strengths. Here, no significant effect of the electric field appears visible. Red: Texas Red Membrane, Green: expressed eYFP. (K-drive:4-12-+chol-005; settings: 488nm-25%, and 561nm-10%)

The second attempt was subsequently complicated by the fact that the 1.5 mm gap of the second chamber inhibited the focussing ability of the confocal microscope. The presence of cholesterol in the studied vesicles is not expected to be a complicating factor. For DOPC vesicles the electrodeformation extend under the addition of cholesterol has namely been found not to be significantly influenced [Gracia *et al.*, 2010]. After two chamber constructions, we decided to prioritise other research branches.

13.5 30%-cholesterol in the liposome membrane does not appear to inhibit FtsA binding and FtsZ polymerisation

The compatibility of cholesterol and membrane associated FtsZ polymerisation was subsequently investigated in liposomes that contain purified FtsZ-A647 and coexpress FtsA and ZapA. Although the sample qualities were generally poor, possibly as a result of undried silica beads in the dessicator, some apparent FtsZ polymerisation was found that seemed associated with the membrane through FtsA. Some polymers also appeared to not be attached to the membrane. However, these were generally colocalised with small membrane aggregates. The polymerisation was furthermore not covering full liposome membranes, but instead appeared regularly localised at the interface of two liposomes. It should be noted that similar behaviour was observed in the control experiments without cholesterol, implying the limited membrane attachment may not be due to cholesterol in the membrane. Alternatively, the observed increased 647 nm intensities may have been invoked through crosstalk between the channels as was sometimes observed. However, the latter explanation is not sufficient as can be seen from figure 13.5.1 (right), where the apparently attached FtsZ polymer

does not localise with the highest 561 nm intensity. Especially in the left image, an elongated liposome is imaged in which FtsZ polymerisation occurs at its pole as well as around mid-plane.

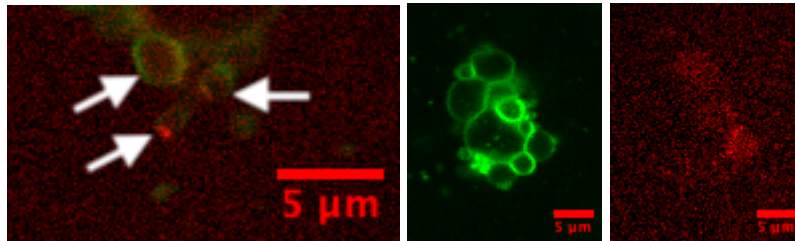


Figure 13.5.1 FtsZ appears to polymerise on a 30%-cholesterol membrane, especially at the interface of two liposomes. In the left image however, an elongated liposome appears to show FtsZ polymerisation at one pole as well as around mid-plane (white arrows). Red: FtsZ-A647, Green: Texas Red Membrane. (K-drive: 20-12-FtsZ+chol-001; 20-12-FtsZ+chol-001; settings: 561nm-1%, 640nm-8%)

Based on the described observations, cholesterol does not appear to inhibit the binding of FtsA to the membrane. The addition of the proteins may have altered the membrane characteristics towards less elongation and more spherical aggregation nevertheless. On the one hand, the observed, mostly spherical, aggregates may be a result of the desiccation process. On the other hand, the sample morphology appeared to be different from the YFP-expressing liposomes in every experiment. Therefore, even though the FtsA membrane attachment may not appear to be affected by the cholesterol in the membrane, the applicability of cholesterol to elongate liposomes to be constricted at mid-plane through FtsZ is limited.

Despite the highly limited sample qualities, in the regular liposome composition without cholesterol, FtsZ has been found to polymerise into a ring-structure in an individual liposome. Additionally, the ring-structure observed was colocalized with a septum that either may have been a result of a division event, or may be a result of higher local protein concentrations. The latter of the explanations may be more likely given the large ring size observed that most likely has not constricted to the extent that would be necessary for the induction of division on itself.

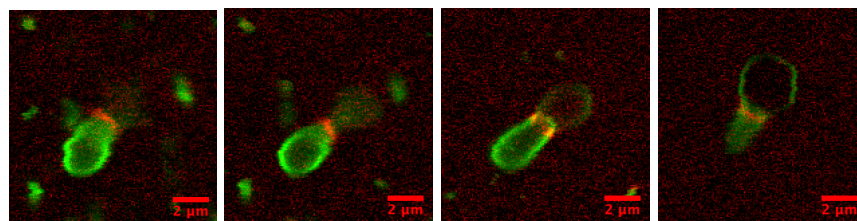


Figure 13.5.1.1 FtsZ may form a ring structure colocalised with a septum in the DO-lipid composition used. $z=0.2; 0.4; 1.0; 2.2 \mu\text{m}$ respectively. Red: FtsZ-A647, Green: Texas Red Membrane. (K-drive: 20-12-FtsZ-chol-003; settings: 561nm-1%, 640nm-8%)

13.6 MinD is recruited to 30% cholesterol membranes, although no waves have been observed

For the cholesterol sample, no waves have been observed for the MinE/MinD DNA ratio (10:5) used. In the dynamic behaviour of the Min system, the acquisition rate is critical to prevent aliasing. Based on values reported by Litschel *et al.* (2018) Min pulsing frequencies around 0.015 Hz may be expected for DOPC:DOPG (4:1) GUVs. However, as indicated by Yu *et al.* (2018) the Min waves are highly dependent on membrane composition and curvature. In accordance with the observed frequencies by Litschel *et al.* (2018), with a 0.5 Hz acquisition rate, waves have been observed before in the Danelon lab. As cholesterol slows down membrane diffusion [Filippov *et al.*, 2003], and affects membrane packing, the wave period characteristics for these liposomes may be influenced however, e.g. due to different binding kinetics of MinE. In the experiment that has been performed with the Min system it has not been elucidated how the Min oscillation period is affected by cholesterol due to the low to non-existent amount of waves observed in the control and the cholesterol samples respectively.

Membrane recruitment was observed in the cholesterol sample. The membrane recruitment may be an initial indication of compatibility of membrane cholesterol with the Min system. It remains to be elucidated whether cholesterol does not interfere with the association and dissociation of MinD, as the waves were not functional in the cholesterol sample (also not prominent in the control sample). As cholesterol partitions within the membrane leaflets, it may either influence MinD binding by its head group pointing outward, or by its induced change in membrane packing. Further experiments need to be performed to elucidate whether alterations in the superficial phospholipid membrane interface compaction as induced by cholesterol may alter association and dissociation rates of MinD, thereby possibly inhibiting the functionality of the Min system.

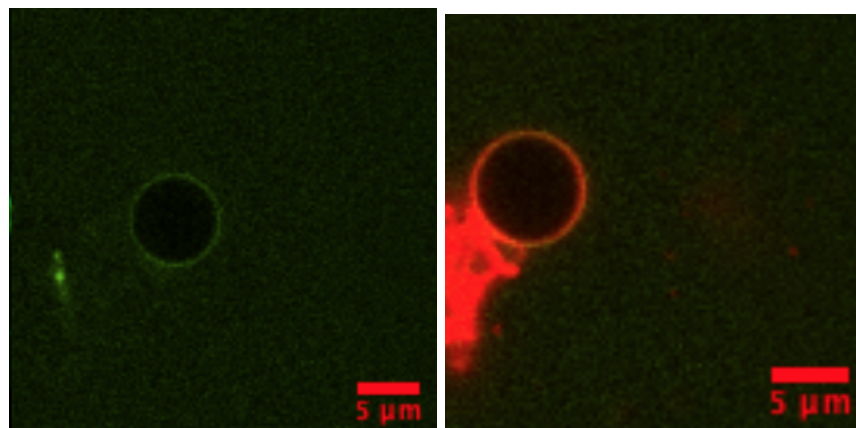


Figure 13.6.1 MinD is recruited to the cholesterol membranes as visualised through the fluorescently tagged MinC binding the MinD on the membrane. Waving was not observed in the extremely low density samples. **Left:** MinC (488nm) channel only. **Right:** Both channels show colocalisation of the recruited MinC with the Texas Red-stained membranes, although the sample quality was poor. Red: Texas Red Membrane, Green: eGFP-MinC. (K-drive: 21-02-MinDE+chol-002; settings: 488nm-1.0%, and 561nm-15%)

13.7 Sucrose addition (100mM) facilitates Min waves in pronouncedly elongated liposomes

Min waves have been reconstituted in liposome samples without cholesterol once. To study the compatibility of the Min waves with sucrose-induced elongation as studied before, 100 mM of sucrose was added to the environment of the liposomes. As a result, the liposomes showed wave-dependent elongation and relaxation consistent with earlier findings [Litschel *et al.*, 2018]. Although, MinD was generally observed attached to the membrane in the elongated liposome state, one observation showed the opposite phenomenon, having MinD recruited to the membrane only in the spherical state. Consequently, it could be speculated that it is a flow rather than the protein binding that induces the temporal shape deformation. The average oscillation frequency observed was $0.05 \text{ Hz} \pm 0.008 \text{ Hz}$.

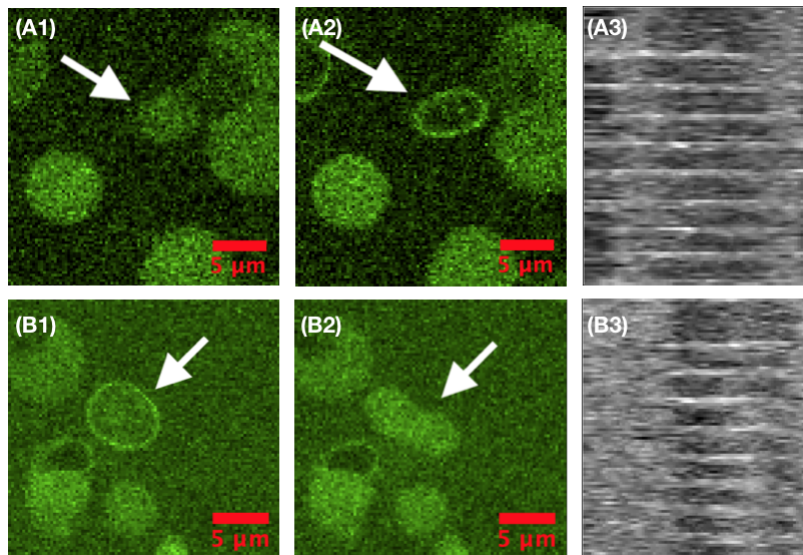


Figure 13.7.1 Min waves in elongated liposomes in 100 mM sucrose. Vesicle A demonstrates MinD recruitment in elongated liposome state, whilst vesicle B shows the exact opposite behaviour. A3 and B3 represent the kymographs of the two liposomes, showing regular oscillations of period $0.05 \text{ Hz} \pm 0.008 \text{ Hz}$. Green: eGFP-MinC (K-drive: 13-03-1016sucrose001(t=36 and 39)/003 (t=1 and 3) respectively)

13.8 Direct cholesterol addition to the liposome environment destroys the liposomes

To put the findings of cholesterol incorporation in the membrane in the context of a minimal cell, it was furthermore attempted to supply liposomes with cholesterol from the external environment, as cholesterol synthesis involves a 37-step synthesis process [Russell *et al.*, 1992]. On multiple occasions cholesterol titrations were therefore performed with 5 mg/mL cholesterol in chloroform. Of the solution 1-3 μL were added to the 8 μL reaction volumes. Everytime however, destruction of the sample followed as depicted in figure 13.8.1. At the time, we explained the observed behaviour as a consequence of the external viscosity of the sample that instantly increases such that the liposome membranes destabilise and may collapse. Alternatively, the chloroform in which the cholesterol is dissolved may dissolve membrane lipids, destabilising the liposomes. Therefore, more dilute solutions of cholesterol may be tried, although the membrane uptake in that case will be highly limited, if even present. Instead, a different cholesterol conveying solution may be used to provide the liposomes with cholesterol, although compatible solutions may be hard to find given the apolarity of cholesterol. Cholesterol suppletion may therefore be expected to either be happening at extremely low rates due to low concentrations, or to be facilitated by carrier molecules, such as BSA that forms C-BSA-C complexes that has been demon-

strated to allow for cholesterol specific incorporation in mitochondria [Martinez *et al.*, 1988]. Alternatively, cholesterol containing SUVs may be used for fusion purposes as described in the context of membrane growth in the review section. In the light of incorporation, fluorescent cholesterol analogues may be interesting to follow the incorporation of cholesterol-like components. This method may also be of interest for the cholesterol partitioning from the lipid beads in relation to the elongation and actual membrane cholesterol contents.

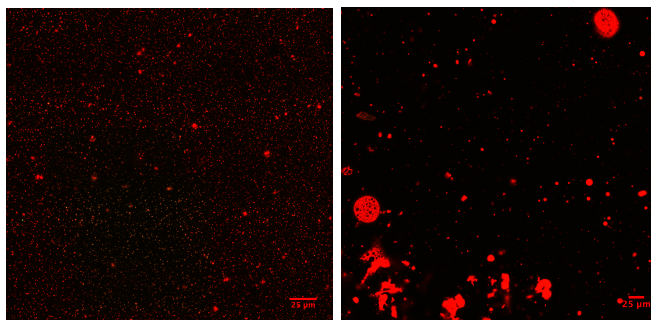


Figure 13.8.1 Sample destruction upon addition of 3 and 1 μL 5 mg/mL cholesterol (in chloroform) respectively. All liposomes have been destroyed, leaving Texas Red aggregates only. (K-drive: 19-12-3uL-001 and 29-01-1uL-003 respectively; settings: 488nm-25%, and 561nm-10%)

14 Discussion

14.1 Cholesterol elongation in context

The cholesterol-induced liposome deformation has been observed before. Nomura *et al.* (2005) observed 'neuron-like tube' formation and assessed this behaviour for different cholesterol contents in both DOPC and Egg-PC GUVs.

Nomura *et al.* found the tube formation to be dependent on the cholesterol content, where the highest influence was observed for 10% cholesterol and a decreasing amount of liposomes and tubes were observed at cholesterol percentages of 40% and higher.

The behaviour observed by Nomura *et al.* is fundamentally different from our observations in the sense that the images provided by Nomura *et al.* indicate an extent of instability that would not be compatible with studying any form of gene-expression due to a loss of observable liposome lumen. In fact, the extended tubes observed by Nomura *et al.* resemble our observations in case the samples suffer from high evaporation, which may also have been the case for Nomura *et al.*

A possible explanation for the elongating effect of cholesterol is local partitioning of cholesterol in less positively curved areas, as cholesterol tends to favour negative curvature areas [Wang *et al.*, 2007]. Here, cholesterol may locally increase membrane rigidity, resulting in elongation of liposomes.

In pure DOPC membranes cholesterol has been described to not have a significant rigidifying effect [Gracia *et al.*, 2010]. Generally, cholesterol does involve increased membrane rigidity [e.g. Petrache *et al.*, 2005] due to its phase compacting effect along with possible local lipid raft formation.

The size dependent difference in elongation provides support for the described elongation mechanism, as smaller vesicles may have less membrane flexibility to allow for distinct localised cholesterol partitioning.

In the context of elucidating the exact mechanism that allows for the observed elongating effect, fluorescent cholesterol analogues may be functional for tracing cholesterol-like components even though one is not observing cholesterol itself. Alternatively, filipin, a highly fluorescent antibiotic mixture obtained from *Streptomyces filipinensis* [Whitfield *et al.*, 1955], may be used for direct cholesterol imaging based on its specific binding to cholesterol. The partitioning behaviour of cholesterol may in this case be influenced by the compound binding however.

14.2 Overall Project in Perspective

We have demonstrated a method for liposome elongation based on the incorporation of 30% cholesterol in DOPC: DOPE: DOPG: Cl(18:1): TxR: PEG-biotin liposomes. With an observed elongation percentage that is about 1.5 times higher than in the same liposomes without cholesterol. A controllable method has been demonstrated that is fully compatible with gene-expression in the

PURE system.

Similar elongating effects were observed under the addition of differing external sucrose concentrations, although the effect of increasing sucrose concentrations on their own were less pronounced than the effect of cholesterol incorporation. Furthermore, sucrose has a maximal elongating effect at 100 mM, and may result in rupturing of liposomes at higher concentrations. Sucrose does reinforce the elongating effect of cholesterol however.

The cholesterol-induced elongation has not yet been placed in the context of a minimal cell from the perspective of external cholesterol suppletion. As described in the results section, carrier molecules such as BSA, or SUV fusion may be deployed to more efficiently transfer cholesterol from the external environment to the gene-expressing liposomes, while evading the need of bringing the liposomes in contact with an apolar solvent.

The cholesterol-based elongation has furthermore shown initial compatibility with both FtsA and MinD binding, although subsequent FtsZ ring formation and Min wave development remain open for investigation. Min waves have shown compatible with (100 mM) external sucrose concentrations. Together sucrose and Min waves induce relatively pronounced oscillating shape deformations in line with earlier observations [Litschel *et al.*, 2018]. It remains to be elucidated what causes the shape transitions, i.e. whether the transitions are mainly induced by protein-membrane binding, or by internal flows. Future experiments could in this light go out to include a lumen dye that could be used to trace fluid flows. Additionally, the observed oscillation frequency of $0.05 \text{ Hz} \pm 0.008 \text{ Hz}$ is different from the frequency reported for DOPC:DOPG (4:1) vesicles only as described by Litschel *et al.* (2018) (0.015 Hz). The combination of a different lipid composition along with external sucrose may thus significantly enhance the oscillatory vesicle behaviour.

The FtsZ-FtsA self-organization was in all cases especially limited to the interface between two liposomes. On one hand the observed septa may be a result of some extend of ring invagination. The relatively big sizes of the rings located at the septa make other explanations for the ring-septum colocalisation, such as locally increased protein concentrations, more feasible however. Figure 13.5.1(left) does show that FtsZ-FtsA may alternatively specifically localise at mid-plane or rather at the poles of an elongated liposome.

Electric fields, in contrast, have not resulted in visible elongation within our microscopy set-up, due to the specialised equipment necessary to achieve higher voltages necessary for more pronounced shape deformations. The approach may still be feasible in the context of gene-expressing liposomes (see review), but was within the scope of this thesis discarded as a research line given both time and material constraints.

Lastly, the question remains whether gene-expressing compatible division can be controllably induced with one of the deployed methods. Several observed events may have constituted division (Appendix D). In all cases, the 2-dimensional observation of the 3-dimensional division event is limiting. In contrast, imaging

flow cytometry allows for direct visualisation of the elongated axes that align with the flow. Unilamellarity and multilamellarity can however barely be distinguished at the objective magnifications (up to 60x) currently provided in the Imagestream®Imaging Flow Cytometer [Luminex Corporation ®, 2018].

15 The future for division in gene-expression liposomes

The present findings show an apparent lack of robust observable division. On the one hand the apparent lack of division may be a result of an actual lack of division. On the other hand, the presently deployed methods may be a complicating factor for direct visualisation of division events.

Confocal microscopy is functional for relatively higher resolutions, but lacks on functionality towards more quantitative aspects. Additionally, movement and influences imposed by trapping methods may interfere with observing division in confocal microscopy. Lastly, confocal microscopy images in 2D, allowing for the possibility that apparently dividing liposomes are still connected in another plane. Limited by the z-stack scanning speed as well as the random sample search, observation of division in confocal microscopy is a rare event.

Imaging flow cytometry may provide more quantitative results towards size, number and morphology distribution instead. In order to gain understanding regarding possible division in cholesterol liposomes compared to non-cholesterol liposomes with or without externally added sucrose, one could think of comparing the liposome size and count between the samples. Possibly, the size and count comparison could be supplemented by a control experiment where the cholesterol liposomes are depleted from cholesterol by β -cyclodextrin directly after liposome formation to ensure that cholesterol does not necessarily affect the size and count of liposomes during the liposome preparation. Size and count comparisons as quantified by flow cytometry have been used as evidence towards division events before [e.g. Sunami *et al.*, 2018]. In our case quantifying liposome count and size would however most likely still not provide us with conclusive data due to the large heterogeneity in sample quality resulting from the natural swelling.

Alternatively, time may be an essential factor determining whether division is observed. In the present experiments, visualisation was started 3 hours after liposome formation to allow for maximum gene-expression. Other groups, such as in the case of M2 protein-induced division, reported fission events after 1 hour however [e.g. Rossman *et al.*, 2010]. Time may therefore have been of influence on the observed lack of division as well, although some earlier screenings did not result in division observation either.

All in all, the observation of division of gene-expressing liposomes is limited by the observation techniques as well as by the heterogeneity imposed by the natural swelling. Given the events that have been observed division may occasionally be taking place. A more robust method may allow for higher observation chances/higher discrimination certainty with respect to actual division. In respect of the creation of more robust division, especially combinations of methods may be promising. Building on the present study, an example of a future

study may be the combination of elongated cholesterol-containing liposomes with FtsZ constriction. Alternatively, sphingomyelin and cholesterol together have been described to largely increase membrane flexibility [e.g. Gracia *et al.*, 2010], opening a door for more membrane-intrinsic division.

References

- [1] Angelova, M. *et al.* (1986). Liposome electroformation. *Faraday Discuss. Chem. Soc.*, 1986, 81, 303-311.
- [2] Angelova M., Dimitrov D.S. (1988) A mechanism of liposome electroformation. In: Degiorgio V. (eds) *Trends in Colloid and Interface Science II. Progress in Colloid Polymer Science*, vol 76. Steinkopff.
- [3] Aranda, S. *et al.* (2008). Morphological Transitions of Vesicles Induced by Alternating Electric Fields. *Biophysical Journal: Biophysical Letters*: L19-L21. doi: 10.1529/biophysj.108.132548.
- [4] CSDN, *et al.* (2015). Fisher's linear discriminant (Linear Discriminant Analysis). Retrieved on 1-3-2019 from: <https://blog.csdn.net/u012303532/article/details/42973897>.
- [5] Döbereiner, H.G. *et al.* (1993). Budding and Fission of Vesicles. *Biophysical Journal*. 65: 1396-1403.
- [6] Filippov, A. *et al.* (2003). The Effect of Cholesterol on the Lateral Diffusion of Phospholipids in Oriented Bilayers. *Biophysical Journal*, 84 (5): 3079-3086.
- [7] Ghouschi, V.P. *et al.* (2015). Opto-Mechanical Design And Development of an Optodigital Confocal Microscope. Master Thesis. DOI: 10.13140/RG.2.2.33261.38884.
- [8] Gracia, R.S. *et al.* (2010). Effect of cholesterol on the rigidity of saturated and unsaturated membranes: fluctuation and electrodeformation analysis of giant vesicles. *Soft Matter*, 2010,6, 1472-1482.
- [9] Henry, S.A. (2012). Metabolism and Regulation of Glycerolipids in the Yeast *Saccharomyces cerevisiae*. *Genetics* 190 (2):317-49. DOI: 10.1534/genetics.111.130286.
- [10] M. Kersbergen, Optimising cell-free gene expression inside cell-sized liposomes, Thesis Bachelor End Project for BSc in Applied Physics performed at the Department of Bionanoscience at the TU Delft, August 2017.
- [11] G. Kockelkoren, De novo synthesis of the ESCRT-III complex as a route for membrane remodelling in a minimal cell framework, Thesis Bachelor End Project for BSc in Nanobiology performed at the Department of Bionanoscience at the TU Delft, March 2018.
- [12] Kumazawa, N. *et al.* (1996). Novel method to form giant liposome entrapping DNA. *Macromol Symp*, 106: 219.
- [13] Lipowsky, R. *et al.* (1992). Budding of membranes induced by intramembrane domains. *J. Phys. II* 2:1825-1840.

- [14] Litschel, T. *et al.* (2018). Beating Vesicles: Encapsulated Protein Oscillations Cause Dynamic Membrane Deformations. *Angewandte Chemie*, 57 (50): 16286-16290.
- [15] Maratinez, F. *et al.* (1988). Cholesterol increase in mitochondria: a new method of cholesterol incorporation. *Journal of Lipid Research*, 29: 1005-1011.
- [16] Nomura, S.M. *et al.* (2005). Changes in the morphology of cell-size liposomes in the presence of cholesterol: Formation of neuron-like tubes and liposome networks. *Biochimica et Biophysica Acta (BBA) - Biomembranes*. 1669 (2): 164-169.
- [17] Nourian, Z., Danelon, C. (2013). Linking genotype and phenotype in protein synthesizing liposomes with external supply of resources. *ACS synthetic biology*, 2(4), 186-193.
- [18] Petrache, H.I. *et al.* (2005). Alteration of Lipid Membrane Rigidity by Cholesterol and Its Metabolic Precursors. *Talking about Biocolloids*, 219 (1): 39-50.
- [19] R Core Team (2015). R: A language and environment for statistical computing. R Foundation for Statistical Computing, Vienna, Austria.
- [20] Rossman, J.S. (2010). Influenza Virus M2 Protein Mediates ESCRT-Independent Membrane Scission. *Vol. 142 (6): 902-913.*
- [21] Russell, D.W. (1992). Cholesterol Biosynthesis and Metabolism. *Cardiovascular Drugs and Therapy*, 6(2): 103-110.
- [22] Sakuma, Y. *et al.* (2015). From Vesicles to Protocells: The Roles of Amphiphilic Molecules. *Life*, 5: 651-675. DOI: 10.3390/life5010651.
- [23] Schindelin, J.; Arganda-Carreras, I. Frise, E. *et al.* (2012), "Fiji: an open-source platform for biological-image analysis", *Nature methods* 9(7): 676-682.
- [24] Shimizu, Y. *et al.* (2001). Cell-free translation reconstituted with purified components. *Nat. Biotechnol.* 19: 751-755.
- [25] H. C. Shum, D. Lee, I. Yoon, T. Kodger and D. A. Weitz, *Langmuir*, 2008, 24, 7651-7653.
- [26] Sunami, T. *et al.* (2018). Flow Cytometric Analysis To Evaluate Morphological Changes in Giant Liposomes As Observed in Electrofusion Experiments. *Langmuir*, 34: 88-96.
- [27] Van Swaay *et al.* (2013). Microfluidic methods for forming liposomes. *Lab Chip*, 2013, 13, 752-767.

- [28] Wang, W. *et al.* (2007). Evidence of Cholesterol Accumulated in High Curvature Regions: Implication to the Curvature Elastic Energy for Lipid Mixtures. *Biophysical Journal*, 92 (8): 2819-2830.
- [29] Whitfield, G.B. *et al.* (1955). Filipin, an Antifungal Antibiotic: Isolation and Properties. *J. Am. Chem. Soc.* 77 (18): 4799-4801. doi:10.1021/ja01623a032.
- [30] Yu, *et al.* (2018). Plasmonic Nanosensors Reveal a Height Dependence of MinDE Protein Oscillations on Membrane Features. *J. Am. Chem. Soc.*, 140 (51), pp 17901-17906. DOI: 10.1021/jacs.8b07759
- [31] Zong, W. *et al.* (2018). Deformation of giant unilamellar vesicles under osmotic stress. *Colloids and Surfaces B: Biointerfaces*. 172: 459-463.

16 Acknowledgements

This thesis would not have been possible without the guidance provided by my supervisor Elisa Godino, MSc. and Dr. Christophe Danelon. Additionally, I would like to thank Duco Blanken, MSc. for borrowing some of his material (e.g. the home made PURE buffer) and for further experienced advice. Also, special thanks to Dr. Zhanar Abil for borrowing her Texas Red-free lipid beads for the imaging flow cytometry calibration and to Dr. Anne Doerr for using her Matlab code for Min wave analysis. I would like to thank Dr. Roland Kieffer, Dr. Shaurya Sachdev and Dr. Pouyan Boukany for their advice and assistance in the development of the electrodeformation protocol. Furthermore, I would like to thank Dr. Peter Rhein for running the Imagestream flow cytometer with us and for making me familiar with the IDEAS® software and for providing me with an initial data analysis template. Lastly, I would like to thank Erwin Swart for his time and Sanquin Amsterdam for letting us analyse our samples with their equipment.

17 Appendix A: Lipid/Sterol Nomenclature

DOPC: 1,2-dioleoyl-sn-glycero-3-phosphocholine (18:1)

DOPE: 1,2-dioleoyl-sn-glycero-3-phosphoethanolamine (18:1)

DOPG: 1,2-dioleoyl-sn-glycero-3-phospho-(1'-rac-glycerol) (18:1)

DLPE: dilauroylphosphatidylethanolamine

DMPC: dimyristoylphosphatidylcholine

Texas Red: Membrane dye 561 nm

Cardiolipin 18:1: Lipid generally found in *E. coli*

Cholesterol: Sterol that is not found in *E. coli*, that partitions within the internal membrane leaflets.

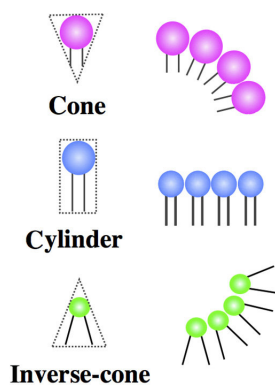


Figure A.1 The lipid shape is determining for the preferential combined morphology [Sakuma *et al.*, 2015]. DOPC is an example of a cylindrical lipid, and DLPE of an inverse-cone shaped lipid.

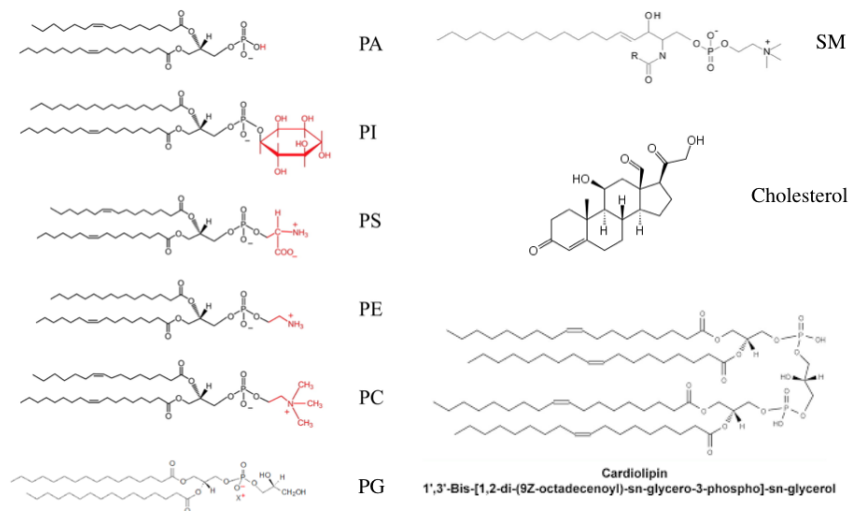


Figure A.2 Overview of the structures of the most important lipid and sterol types in the current context. The nomenclature mentioned for the phospholipids is here directed at the head groups [Figure adapted from Henry *et al.*, 2012].

18 Appendix B: Electrodeformation Chamber Construction

The initial objective was to observe liposome shape deformation from prolate to oblate shapes according to what has been described in literature [e.g. Aranda *et al.*, 2008]. For this purpose we constructed two electrodeformation chambers with different electrode gap widths to reconstitute different uniform electric field strengths according to equation 5.

$$\vec{E} = \vec{V}/d \quad (5)$$

The maximal uniform field strength that therefore can be obtained is fully dependent on the voltage source and the electrode gap width. Given the maximal voltage output of the oscilloscope we connected to the copper electrodes ($25V_{pp}$), we had to minimise the gap width in order to obtain field strengths similar to the ones described to deform liposomes, i.e. $\pm 0.1kV/cm$. To achieve similar field strengths as described in literature, we constructed two electrodeformation chambers with gap widths of 4.5 and 1.5 mm respectively.

In the chamber construction that was done with Dr. Roland Kieffer, we chose to use copper electrodes over platina electrodes from a cost efficiency perspective. As copper is corrosion sensitive however, we had to ensure the electrodes would not be able to get in contact with the solutions. Therefore, we separated the electrodes from the solution through a thin coverslip adhered with Norland Optical Adhesion 81 (Noah81) glue. It should be noted that the vertical distance between the solution and the electrodes thereby may negatively influence the net electric field strength experienced by the liposomes, although this we expect to be only of minor influence. The desired field strengths in both chambers were therefore $0.03kV/cm$ and $0.08kV/cm$ for the two chambers respectively. A schematic depiction of the chamber construction is given in figure B.1 below.

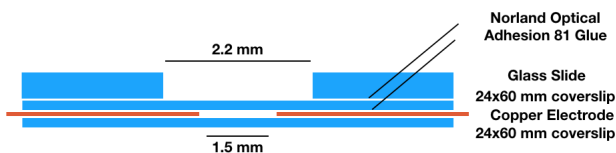


Figure B.1 Schematic image of the electrochamber construction. The copper electrodes were glued between two thin No.0 coverslips with Noah81. On top of the coverslip construct, a thick glass slide was subsequently glued in which a small hole was drilled to contain the liposome solution. Note that the construction depicted is the second chamber we constructed. The first chamber made had a gap width of 4.5 mm that was equal in diameter to the hole drilled in the glass slide. In the first case analysis at least is easier as one can look throughout the sample and is not constricted to the middle of the solution.

19 Appendix C: Additional Images and Data on the Morphology and Expression of Cholesterol Liposomes (30%) under the Addition of External Sucrose (0-200 mM)

Overview images of the effect of sucrose on YFP-expressing cholesterol (30%) liposomes are depicted in figure C.1. Especially for sucrose concentrations of 200 mM the total amount of liposomes does decrease, although less than for the non-cholesterol liposomes.

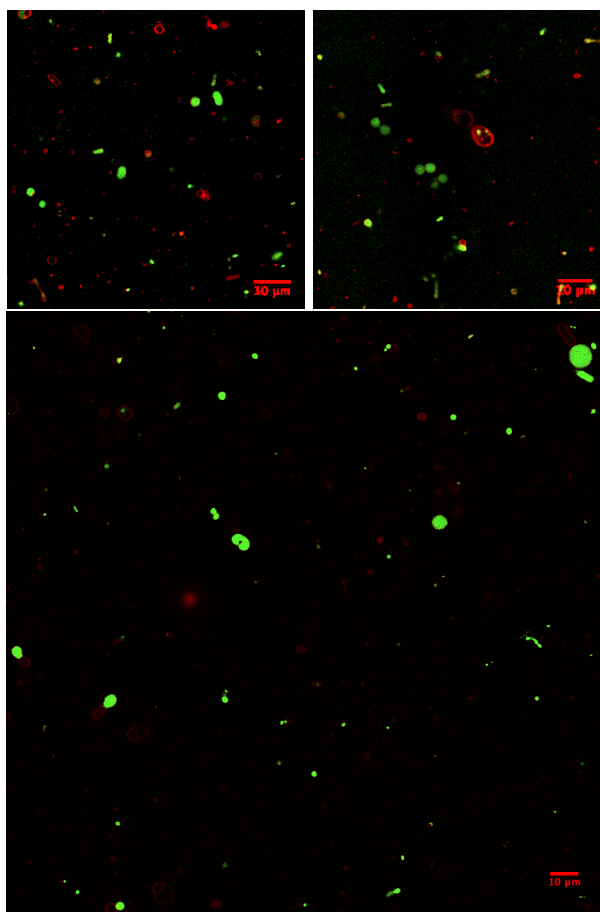


Figure C.1 Cholesterol induced non-sphericity in liposomes with increasing sucrose concentrations in the external environment (0, 100, 200 mM respectively) (time>3 hours). Note that the cropped areas increase in size due to a decreasing liposome density for higher sucrose concentrations. (K-drive: 18-12-001)

Manually counted confocal images indicate there is no difference between the percentage of expressing liposomes for the cholesterol and non-cholesterol liposomes within an external sucrose range between 0 and 200 mM as depicted in figure C.2.

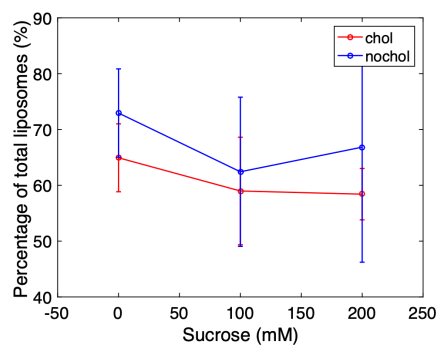


Figure C.2 Percentage of expressing liposomes on the total liposome population (for both (30%) cholesterol liposomes and liposomes without cholesterol) for different external sucrose concentrations (0-200 mM). On average ± 1000 liposomes have been counted per data point with a minimum of 350 liposomes in low-density samples.

20 Appendix D: Observed Events that resemble or suggest Fission

Two most notable events related to fission have been recorded and are displayed in the figures below.

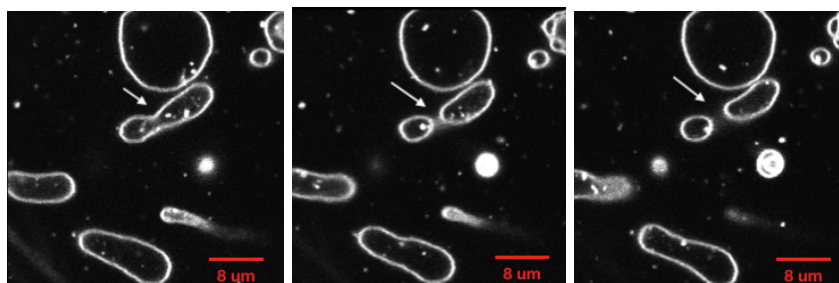


Figure D.1 One possible division event (2D) observed in a cholesterol (30%) containing liposome. The shadow in the back of the constriction site however increases the likelihood that the liposome is still connected in another plane, as was observed at later times. (K-drive: 20-11-300suc-2012; t=49:51 (2s interval))

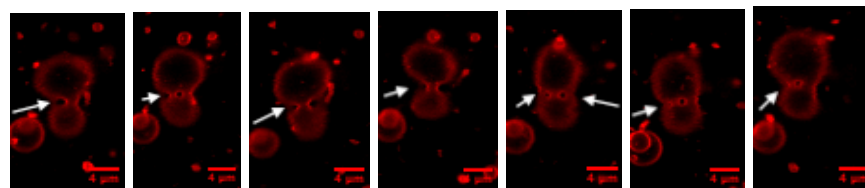


Figure D.2 Display of an endocytosis-like fission event in a cholesterol vesicle (Texas Red channel only). (K-drive:11-01-007; t=12:18)

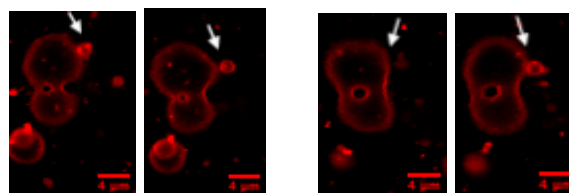


Figure D.3 Display of an endocytosis-like fission event in a cholesterol vesicle (Texas Red channel only). (K-drive:11-01-007; t=19:21 and t=24:25 resp.)

21 Appendix E: Fischer Linear Discriminant Analysis

For sensible flow cytometry data analysis generally dimensional reduction is carried out through a principal component analysis. One functional data analysis technique used in flow cytometry context is Fischer Linear Discriminant Analysis (LDA), an unsupervised machine learning technique.

Using Fischer LDA, the direction of largest variability in the data is found to project the data on. For two normally distributed parameters with equal covariances, the ratio S between the variances between both characteristics $\sigma_{between}^2$ and within σ_{within}^2 the characteristics is determined following equation 6.

$$S = \frac{\sigma_{between}^2}{\sigma_{within}^2} = \frac{(\vec{w} \cdot \vec{\mu}_1 - \vec{w} \cdot \vec{\mu}_0)^2}{\vec{w}^T \Sigma_1 \vec{w} + \vec{w}^T \Sigma_0 \vec{w}} = \frac{(\vec{w} \cdot (\vec{\mu}_1 - \vec{\mu}_0))^2}{\vec{w}^T (\Sigma_0 + \Sigma_1) \vec{w}} \quad (6)$$

Here, $\vec{w} = \Sigma^{-1}(\vec{\mu}_1 - \vec{\mu}_0)$ and $\vec{\mu}_0$ and $\vec{\mu}_1$ are the averages of the individual parameters. In other words, $\vec{w} \in N(0, 1)$, or \vec{w} is a normally distributed variable within the interval between 0 and 1. The covariance matrix Σ conveys the relation between the two parameters under investigation and is a main topic of experimental interest as it determines the extend to which observed characteristics can be distinguished.

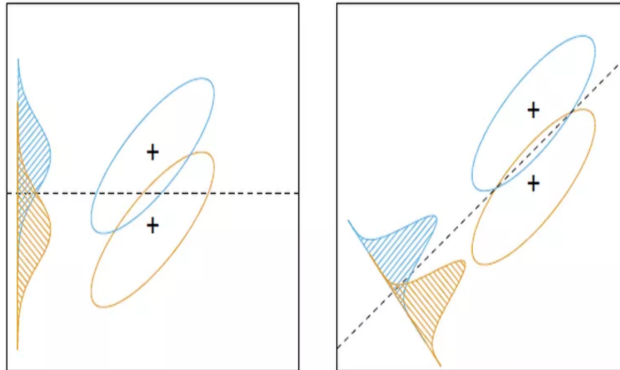


Figure E.1. The principle behind Fischer LDA is class discrimination based on two normally distributed characteristics [CSDN *et al.*, 2015].

In what direction the classification has to occur is dependent on the optimal projection found with the LDA. Orthogonal to the projection line are the residues, amongst which is the uncorrelated noise that may, given significant separation, account for different group-intrinsic characteristics. The projection in essence

maximises the mean difference between both classes, while minimising the class-internal variances.

For variance ratio's S below 1, no group distinction can feasibly be made. In contrast, ratio's of S above 3 are strong indicators for distinguishing properties. The boundaries outlined are used in the feature finder tool in the imaging flow cytometry IDEAS® software (Image Data Exploration and Analysis Software) from Luminex Corporation.

Elongated liposome shapes can in this way be theoretically distinguished through a characteristic intensity regression related to their intrinsic membrane to volume ratio.

Suppose an elongated liposome can be approximated by an ellipsoid with volume and membrane area given by equations 7 and 8.

$$V = \frac{4}{3}\pi xyz \quad (7)$$

$$A = 2\pi x^2 \left(1 + \frac{z^2}{ex^2} \cdot \operatorname{arctanh}(e) \right) \quad \text{where} \quad e^2 = 1 - \frac{z^2}{x^2} \quad (z < x) \quad (8)$$

The ratio between the volume and the membrane area for elongated liposomes would consequently involve non-linear multidimensional regression.

We can approximate the relation between liposome volume and membrane area through a linear relation as can be done in the case of spherical liposomes.

For spherical liposomes, the volume-to-area ratio is given through equation 9.

$$\frac{V}{A_{spherical}} = \frac{\frac{4}{3}\pi r^3}{4\pi r^2} = \frac{r}{3} \quad (9)$$

In the case of spherical liposomes, the slope coefficient therefore is equal to $\frac{1}{3}$.

In the case of elongated liposomes approximated as ellipsoids, x and z should first be chosen as approximate constant values given the degree of elongation to be quantified with a linear approximation. Hereby, we only allow the y axis of the ellipsoid to vary. Finally, the volume-to-area ratio is given by equation 10.

$$\frac{V}{A_{ellipsoid}} = \frac{2yz}{3x} * \frac{1}{1 + \frac{z^2}{\sqrt{(1-\frac{z^2}{x^2})} * x^2} * \operatorname{arctanh}(\sqrt{(1-\frac{z^2}{x^2})})} \quad (10)$$

Educated guesses based on the imaging flow cytometry data acquired in this work, may give sensible $\frac{x}{z}$ -ratio's between around 1.1 and 3. Plugging these values in equation 10, results in slope coefficients between 0.32 and 0.18 respectively. Therefore, in distinguishing elongation shape, the degree of elongation is, as was to be expected, of paramount importance.

As significantly more approximations need to be made for the elongated liposome case, these populations will suffer from higher intrinsic noise, complicating Fischer Linear Discriminant Analysis. For the higher elongation factors however, we might be able to distinguish populations based on set parameter values for x and z .

22 Appendix F: Imaging Flow Cytometry Data Analysis

In a dot plot with the side-scatter (SSC) signal versus the Texas Red intensity, we first distinguish liposomes (and aggregates/dye precipitates) from the speed beads that run along in the flow cell, see figure F.1.

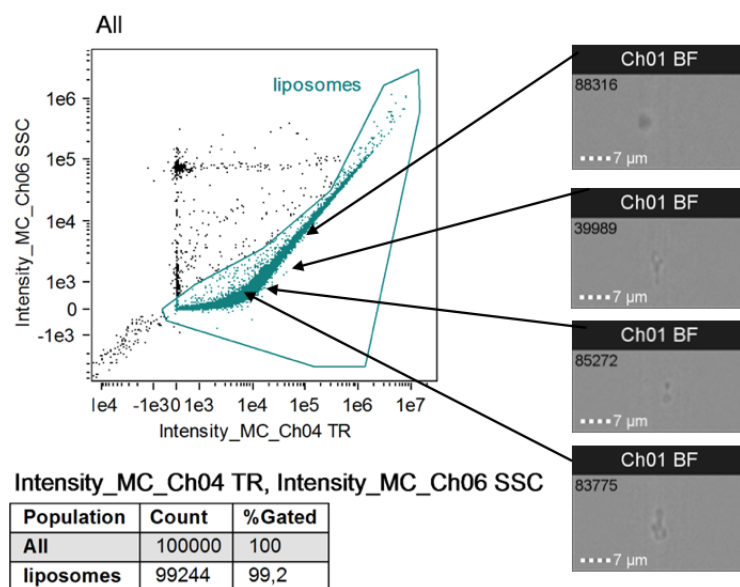


Figure F.1 Dot plot of the side-scatter signal versus the Texas Red intensity. Due to their different refractive index, the speed beads in the flow cell show higher SSC intensities, along with their general lack of Texas Red signal as opposed to the liposomes (and aggregates/dye precipitates).

After selecting the population from figure F.1, brightfield contrast gating was performed to distinguish liposomes from dye precipitates. An empirical threshold of 0.15 for the brightfield contrast value was determined based on individual images. In this way, still about 50% of the detected particles were generally classified as liposomes, unable to distinguish for e.g. multilamellarity given the magnification.

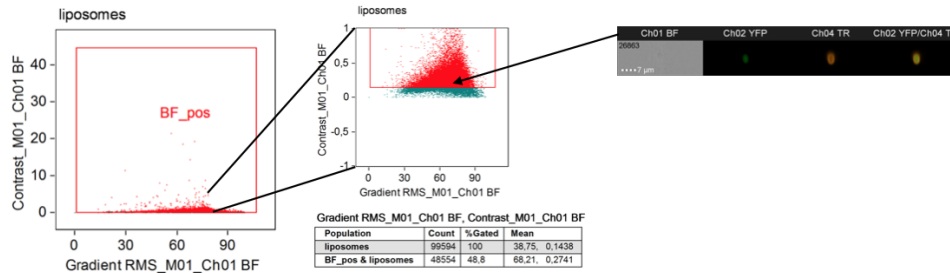


Figure F.2 To distinguish liposomes from aggregates and dye precipitates, a minimal bright-field contrast value was coupled to the fluorescence intensity to ensure at least some extend of liposome-like morphology.

Subsequently, as in regular flow cytometry experiments, intensity dot plots were made for the YFP intensity versus the Texas Red Intensity. From the dot plots as depicted in figures F.3 and F.4, it followed that, with equal thresholds, the YFP-expression levels in the 30%-cholesterol liposomes was in general about 2-3 times higher than in the non-cholesterol vesicles. Here it should be noted that the expression percentages were extremely low. The low percentages could either be attributed to large amounts of non-liposomal objects that are still treated as liposomes, or, most likely, the percentages could be due to the limited 488nm-laser power that we used at the maximal output.

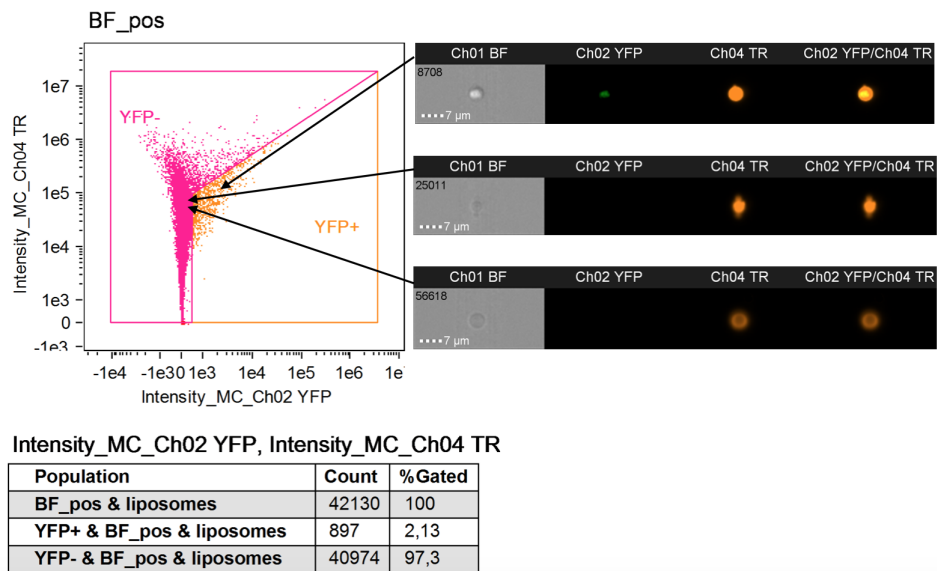
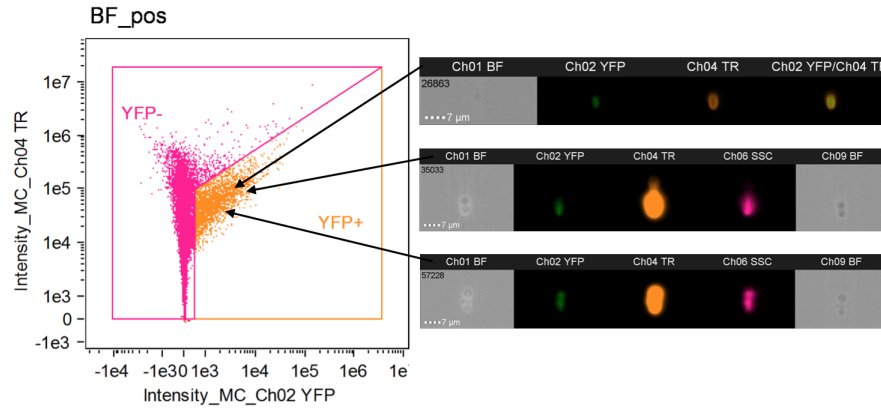


Figure F.3 Dot plots for YFP vs. Texas Red Intensity with the accompanying selections for non-cholesterol liposomes.



Intensity_MC_Ch02 YFP, Intensity_MC_Ch04 TR

Population	Count	%Gated
BF_pos & liposomes	48554	100
YFP+ & BF_pos & liposomes	2510	5,17
YFP- & BF_pos & liposomes	45863	94,5

Figure F.4 Dot plots for YFP vs. Texas Red Intensity with the accompanying selections for 30%-cholesterol liposomes.

Lastly, all resultant populations (i.e. YFP expressing and non-expressing cholesterol and non-cholesterol vesicles) were compared for their elongation given their size category. We determined 5 distinct size categories (0-1 μm ; 1-4 μm ; 4-7 μm ; 7-10 μm and >10 μm) and compared the elongation percentages for each size category in the different resultant populations. For the first experiment after one night liposome storage the results are depicted in figure F.5. Based on the raw results presented in figure F.5, the more quantitative analysis was carried out resulting in figure 13.3.1 in the main text. Note that liposomes qualified for elongation in this study only when their aspect ratio is between 1.4 and 5.0, which are carefully chosen boundaries that were deduced suitable from the confocal microscopy experiments.

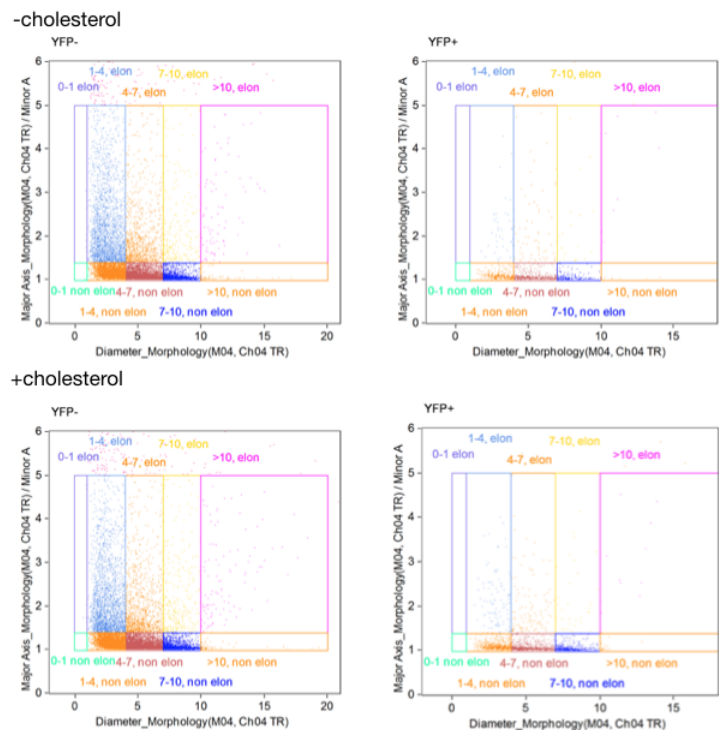


Figure F.5 Scatter plot for aspect ratio's versus diameter for -chol,-YFP; -chol,+YFP; +chol,-YFP; +chol,+YFP respectively. The apparent difference between -YFP and +YFP is essentially to be attributed to the different amounts of liposomes (raw data).

Additionally, an attempt was made to quantify the invagination behaviour in the cholesterol liposomes. The feature tool in the IDEAS®software appeared not able to distinguish such invagination however, and the quantification therefore stopped after a single manual search, see figure F.6 for some images.



Figure F.6 Collection of some invaginated and budding cholesterol liposomes as imaged during imaging flow cytometry.